國立交通大學

電信工程學系

碩士論文

寬頻圓極化天線設計

Design of Wideband Circularly Polarized Antennas

研 究 生：柯智元

指導教授：周復芳　博士

中 華 民 國 九 十 七 年 六 月

寬頻圓極化天線設計

Design of Wideband Circularly Polarized Antennas

研 究 生：柯智元　　Student: Jhih-Yuan Ke

指導教授：周復芳　博士　Advisor: Dr. Christina F. Jou

國 立 交 通 大 學

電 信 工 程 學 系 碩 士 班

碩 士 論 文

A thesis

Submitted to Department of Communication Engineering

College of Electrical and Computer Engineering

National Chiao Tung University

In Partial Fulfillment of the Requirements

For the Degree of

Master of Science

In Communication Engineering

June 2008

Hsinchu, Taiwan, Republic of China

中 華 民 國 九 十 七 年 六 月

寬頻圓極化天線設計

研 究 生：柯智元　　指導教授：周復芳　博士

國立交通大學電信工程學系碩士班

摘　　要

本研究主要針對寬頻圓極化天線以及應用於無線區域網路之雙頻天線作設計及探討，並分析這兩種天線的模擬與實驗的結果。

首先，提出一種平面寬頻天線設計概念，在天線上增加寄生元件以提升頻寬，為了達到激發正交能量的目的，採取非對稱饋入方式，接著為了將低頻帶之相位差拉到九十度附近，在天線的輻射器下方所對應的接地面上截出一塊槽孔，最後再配合接地面與輻射器上的開槽，不僅提升了中心頻率在 5.6GHz 上的阻抗頻寬達到121%，也近一步達到圓極化激發模態，並且將中心頻率在 4GHz 的軸比頻寬拓展為40%，順利激發左手圓極化波。

在一般的雙頻天線激發方式，常使用兩段分枝各自激發高低頻段，接著，提出一種拉近兩個頻帶的方式，在兩分枝後方加上一塊貼片，分別將高低頻段匹配在5.8GHz 以及 2.4GHz 的無線區域網路頻段。

Design of Wideband Circularly Polarized Antennas

Student: Jhih Yuan Ke Advisor: Dr. Christina F. Jou

Department of Communication Engineering

National Chiao Tung University

ABSTRACT

This thesis mainly focus on the design and discuss of wideband circularly polarized antennas and dual band antennas for wireless LAN purpose. Furthermore, the results from simulation and experimentation belong to the two kinds of antenna will be analyzed.

At first, it would be proposed a concept designing planar wideband antennas in which improving bandwidth by way of adding parasitic elements. In order to achieve orthogonal energy exciting, it employs asymmetric-fed. Truncate a slot in the ground plane corresponding to radiator so as to pull the phase difference in lower band to the vicinity of 90 degrees. Finally, embedding slit both in the radiator and the ground plane of the antenna. It would be not only improved the impedance bandwidth to 121% at the center frequency of 5.6GHz, and further excited circularly polarized modes. Moreover, extending the bandwidth of axial ratio to 40% at the center frequency of 4GHz, and exciting the Left Hand circularly Polarized waves successfully.

In general, the higher and lower band is exciting through two branches separately. It would be proposed that adding a patch in the rear of the two branches and the higher and lower band will be matched to the wireless LAN band in which 5.8 GHz and 2.4GHz.

ACKNOWLEDGEMENT

在電信所的兩年研究生活中，疑惑以及陌生充斥在未知的下一秒，隨之而來，是在驚喜中了解與熟悉。首先我要感謝的是指導教授周復芳博士，在研究過程中不厭其煩的給予協助，在日常生活當中，良師益友的身份，著實為研究領域以外帶來另一種踏實。同時感謝口試委員吳霖堃博士以及王健仁博士的不吝指導，在學生囿限的知識領域外，激盪更全盤的思考與認知，為這篇論文增添了不少價值。

在研究主題上，感謝俊緯學長細心的指導，從設計到量測都給予全力的支持，生活中遇到種種的問題，更仰賴您的中流砥柱形成最強力的後盾，未知帶來的疑慮因此消散於無形。感謝玠瑝與奕霖兩位學弟，在討論中盡心盡力，研究過程中的鼎力相助，讓我的學習更加順利。同時要感謝我的學習伙伴：積極樂觀的沛遠，熱情奔放的志豪，沉默穩重的廉昇，胸有成竹的昱舜，以及誠懇浪漫的昭竹，在兩年的碩士生涯中有幸與你們同窗學習，讓小小的實驗室瀰漫幸福的味道。感謝學長匯儀、錦福、智鵬、宜星在研究上所樹立的典範，雖然我還有許多需要努力的空間，但努力的方向卻非常的明確。最後要感謝實驗室中的新生代：深謀遠慮的子哲，篤志力行的昭維，以及胸無城府的宗廷，在你們的加入後，為實驗室帶來一片祥和之氣，感謝你們的付出與投入，輔助世代交替的運作很快的步上軌道。人生的旅途上，因為有分岐點而帶來了不同的選擇，在柳暗花明前的山窮水盡，這些默默給予支持的朋友，聽我開心伴我失意。我想感謝一直支持著我的明傑、有德、柏勳、礎宇…專科及二技的同學們，帶我回到夢幻國度的志諭、登捷、志元、嘉晏…國中同學們，伴我走過不同人生際遇的夜哥、豪哥、建衛、香崎…一路上的好朋友，因為有你們陪伴與支持，讓我更義無反顧的堅持下去。

最後我要感謝我最愛的父母親和兄妹，在求學的路上給予我最大的支持和包容；感謝貼心的女友雅鈴無怨無悔的陪伴，讓我無後顧之憂的完成碩士學業。在此僅以小小的研究成果，獻上無比的感恩，並與你們分享我的喜悅。

CONTENTS

LIST OF TABLES

LIST OF FIGURES

CHAPTER 1

Introduction

1.1 Background and Motivation

Remarkable advances have been made in wireless communication. Generally speaking, it can be divided to several stages according to the mechanism was employed by each period. The first, cellular system was deployed and analog transmission was applied to construct communication networks. This so-called first-generation (1G) mobile technology which involves AMPS (Advanced Mobile Phone System) and NMT (Nordic Mobile Telephone) was developed since 1980s. The next generation of mobile technology was founded because of 1G accounted for the drawbacks such as insecure connection, lavish spectrum allocating and heavy weight. Second-generation (2G) mobile technology which includes GSM (Globe System for Mobile communications), TDMA (Time Division Multiple Access), and CDMA (Code Division Multiple Access) started at 1990s. Utilizing digital coding to compress and encrypt information, 2G not only improves the spectrum efficiency and communicating security but adds many personal services. The most commonly used multimedia and demands for high speed excites the upgrade of mobile communication systems, and further, the third-generation (3G) mobile technology which comprises UMTS (Universal Mobile Telecommunications System), CDMA2000, and TD-SCDMA (Time Division - Synchronous CDMA) was produced at 2000s. It provides high speed, high quality and versatility on mobile communications.

Recently, the development of wireless communication has progressed rapidly such that many applications based on wireless transmission attract much attention. To be in

opposition to more and more demand for channels allocating, not only the systems and antennas are specified to the corresponding spectrum. A device contains more than one purpose give rise to the benefits on diminution in volume, reduction of cost and manifold functions. Therefore, there is a tendency towards multiband integration as Apple iPhone [1] and HTC Touch Phone [2] of nowadays. Such handsets provide the connection services over 2G, 3G, Blue Tooth, HSDPA (High-Speed Downlink Packet Access), GPRS (General Packet Radio Services), Wi-Fi (Wireless Fidelity), GPS (Globe Positioning System) and EDGE (Enhanced Data rates for GSM Evolution). The assignment of an antenna for a specification would lead to not merely dissipative in spatial but interference amid antennas; and further, the requirement of spectrum extend incessantly. The wideband antenna would be an appropriate solution to achieve the anticipation of users effectively.

On the other hand, GPS applications get more attention today since the complete abilities of navigation enables the traveling information provided through location, speed, direction and time becoming more accurate. As considering the view of transferring, the circularly polarized technique would accentuate the significance of polarization undoubtedly. Over and above the well-known specification of inclemency counteracting, the circularly polarization possess the tolerance of misalignment between transmitting and receiving antennas. This is especially suitable for mobile devices and RFID (Radio Frequency Identification) consequently. A planar monopole antenna with wideband of circularly polarized bandwidth will be introduced.

The technology of wireless LAN is applied to notebooks and handset devices nowadays. The rule of thumb in design is reduction of entire system size and hence the requirement of antenna size accompanies the limitation of spatial size. A compact wireless LAN antenna will be considered.

1.2 The Characteristics of Proposed Antennas

In recent years, planar antennas receiving much attention owing to their inherent characteristics such as easy fabricating, light weight and low profile. In addition, a monopole antenna consists of a radiator and a large enough ground plane. It can be seen as a dipole antenna through image theorem and hence it possesses dipole-like radiating behaviors as wider bandwidth and Omni-directional radiating pattern [3]. The surface current distribution on the monopole antennas appear linear motion with phase variation, and hence radiate linear polarized wave in far-field region.

The first antenna has dimensions of 60 mm×40 mm and is etched on a 1.6 mm FR4 substrate with a dielectric constant of 4.4. Based on asymmetric feeding and truncated monopole antenna design concept, a planar monopole antenna with wideband of circularly polarized bandwidth has been fabricated. It can be obtained 120% impedance-bandwidth centered at 5.6 GHz. Otherwise; it possesses 40% 3dB-axial-ratio bandwidth with center frequency at 4 GHz and achieves LHCP wave excitation at broadside direction.

The second antenna has dimensions of 45 mm×14.5 mm and is etched on a 1 mm FR4 substrate with a dielectric constant of 4.4. Based on two branches assignment and reflect patch design concept, a compact antenna for wireless LAN purpose has been fabricated. It can operate over ISM band and the upper band of 802.11a.

1.2.1 Review of Circularly Polarized Antennas

To achieve circular polarization, as a general rule of thumb, two modes possess equal magnitude and 90 degree out of phase must be excited. The relevant designs have been studied extensively and many various approaches have been proposed.

Microstrip Patch Antennas (MPA) are mainly utilized to produce circular polarization just because of their inherent advantages such as low profile, light weight, easy of fabrication and low cost. First, the theoretical prediction of nearly square patch antennas have been developed to avoid senselessly trial-and-error owing to their simply structures. A cavity model was proposed in [4] to plumb patch antennas about nearly square, corner truncated and capacitive loaded individually as shown in Fig. 1-1. The estimation for central frequency of circular polarization and polarized sense can be completed via physical size and feeding points. In order to extend the discussion over various feeding position and thicker substrate for wideband manipulation, a modified formula was further investigated [5-6]. Based on adequate design, patches with various modifications possess circularly polarized ability consequently [7]. To improve circularly polarized performance, various shaping techniques were applied. Adding slot on the patch of conventional probe-fed antennas not only widens bandwidth [8] as shown in Fig. 1-2 but also further reduces apparel since lengthening the path of surface current path [9-11] as shown in Fig. 1-3.

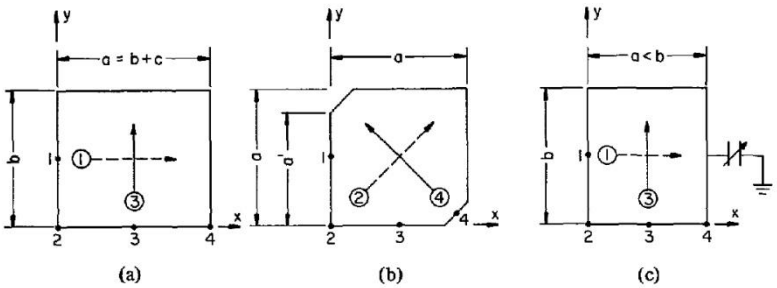

Fig. 1-01 Three prototypes of circularly polarized antenna design (a) nearly square patch, (b) corner truncated patch, and (c) capacitive loaded patch [4]

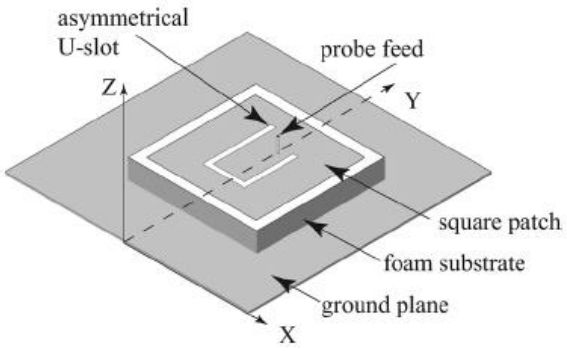

Fig. 1-02 Patch antenna embedded an asymmetric U-slot [8]

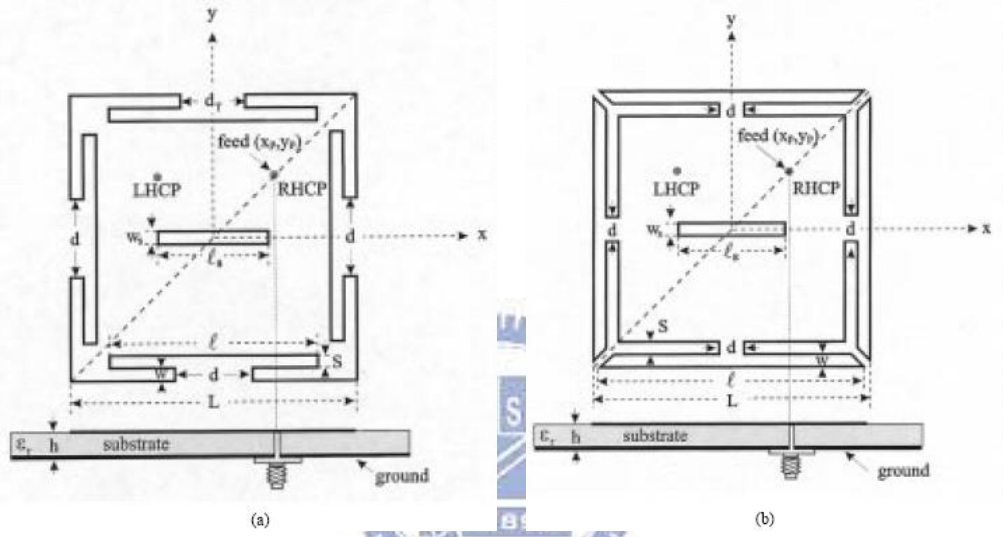

Fig. 1-03 Patch antennas embedded (a) T-slot and (b) Y-slot [10]

For the request of phase difference, much avenues focus on the feeding network and the shape of radiator of antennas. The hybrid coupler must be the direct idea to separate two modes and identical magnitude caused by balance structure and quadrature exciting by differential current paths can be achieved [12-13] as shown in Fig. 1-4. In order to meet wider bandwidth over traditional patch antennas, the stacked patch antenna consists of a driven patch, a parasitic patch and a additional substrate with thicker height and lower dielectric constant was presented [14-16] as shown in Fig. 1-5. Spiral antennas [17] as shown in Fig. 1-6 and sinuous antennas [18] possess inherent wideband manipulation since their own active region according to various frequencies.

For diminution of antenna size, slot antennas [19-21] as shown in Fig. 1-7 and annular-ring antennas [22-24] as shown in Fig. 1-8 was investigated to provide circular polarization over wideband. Other special design such as sequential-rotation subarrays with either linearly polarized antennas [25] or circularly polarized antennas [26] as shown in Fig. 1-9 was analyzed and the wideband operation was obtained.

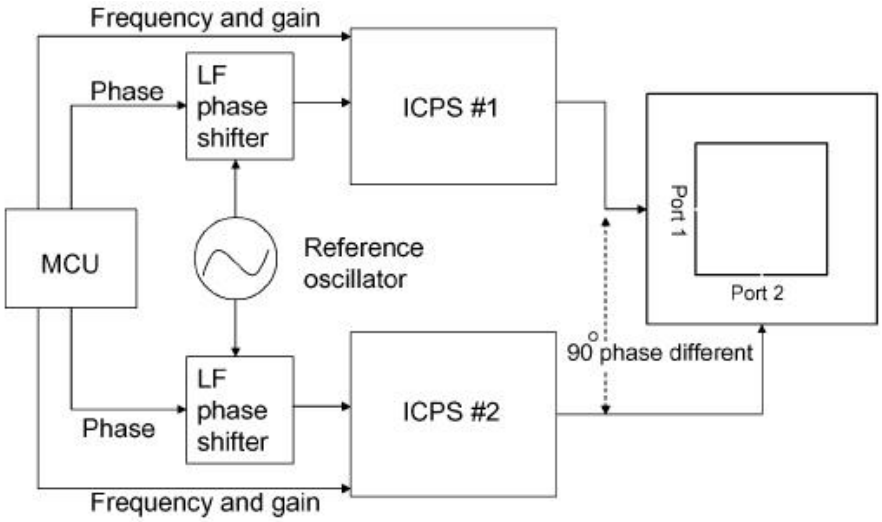

Fig. 1-04 Design of Circularly polarized transmitter via dual feed [12]

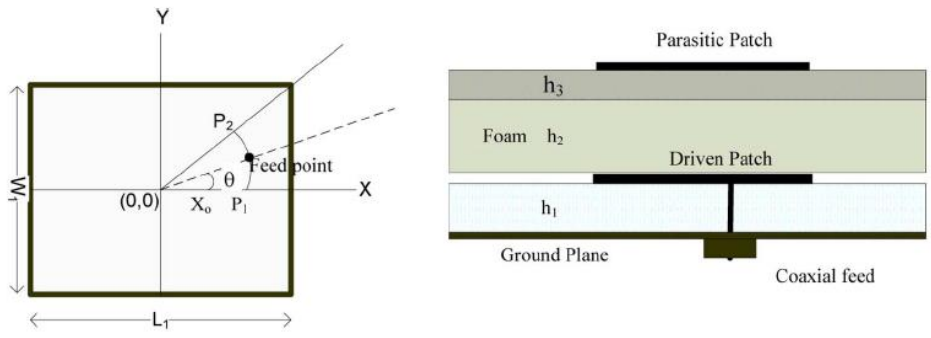

(a) (b)

Fig. 1-05 Stacked patch antennas (a) Feeding schema of driven patch (b) Cross-section view of the stacked patch antenna [15]

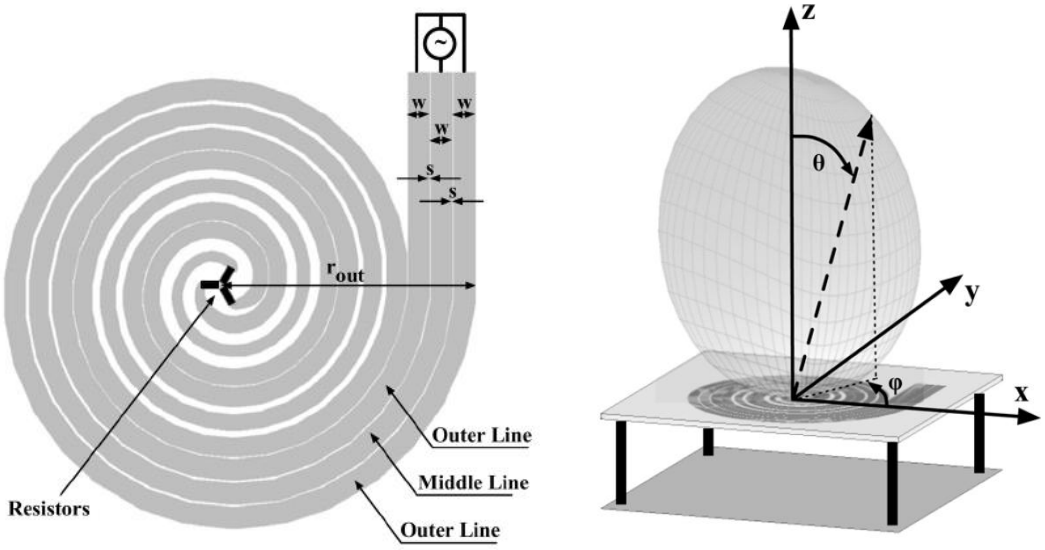

(a) (b)

Fig. 1-06 Spiral antennas (a) 3-arms spiral antenna fed from outer edge (b) The 3-arms spiral was mounted above a ground plane to achieve unidirectional radiation pattern [17]

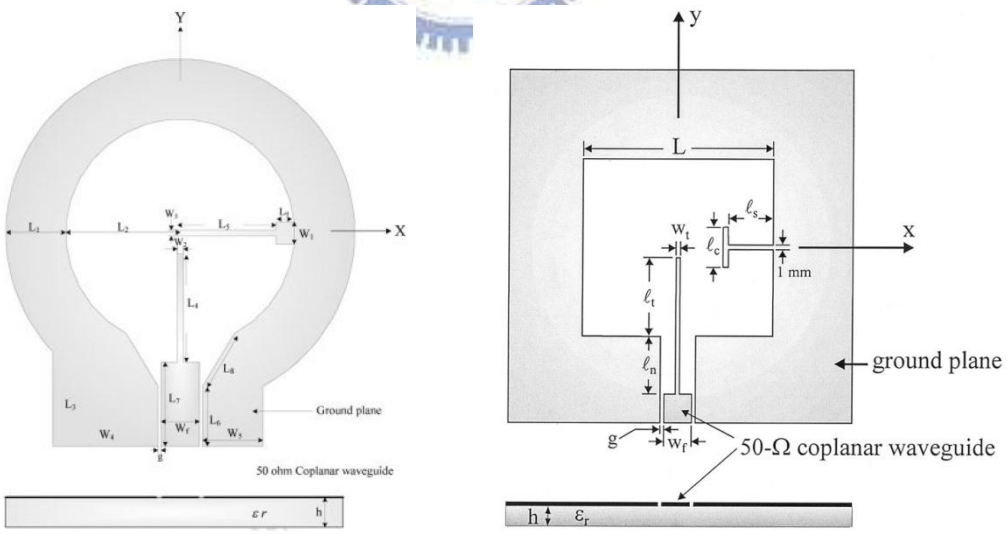

(a) (b)

Fig. 1-07 Slot antennas (a) Circular slot antenna with CPW fed [19] (b) Square slot antenna with CPW fed [20]

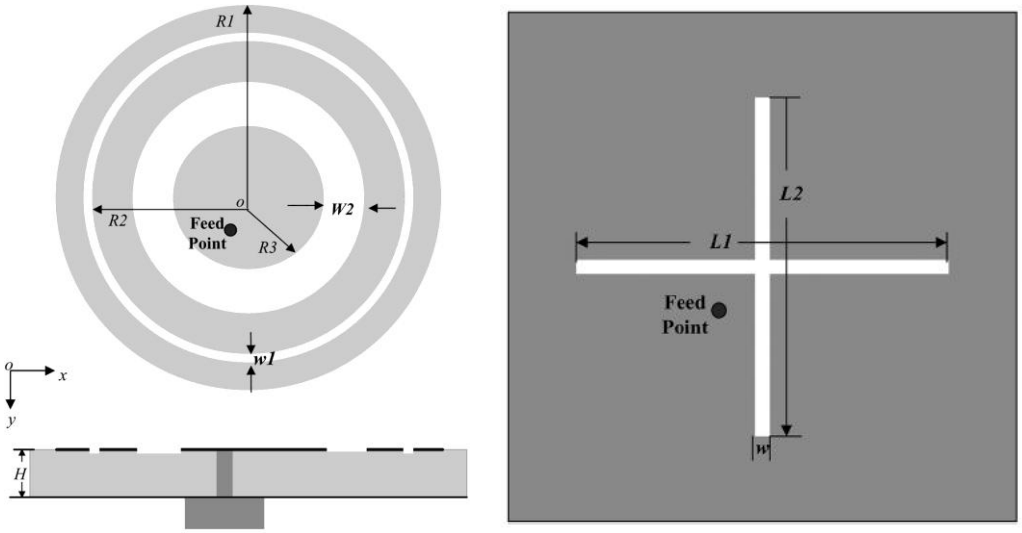

(a) (b)

Fig. 1-08 Annular-ring antennas (a) Schema of Annular ring patch and the side view of configuration (b) Cross-slot ground plane [24]

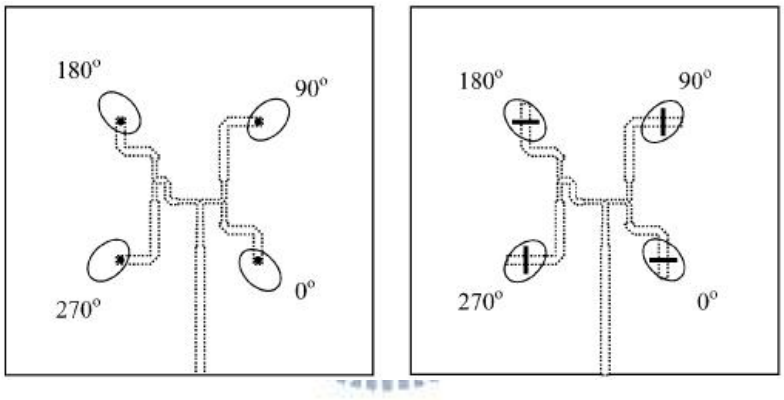

(a) (b)

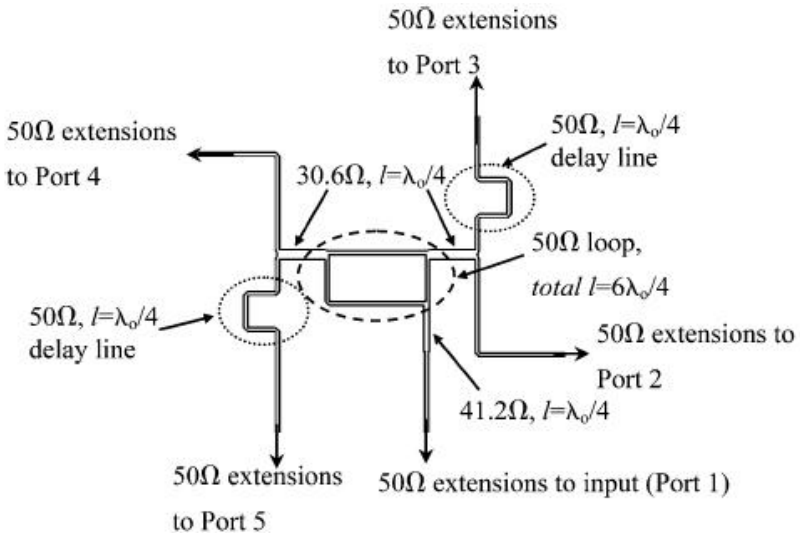

(c)

Fig. 1-09 Sequential-rotation subarray with dielectric resonator antennas (DRA) (a) Schema of probe-fed elliptical DRAs. (b) Schema of narrow-slot-fed elliptical DRAs (c) Geometry of hybrid ring feeding network [26]

1.3 Thesis Framework

In this thesis, the wideband circularly polarized antennas will be introduced in ***Chapter 2***, the compact antenna design will be presented in ***Chapter 3***, and finally, the future work will be considered in ***Chapter 4***.

In ***Chapter 2***, the behavior of polarization will be discussed at ***2.1.1 polarization***. The linear polarization can be seen as a component to compose other derivations and it will be mentioned at ***2.1.2 Linear Polarization***. Actually, the elliptical polarization which ***2.1.3 Elliptical Polarization*** referred to often exists in nature, and the circular polarization considered at ***2.1.4 Circular Polarization and Axial Ratio*** usually possesses tolerance. Axial ratio will be introduced to classify the types of polarization. Influence caused by mismatching in polarization will be mentioned at ***2.1.5 Polarization Mismatching***. Focus the viewpoint to the antenna design and the configuration of proposed wideband circularly polarized antenna will be further presented at ***2.2.1 Schema of Antenna Structure***. The development of the antenna will be introduced at ***2.2.2 Considerations during Design Procedure***. Consequently, the variables of design will be discussed at ***2.2.3 Parametric Studies*** and experimentation will be established to verify the concept of anticipation through ***2.2.4 Results of Simulation and Measurement***.

In ***Chapter 3***, the wireless LAN technology will be introduced at first. The detail information about the wireless LAN will be discussed at ***3.1.1 Protocols and Spectrum Allocation***. Turn to antenna design, the architecture of proposed wireless LAN antenna will be presented at ***3.2.1 Schema of Antenna Structure***. The variables of design will be further discussed at ***3.2.2 Parametric Studies***. Finally, ***3.2.3 Results of Simulation and Measurement*** will validate the achievement of design.

CHAPTER 2

Design of CPA with Wideband Characteristic

2.1 Circularly Polarized Wave Propagation

In recent years, the applications of circularly polarized wave propagation have attracted much attention owing to their significant superiority on resistivity of inclemency weather over linearly polarized wave propagation. These applications are especially employed in modern communication systems sensitive to atmospheric variation such as radar tracking, navigation, satellite communication and mobile systems. Furthermore, the unconsidered risk of misalignment simplifies set-up process and benefits receiving ability.

2.1.1 Polarization

According to the concept of displacement current, James C. Maxwell got agreement with other electromagnetic equations and predicted the existence of electromagnetic wave since more than a century ago. In the far-field region, energy radiation caused by current distribution on antennas can be seen as a transverse electromagnetic (TEM) wave – the components of electrical field (E), magnetic field (H) and propagating direction are perpendicular each other none the less because they vary with time. The term ***Polarization*** can only use the trajectory of time-varying E in space to identify behavior of microwave radiation due to the relation between E and H as (2-1).

Generally, infinitesimal current I with $\Delta z \ll \lambda$ in length on the antenna can be seen as an equal length ideal dipole possesses both uniform magnitude and phase [3]. Such an ideal dipole illuminates in free space to form a doughnut-like radiation pattern

without inner hollow and hence polar plots with omnidirection and figure-of-eight are revealed through the cross-section vertical and horizontal to the dipole separately. In a practical sense, H-plane presents the vertical cutting mentioned above as it contains H vector and E-plane indicates the other for the same reason. The wave is referred as to a planer wave while observation point is stationed adequately far from radiating source, and its E vector and H vector are co-located on the constant phase plane. Selecting any constant phase plane as an observation plane with time-varying condition, a trajectory constructed by the tip of E vector can be obtained.

$$\frac{E_\theta}{H_\phi} = \frac{\omega\mu}{\beta} = \frac{\omega\mu}{\omega\sqrt{\mu\varepsilon}} = \sqrt{\frac{\mu}{\varepsilon}} = \eta \tag{2-1}$$

where η is the intrinsic impedance of the medium, and

$$\vec{E} = E_\theta \hat{\theta} = \frac{I\Delta z}{4\pi} j\omega\mu \frac{e^{-j\beta r}}{r} \sin\theta\hat{\theta} \tag{2-2}$$

$$\vec{H} = H_\phi \hat{\phi} = \frac{I\Delta z}{4\pi} j\beta \frac{e^{-j\beta r}}{r} \sin\theta\hat{\phi} \tag{2-3}$$

2.1.2 Linear Polarization

It would be examined further the radiating properties of ideal dipole referred before. Once the dipole vertical to ground is placed in free space, the tip of time-varying E vector will go back and forth along a straight line perpendicular to ground and the wave is so-called vertical polarization. Horizontal polarization presents time-varying E vector varies with the straight line parallel to ground by the same token. The situation a wave polarized in the x-direction is traveling along the +z-axis can be written as following:

$$\vec{E} = \hat{x}E_x e^{-jkz} \tag{2-4}$$

To deserve to be mentioned, 45-degrees polarization is obtained as the included

angle of 45 degrees between dipole and ground plane is installed. It would be obtained in the situation such as dual-polarized application. After the discussion of three kinds of the polarization type, it can be attached the triple to linear polarization because of the orbits caused by them are linearity.

A coordinate system is further established on an observation plane to describe the behaviors of polarization through two orthogonal bases – E_V and E_H, which means that the electric field distribution in free space would be composed of E_V and E_H even through it varies with time. The classifications of polarization are completed according to combinations of the bases and hence circular polarization and elliptical polarization will be considered.

2.1.3 Elliptical Polarization

The elliptical polarization will be produced while the E vectors against time on the observation plane would be reduce to a generating set includes two perpendicular vectors. In other words, the tips of vectors on the observation plane depict an ellipse with respect to time varying. It would be judged which is a left polarization or right polarization according to phase relation between these two components. Take a simple example; it is a left polarized wave as observer faces the incoming wave and the vector combined by generating set rotates clockwise. It can be considered the situation a wave of which x-component leads y-component by +90 degrees is traveling along the +z-axis forms the right hand elliptically polarized wave. It would be expressed as following:

$$\overline{E} = \hat{x}E_x e^{-jkz} - \hat{y}jE_y e^{-jkz} \qquad (2\text{-}5)$$

The expression gives a good account of the fact that an elliptical polarized wave can be decomposed to a couple of linear polarized waves which are perpendicular each other in space as well as are 90 degrees out of phase. In physical sense, it presents this

phenomenon obviously and hints elliptical polarization can be as a general solution to derive other polarized types. Generally speaking, elliptical polarization is a kind of conventional polarization type in everyday life.

2.1.4 Circular Polarization and Axial Ratio

Circular polarization would be constructed as imposing a restriction of generating components with equal quantity on the elliptical polarization. As implied by the name, the vector remains constant in length and rotates around in a circular path. Similarly, the discrimination between left-hand circular polarization (LHCP) and right-hand circular polarization (RHCP) will be done through the rotational sense by vector as the wave travels toward the observer.

After the discussion, it would be derived to the question which one parameter could identify the types of polarization. It should be concentrated on the interpretation of axial ratio and the extended discussion of elliptical polarization will be considered.

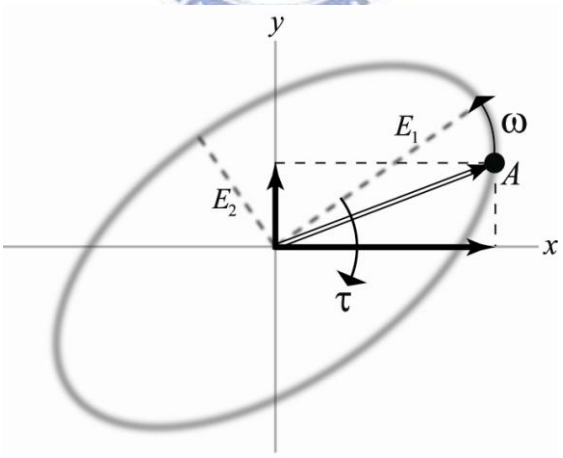

Fig. 2-01 RHEP with traveling direction in the +z-axis and tilt angle τ with respect to the principle axis

As shown in Fig. 2-01, at first, the spatial configuration attracts more attention about that coordinate transformation would be employed to simply analysis just because the

bases are non-unique and it leads into Fig. 2-02. Turning to the observation on time domain, the elliptical trajectory is formed along the time with angular frequency ω.

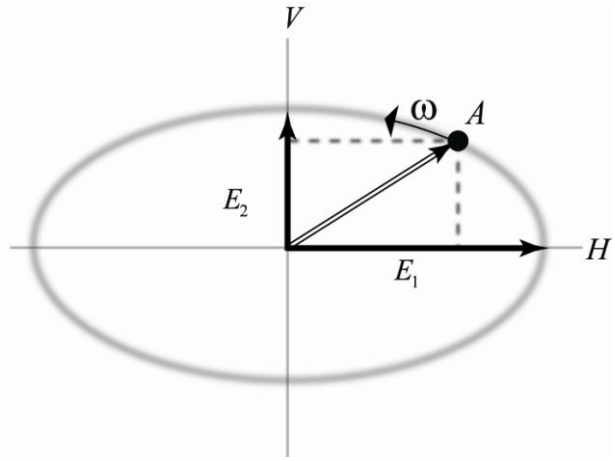

Fig. 2-02 Modified-axis RHEP presentation

The H-component equals to E_1 and no V-component as point A lies on the H-axis, similarly, the V-component equals to E_2 and no H-component as point A lies on the V-axis. The H-component leads V-component by 90 degrees according to the pasting angle is about 90 degrees. Polarized behavior can be described in terms of space and time and axial ratio can be written as following:

$$AR = 20\log\left|\frac{E_{\max}}{E_{\min}}\right| \tag{2-6}$$

Where $E_{\max}$ means maximum value of E along major axis and $E_{\min}$ means maximum value of E along minor axis. In conclusion,

(1) ***Linear polarization***: ($AR \to \infty$)

Uni-axis or bi-axial with in phase

(2) ***Elliptical polarization***: ($AR \geq 0dB$)

Bi-axis with quadrature phase

(3) ***Circular Polarization***: ($AR = 0dB$)

Bi-axis with identical magnitude and quadrature phase

2.1.5 Polarization Mismatching

The power gain is used to quantify the efficiency of transforming the energy from the feeding to the radiating edge of an antenna. Owing to the reciprocity of antennas the transmitting ability presents the receiving performance. It should be considered as following:

$$G = \frac{4\pi}{\lambda^2}\varepsilon_{ap}A_p = \frac{4\pi}{\lambda^2}\left(e_r\varepsilon_t\varepsilon_s\varepsilon_a\right)A_p \qquad (2\text{-}7)$$

There are many parameters relate to the physical specification of antennas: power gain G, wavelength corresponding to operating frequency λ, physical aperture area A_p, radiation efficiency e_r, aperture taper efficiency ε_t, spillover efficiency ε_s and achievement efficiency ε_a. Besides the cross-polarization efficiency ε_{cr} involved in the achievement efficiency mentioned above, it is not necessary for the purpose of this section to discussion particularly. Cross polarization is caused by the non anticipative polarization: for instance, LHCP appears on RHCP antenna and vertical polarization appears on horizontal polarization antenna. The energy will be partly dissipated on account of the negligence during designing process.

Turning the observation to receiving systems and some loss the system configuration leads into will be concerned. Impedance mismatching arises as the maximum power transferring is uncompleted. Polarization mismatching occurs in the circumstance such as imperfect alignment or incorrect sense of polarization. These reasons extra drop the system efficiency without involving by power gain and it should pay much attention on system installation and choice of polarized states accordingly.

Actually, the waves almost all propagate according to the linearly polarization and suffer foul environment such as misalignment, destructive interference, reflection and

attenuation. The improving of system efficiency can be achieved by introducing circularly polarized antenna as receiving antenna.

2.2 Wideband Planar Circularly Polarized Antenna

In this chapter, the circular polarization design of a monopole antenna fed through microstrip line is proposed. The proposed antenna is single feed and the required two orthogonal resonant modes excited over wide bandwidth through adding parasitic elements and truncating both the radiator and ground plane. To obtain a good impedance matching, the parasitic element was introduced [27]. The inherent characteristic of monopole antennas, linear polarization, leads to the difficulty for circular polarization exciting. According to the asymmetric feeding, the orthogonal mode was generated handily and the proposed antenna possesses basically circular polarization in a narrow bandwidth. Truncate the ground plane of proposed antenna and the phase difference between two orthogonal modes approaches to the vicinity of 90 degrees over wide bandwidth. Adequate embedding slots both into radiator and ground plane achieves wideband no matter in impedance bandwidth or 3-dB axial ratio bandwidth.

Circularly polarized antennas with wideband characteristic would benefit its operating region. Fig. 2-03 shows the configuration of our proposed wideband planar circularly polarized antenna. It would be etched on 1.6 mm FR4 double side substrate with relatively permittivity ε_r =4.4 and loss tangent $\tan\delta$ =0.024. The overall sizes of the antenna is about ($L\times W\times H$) $60\times 40\times 1.6$ mm^3. The proposed antenna possesses about 40% bandwidth of 3dB axial ratio at center frequency of 4GHz and excites LHCP wave at broadside direction. It would be obtained 121% bandwidth with center frequency of 5.6GHz.

2.2.1 Schema of Antenna Structure

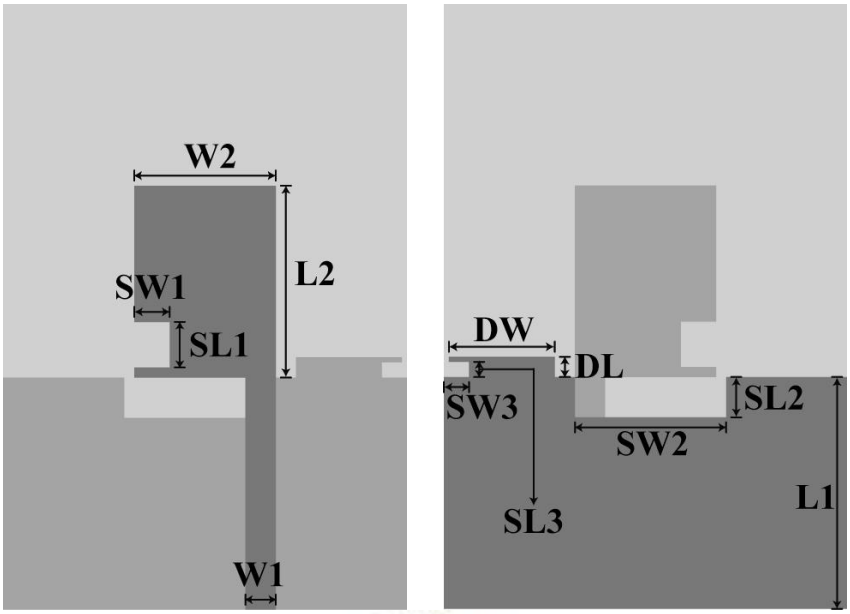

(a) (b)

Fig. 2-03 Geometry of the proposed antenna (a) Top side view (b) Back side view

The geometry of the proposed antenna was shown as Fig. 2-03. There are three gradations of gray color to distinguish the arrangement via scenograph and they are light gray, gray and dark gray respectively. Because of the light gray always means substrate and hence it should be considered only on the others. The dark gray used to present the side near observer in this expression. Top side view of the proposed antenna was displayed in Fig. 2-03 (a) and a radiator with the size of $L2\times W2$ was connected to feeding point via a microstrip line with the size of $L1\times W1$. A slot with the size of $SL1\times SW1$ was embedded on the radiator. Turn the proposed antenna to the other side and it can be seen as Fig. 2-03 (b). At first, a ground plane with the size of $L1\times 40mm$ was etched on the side of proposed antenna in origin case. A perturbation with the size of $DL\times DW$ was added to upper left of the origin ground plane, and then embedded a slit with the size of $SL3\times SW3$ to lower left of the perturbation. Finally, truncate a slot

with the size of $SL2 \times SW2$ aligning to the lower edge of radiator on top side and the proposed antenna was established. Table 2-01 states the optimization of the architecture.

(Unit: mm)

Topside	L1	W1	L2	W2	SL1	SW1
	23	14	19	14	4.5	3.5
Backside	DL	DW	SL2	SW2	SL3	SW3
	2	9.5	4	15	1.5	2.5

Table 2-01 Parameters of Antenna Optimization

2.2.2 Considerations during Design Procedure

A.*Wideband Operation*

In the application of planar monopole antennas is popular among the ultra wideband (UWB) antennas design since these advantages such as low profile, cheaper cost, less cross-polarization, wideband operation and omni-directional pattern provide the further benefit of easy fabricating to circuit boards. A simple design to achieve wideband can be done via adding a rectangular parasitic element near the monopole radiator as shown in Fig. 2-04 [27]. The characteristics of the monopole antenna introduced late was calculated according to Ansoft High Frequency Structure Simulator (HFSS) [28] software.

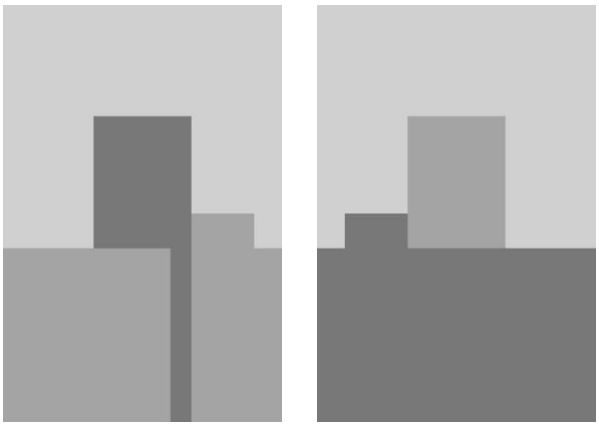

(a) (b)

Fig. 2-04 A wideband antenna with a square parasitic element (a) Top side view (b) Back side view [27]

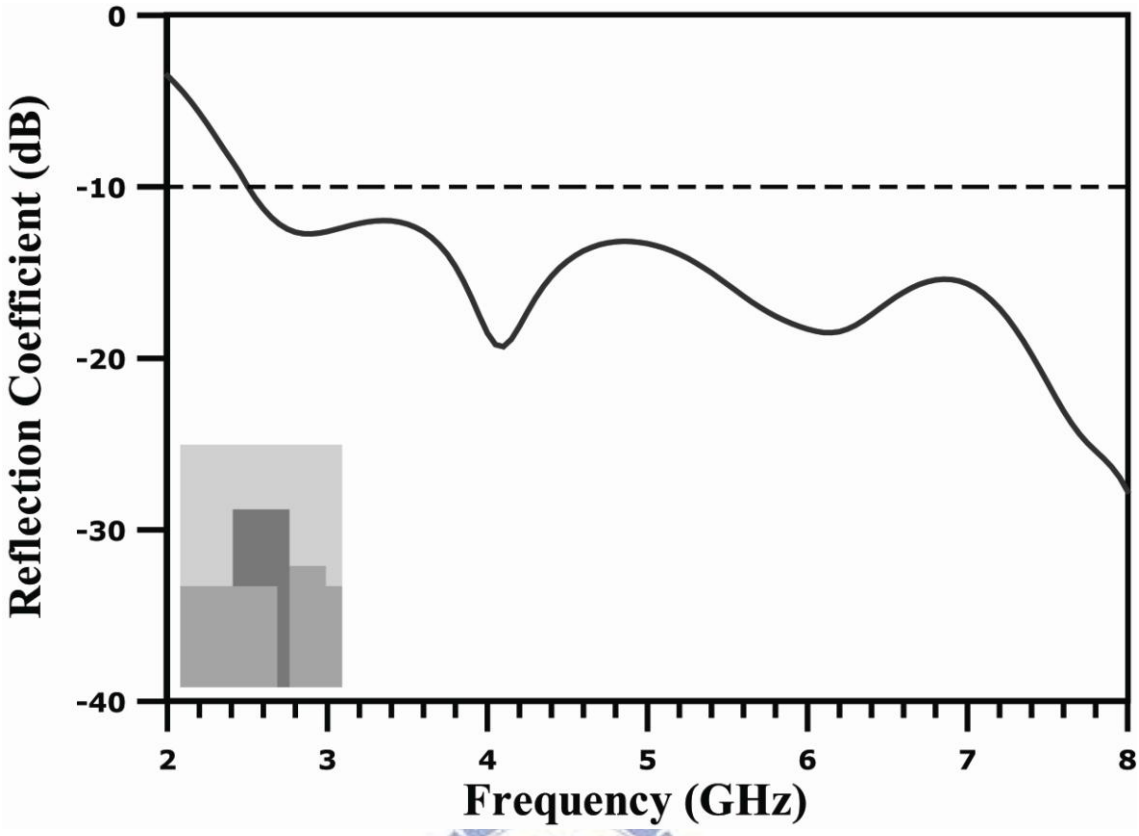

Fig. 2-05 Reflection coefficient of the antenna as shown in Fig. 2-04

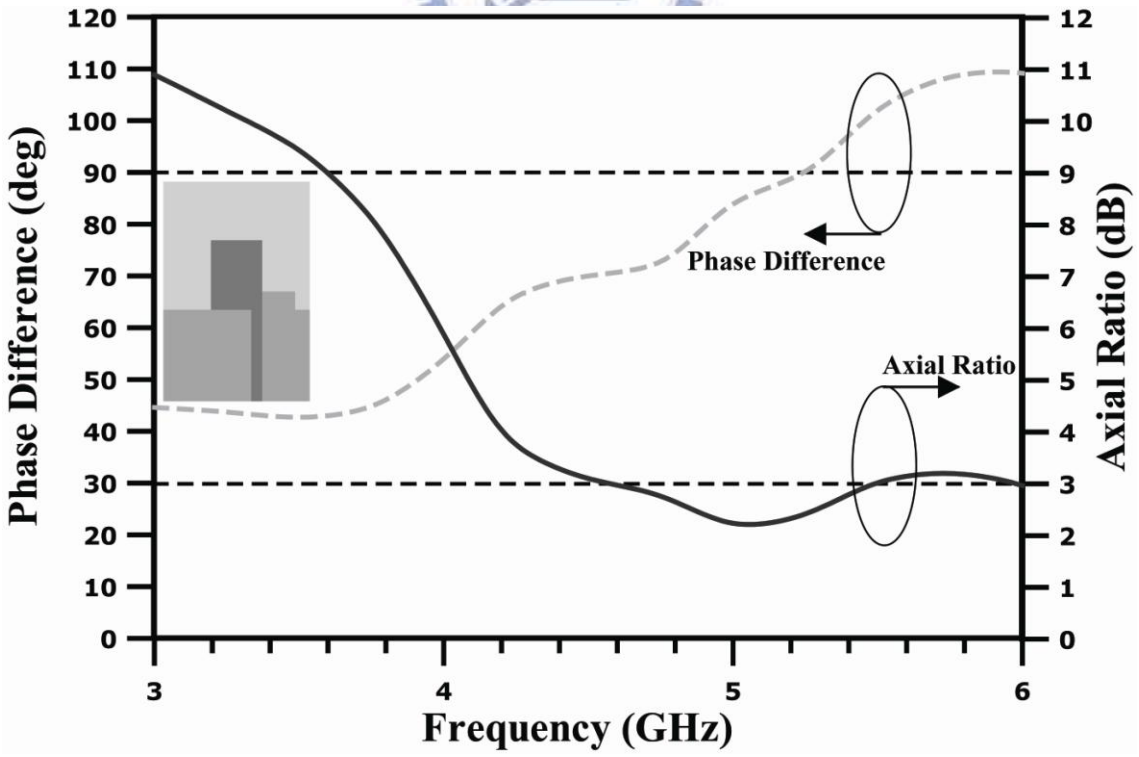

Fig. 2-06 Phase difference and axial ratio of the antenna as shown in Fig. 2-04

It can be obtained wider bandwidth via adding rectangular parasitic as shown in Fig. 2-05 and slightly circular polarization was presented surrounding 5 GHz as shown in Fig. 2-06. It will be further discussed about the offset feeding technology related to circular polarization.

B.*Asymmetric Feeding*

It can be easily divided feeding technologies to two kinds of central feeding and asymmetric feeding and theses two feeding manner would cause differential surface current distribution on the antennas. In Fig. 2-07, the center-feeding was occupied and the surface current almost presents the linearly variation in Fig. 2-08. Absenting of orthogonal terms, it is very difficult to form a circular polarization. As the modify was employed to feed to form an asymmetric feeding as shown in Fig. 2-09 and the surface current distribution presents the orthogonal component was generated to achieve circularly polarization as shown in Fig. 2-10. The circularly polarization will be excited as the orthogonal components possess the same energy and 90 degrees out of phase.

Pay the attention to Fig. 2-11, the comparison of phase difference between these two kinds of feeding technique was presented. In the case of central feeding, phase difference varies acutely over wide bandwidth. On the other hand, asymmetric feeding retains tardy variation of phase difference over wide bandwidth. Corresponding to Fig. 2-12, asymmetric feeding possesses lower and almost steadfast axial ratio and hence it can be concluded asymmetric feeding technique improves circularly polarized performance effectively.

For circularly polarization purpose, the orthogonal components can be arisen from asymmetric-feeding technology and the wideband characteristic can be achieved through adding the parasitic element in the ground plane as mentioned before. Combining these two mechanisms turns up the prototype of antenna design.

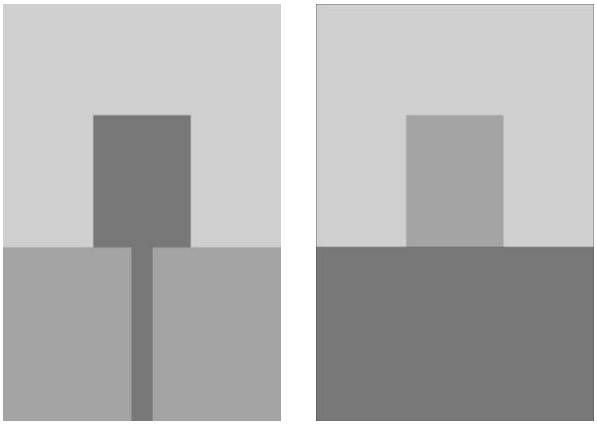

(a) (b)

Fig. 2-07 A central feeding monopole antenna (a) Top side view (b) Back side view

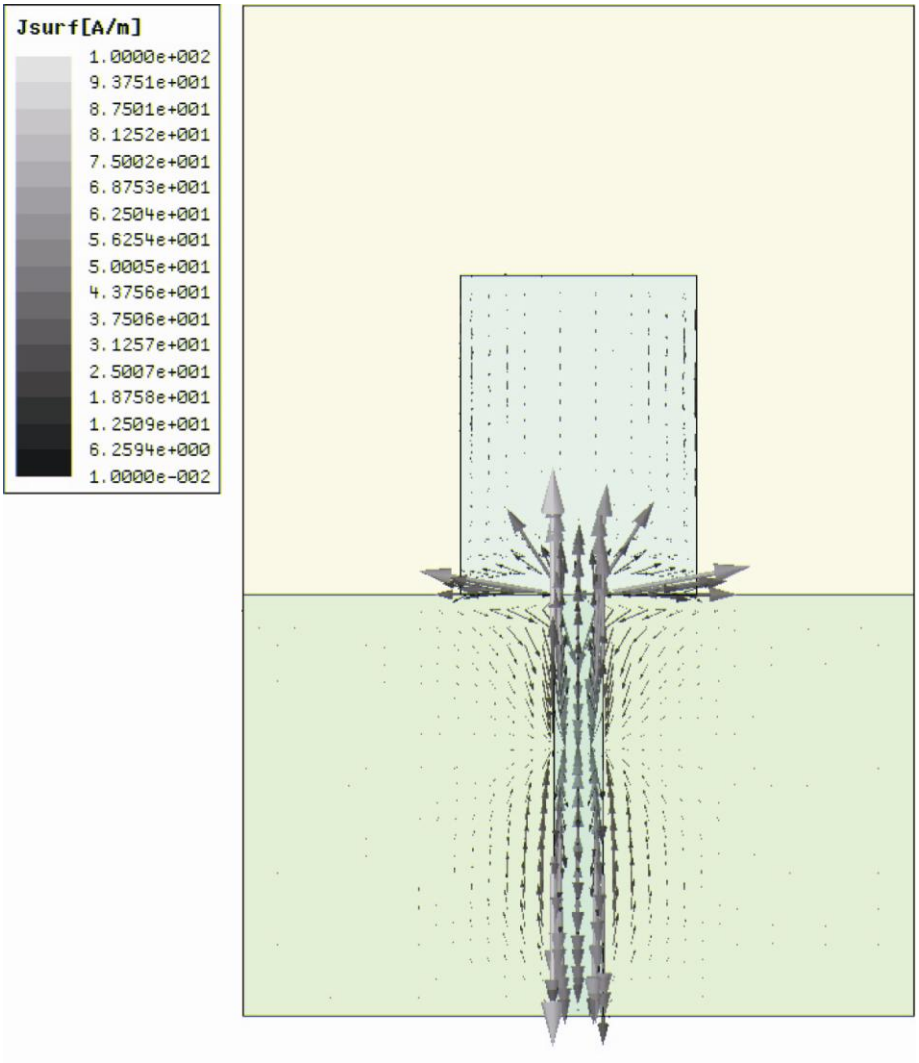

Fig. 2-08 Surface current distribution for the antenna geometry as shown in Fig. 2-07

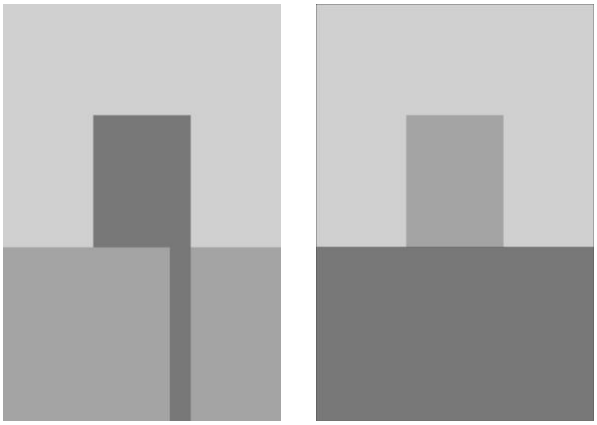

(a) (b)

Fig. 2-09 An asymmetric feeding monopole antenna (a) Top side view (b) Back side view

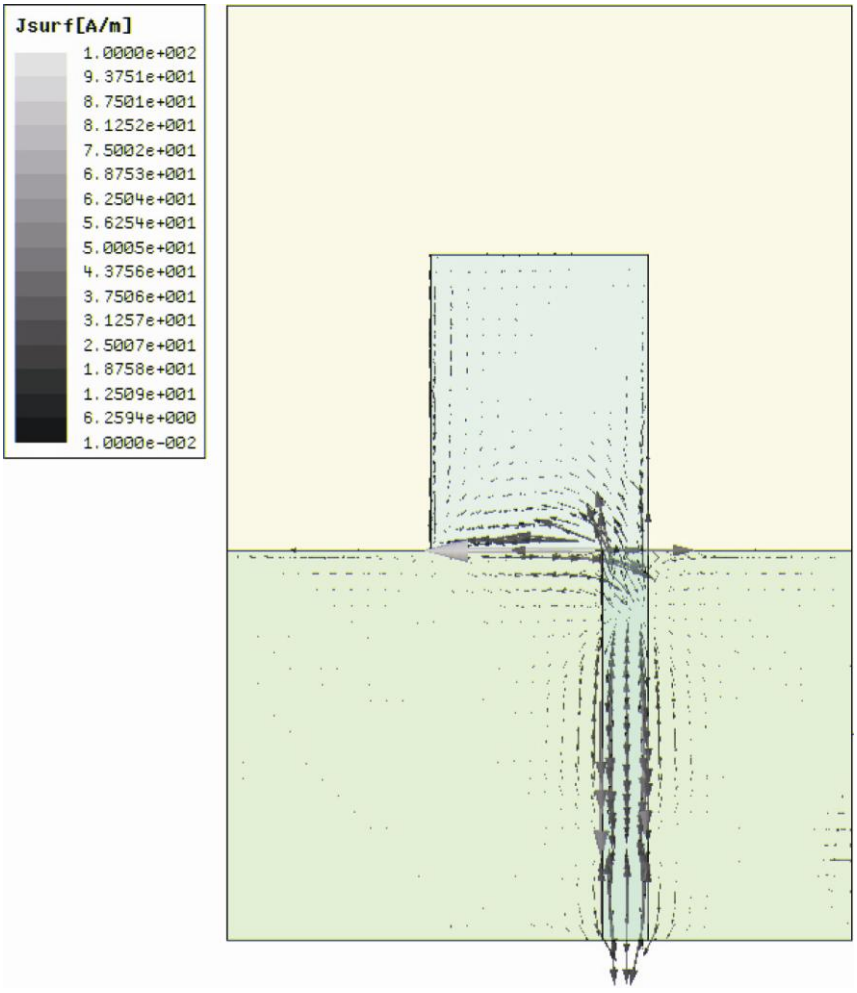

Fig. 2-10 Surface current distribution for the antenna geometry as shown in Fig. 2-09

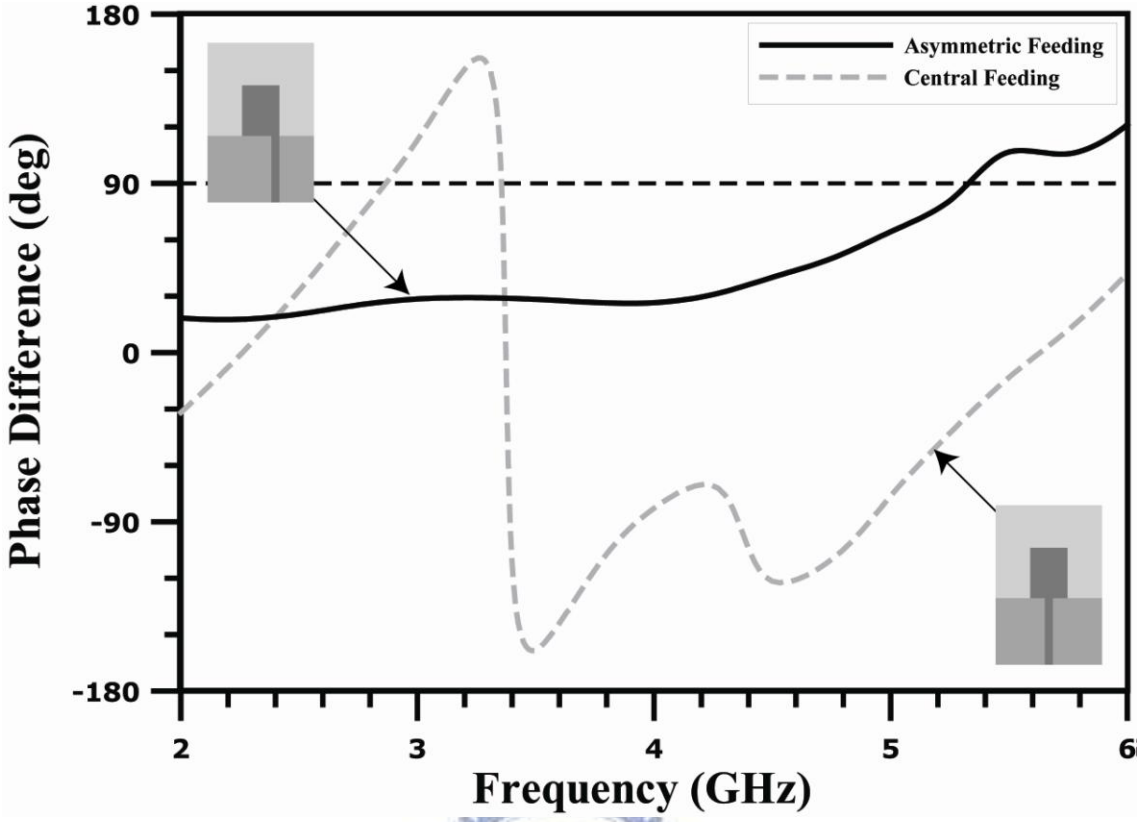

Fig. 2-11 Comparison of phase differences between asymmetric feeding and central feeding

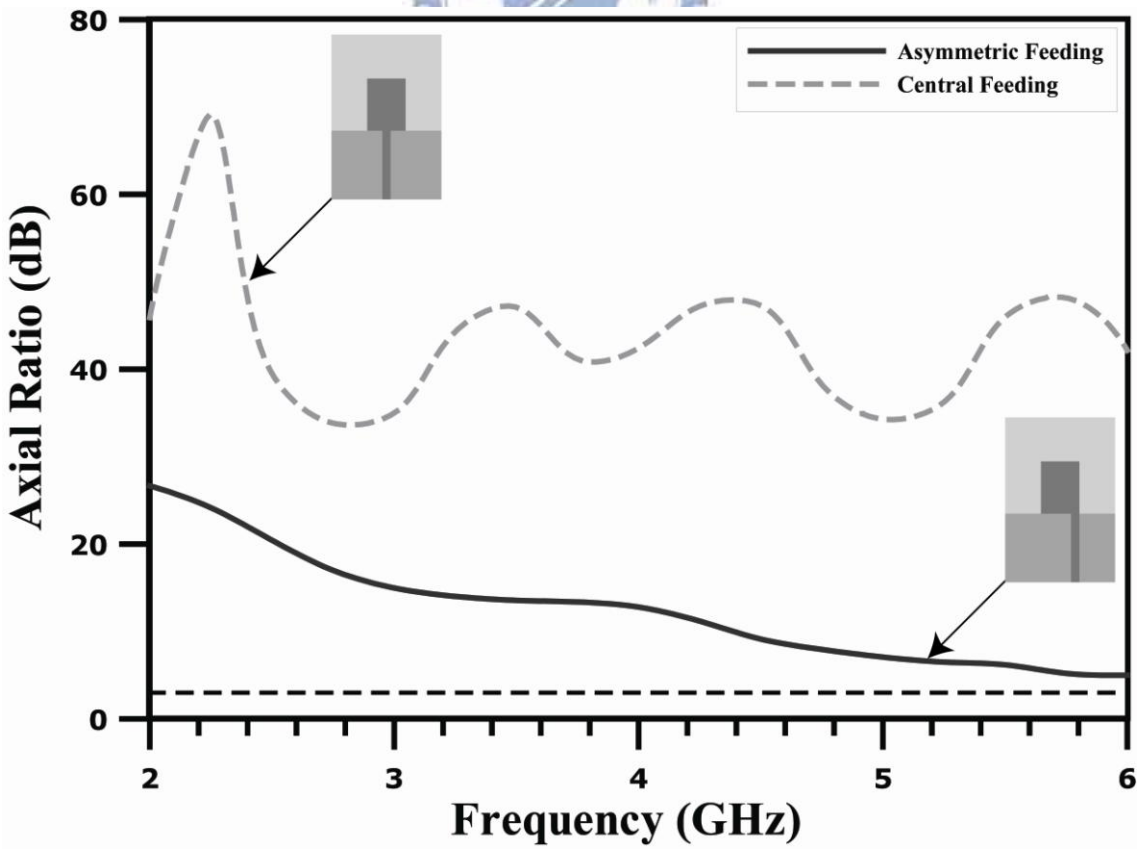

Fig. 2-12 Comparison of axial ratio between asymmetric feeding and central feeding

C. *Improving of Phase Difference over Wide Bandwidth*

Even though the impedance bandwidth with wideband characteristic can be achieved through shaping the parasitic element adequately, it is still narrowband on circularly polarized sense. The phase difference appears below 90 degrees about the geometry before ground plane truncating. This situation could be improving by truncating a ground slot with the size about $SL2 \times SW2$ under the radiator. Fig. 2-13 illustrates the geometry of truncated place. Pay attention to the curve of ***W/O Ground Slot*** in Fig. 2-14 and the intersection to 90 degrees can be obtained. It possesses the great fall beside the intersection point, and hence, the narrowband circular polarization further generated. On the other hand, the curve of ***With Ground Slot*** in Fig. 2-14 presents the tendency nearby 90 degrees. Corresponding to the axial ration as shown in Fig. 2-15, it can obtain easily that axial ration bandwidth was broadened after truncating the ground plane.

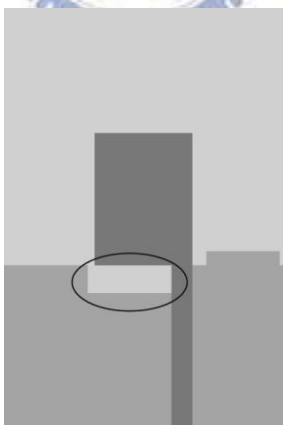

Fig. 2-13 Truncate a slot in the ground plane of the antenna

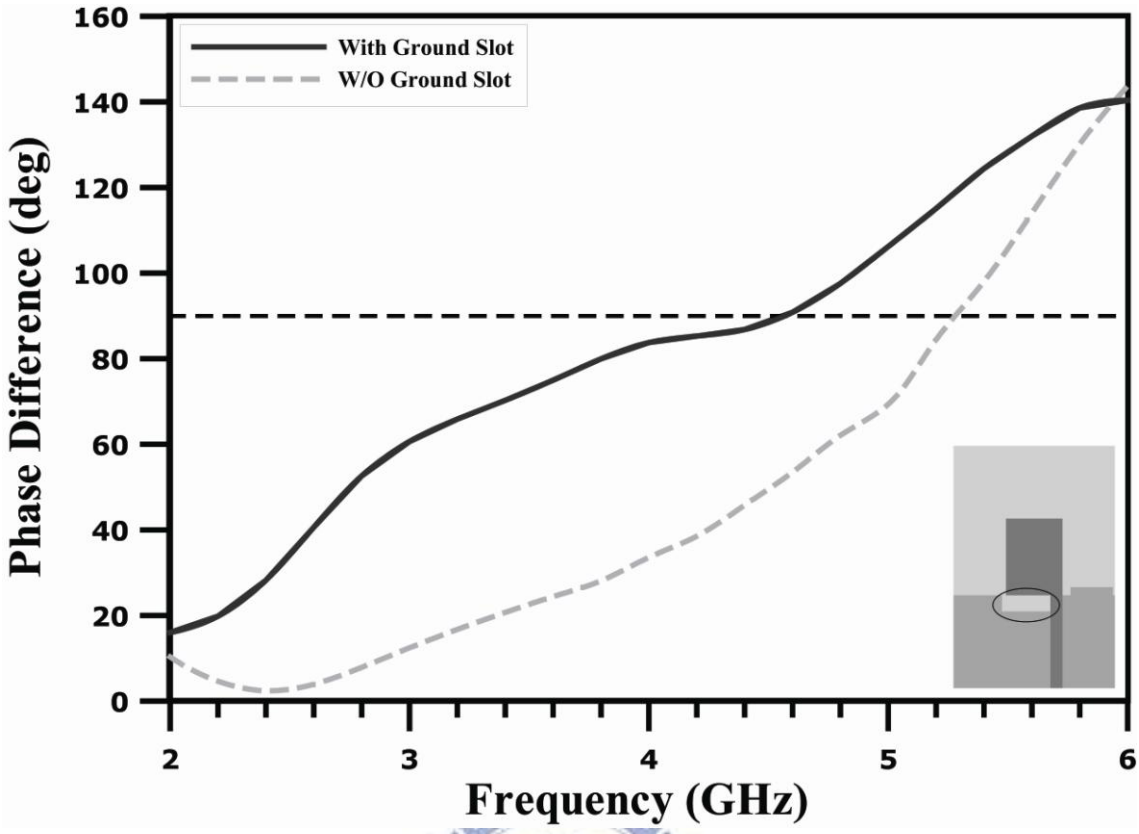

Fig. 2-14 Comparison of phase differences related to ground plane truncating

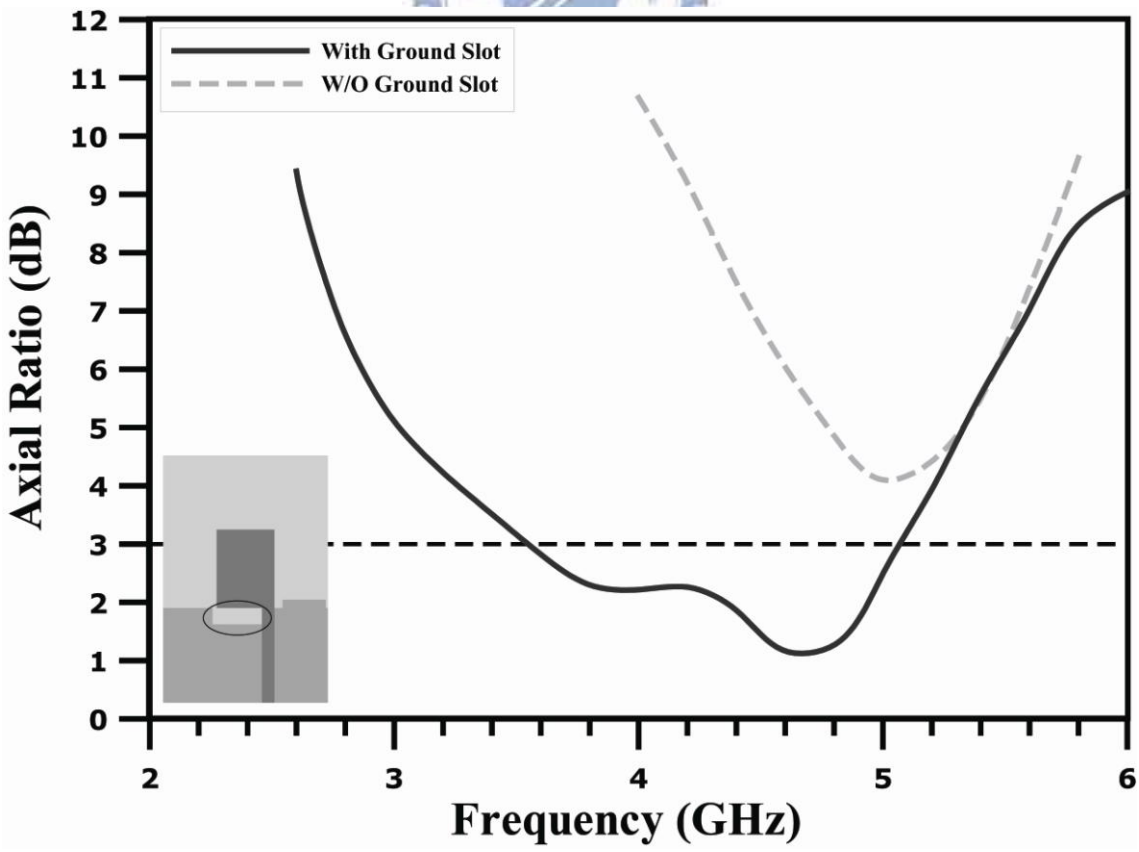

Fig. 2-15 Comparison of axial ratio related to ground plane truncating

D.*Adequate Matching to Vicinity of 90-Degrees*

After pulling up the phase difference, impedance matching maybe inferior to the origin design of wideband purpose and adequate matching need to enforce so as to hold out the performance. It can be obtained the curve of phase difference further adjoins 90 degrees line through embedding both slits at radiator and parasitic element on the ground plane in Fig. 2-16. Pay attention to Fig. 2-17, it can be obtained directly that the phase difference approach 90 degrees no matter at 4.4 GHz or 5.6 GHz after embedding these slits. Matching to vicinity of 90 degrees can be achieved via adequate assigning the slits both at radiator and ground plane. A wideband axial ratio bandwidth can be obtained in Fig. 2-18.

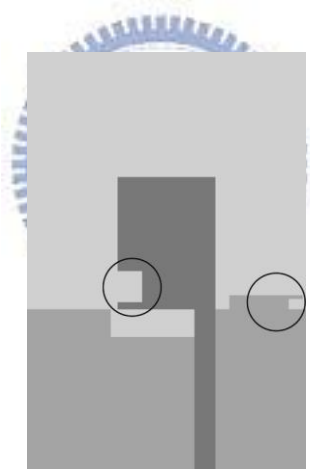

Fig. 2-16 Embed slits both in radiator and ground plane of the antenna

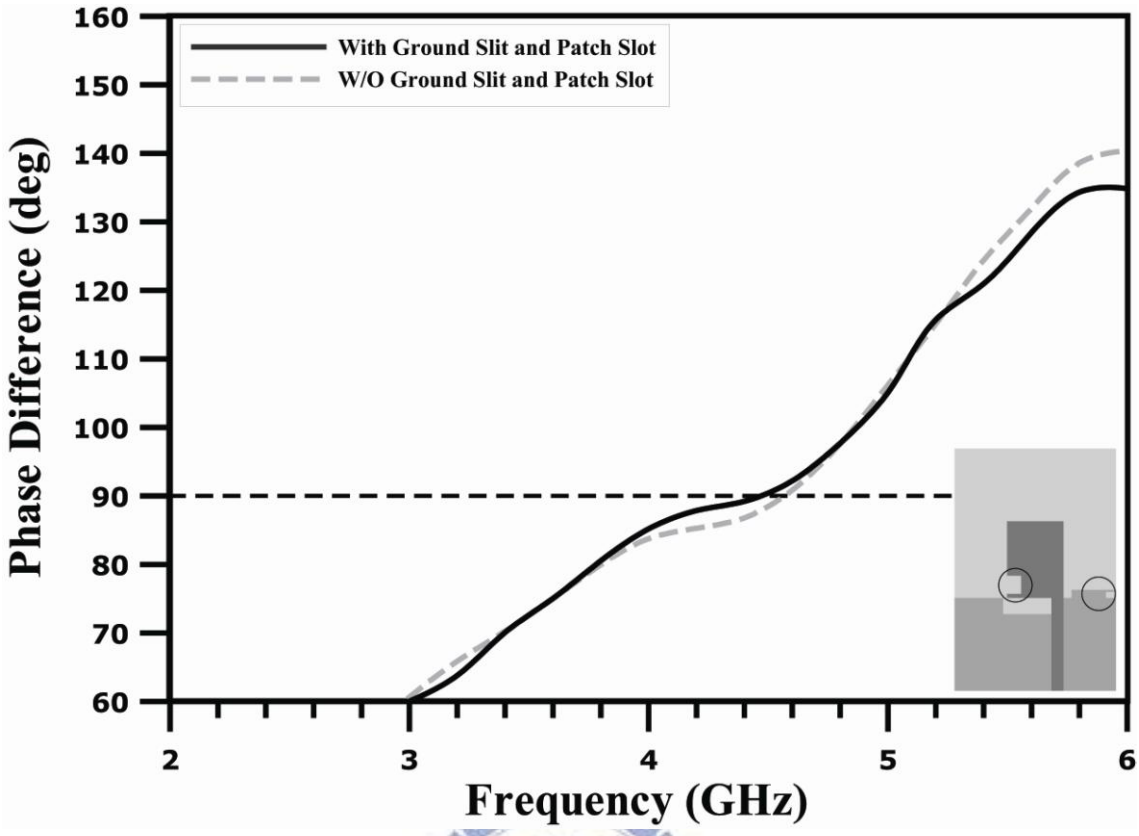

Fig. 2-17 Comparison of phase differences related to slits embedding

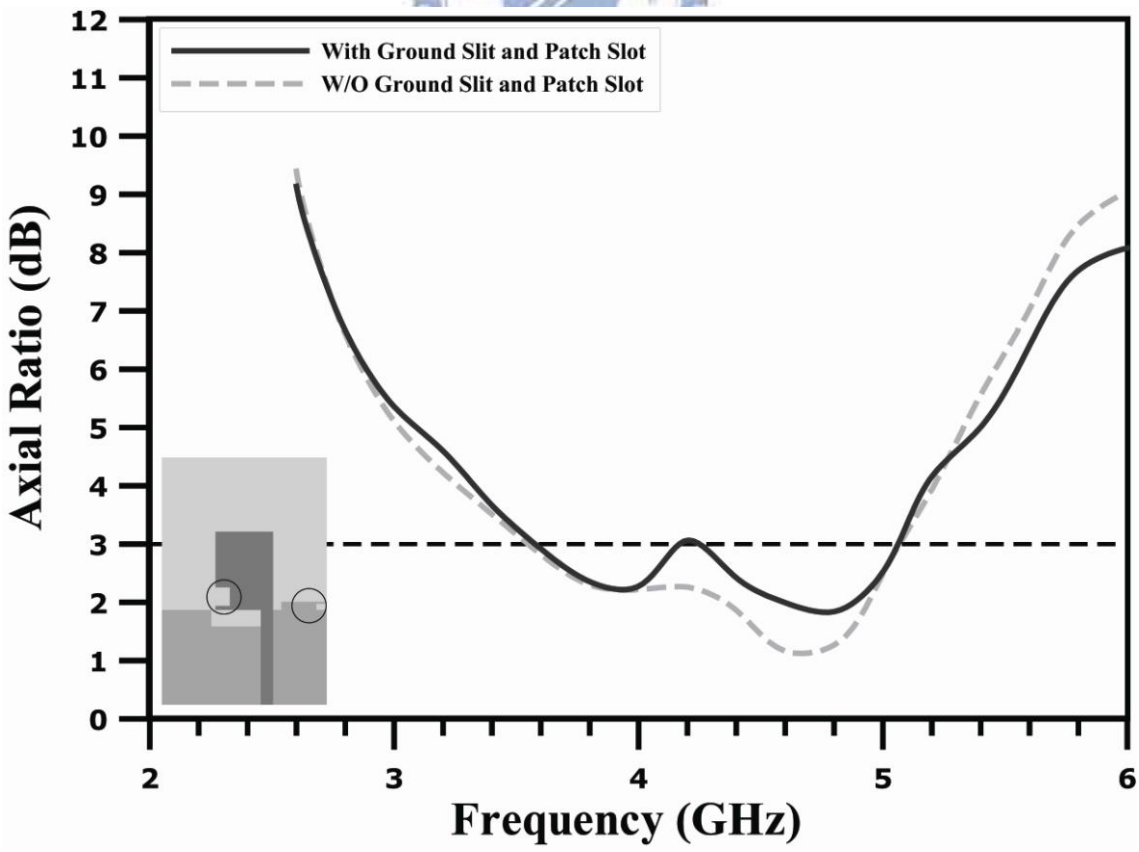

Fig. 2-18 Comparison of axial ratio related to slits embedding

2.2.3 Parametric Study

Some parameters influence the variation of phase difference in distinct bands, the optimized circularly polarization can be achieve according to these analysis. An example with *L1*=23mm, *W1*=14mm, *L2*=19mm, *W2*=14mm, *SL1*=4.5mm, *SW1*=3.5mm, *DL*=2mm, *DW*=9.5mm, *SL2*=4mm, *SW2*=15mm, *SL3*=1.5mm and *SW3*=2.5mm is selected to show the design of the proposed circularly polarized monopole antenna. It is found that the input impedance is much related to *SW1*, *SL2*, *SW2* and *DL* and the circular polarization axial ratio is mainly controlled by the *SL1*, *SW1*, *SL2* and *DL*.

A.*Parametric Study of Reflection Coefficient*

At first, it varies the position of the mode at vicinity of 5.5 GHz and the mode moves to lower band as *SW1* increased as shown in Fig. 2-19. It not only controls the motion of the mode of 5.5 GHz but also relates to matching of the mode of 4.0 GHz.

The parameter of *SL2* widely affects all of the modes bounded 2 GHz to 8 GHz as shown in Fig. 2-20 and it will be composed with the result of surface current distribution in Fig. 2-32.

The parameter of *SW2* influences the matching of each mode, this exists a trade-off in design since it controls the matching of each mode in unequal sense as shown in Fig. 2-21.

The last parameter *DL* affects the matching of 2.2 GHz, 4.0 GHz and 7.0 GHz directly and controls the motion of 5.5 GHz as shown in Fig. 2-22.

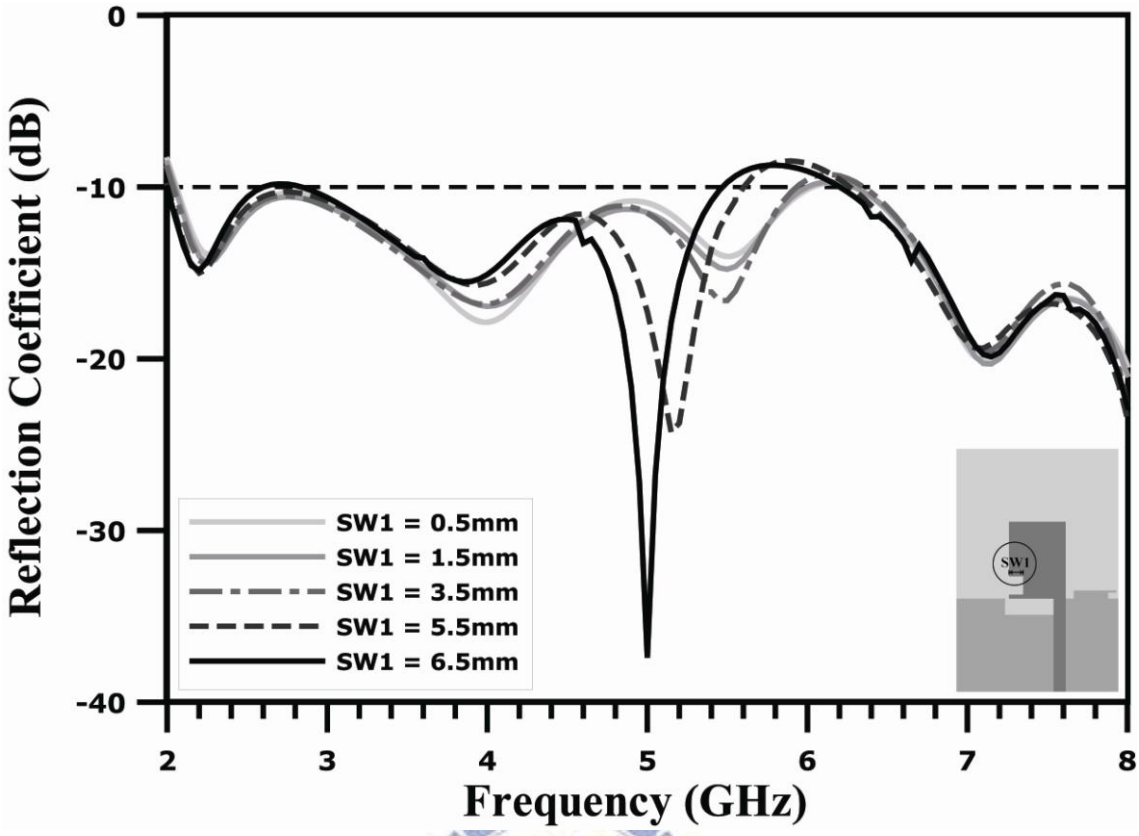

Fig. 2-19 Parametric study of *SW1* for reflection coefficient

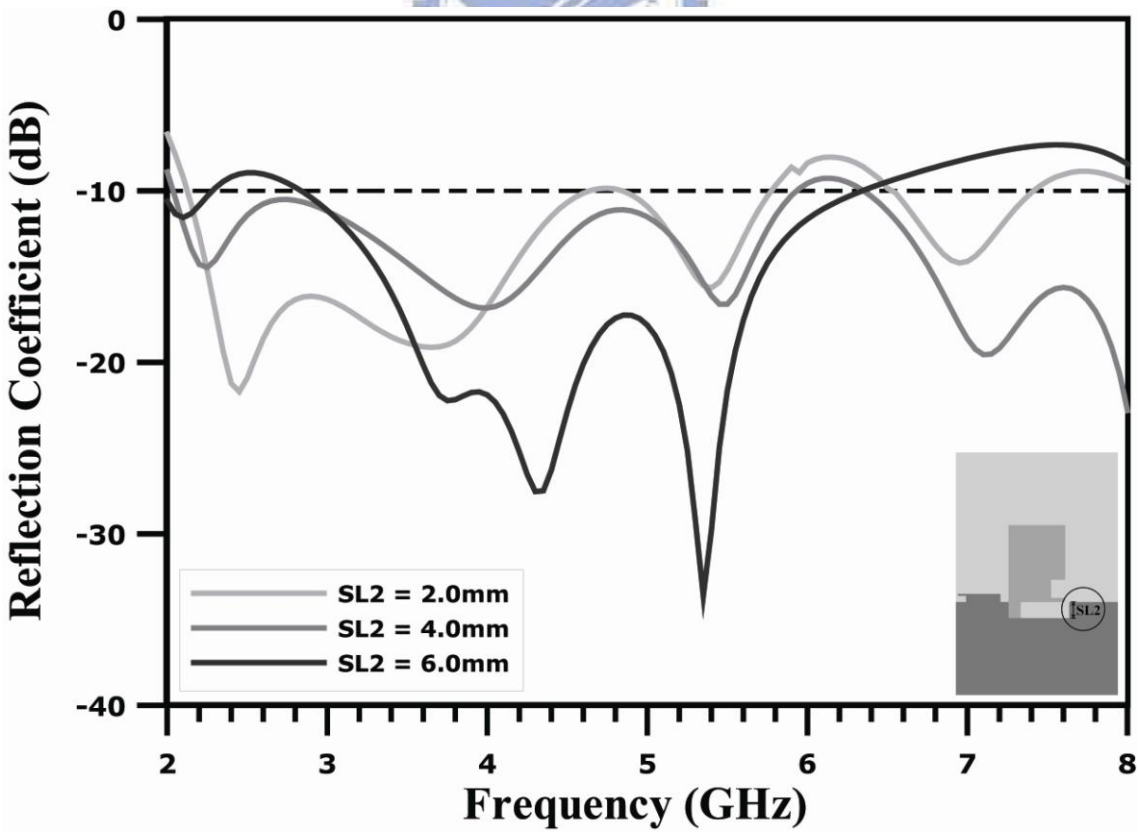

Fig. 2-20 Parametric study of *SL2* for reflection coefficient

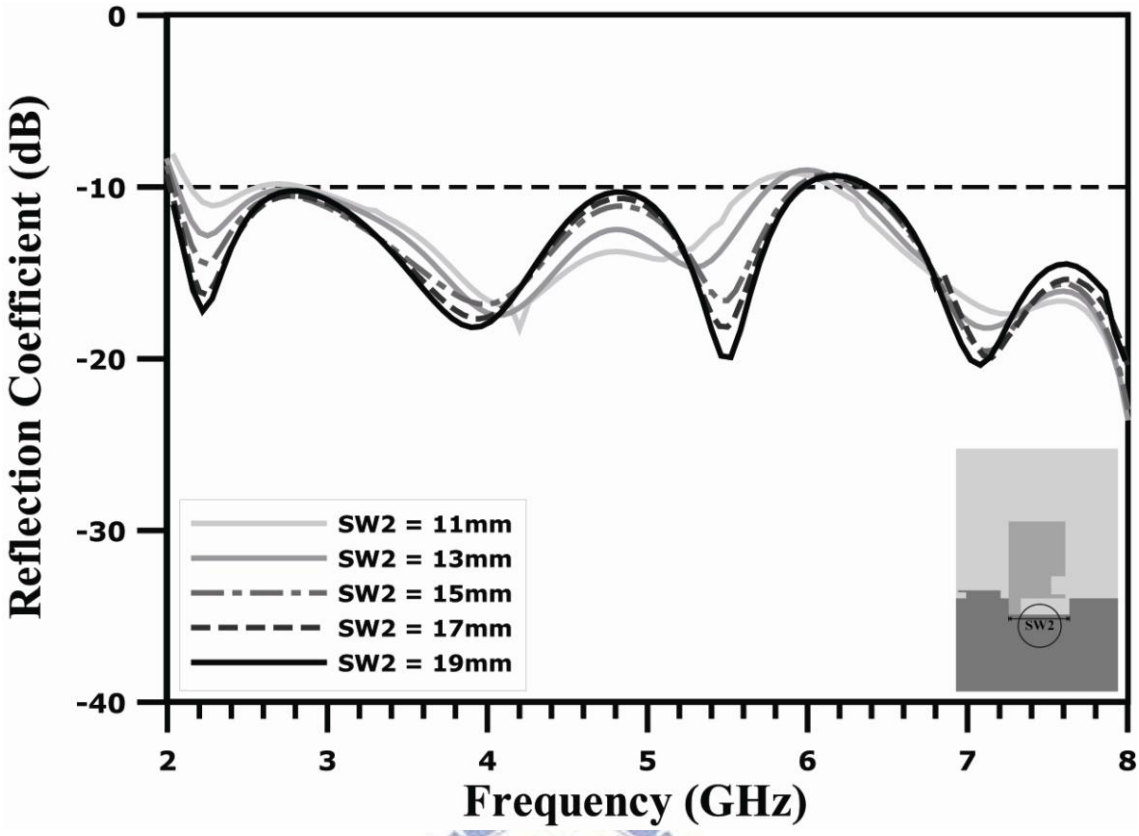

Fig. 2-21 Parametric study of *SW2* for reflection coefficient

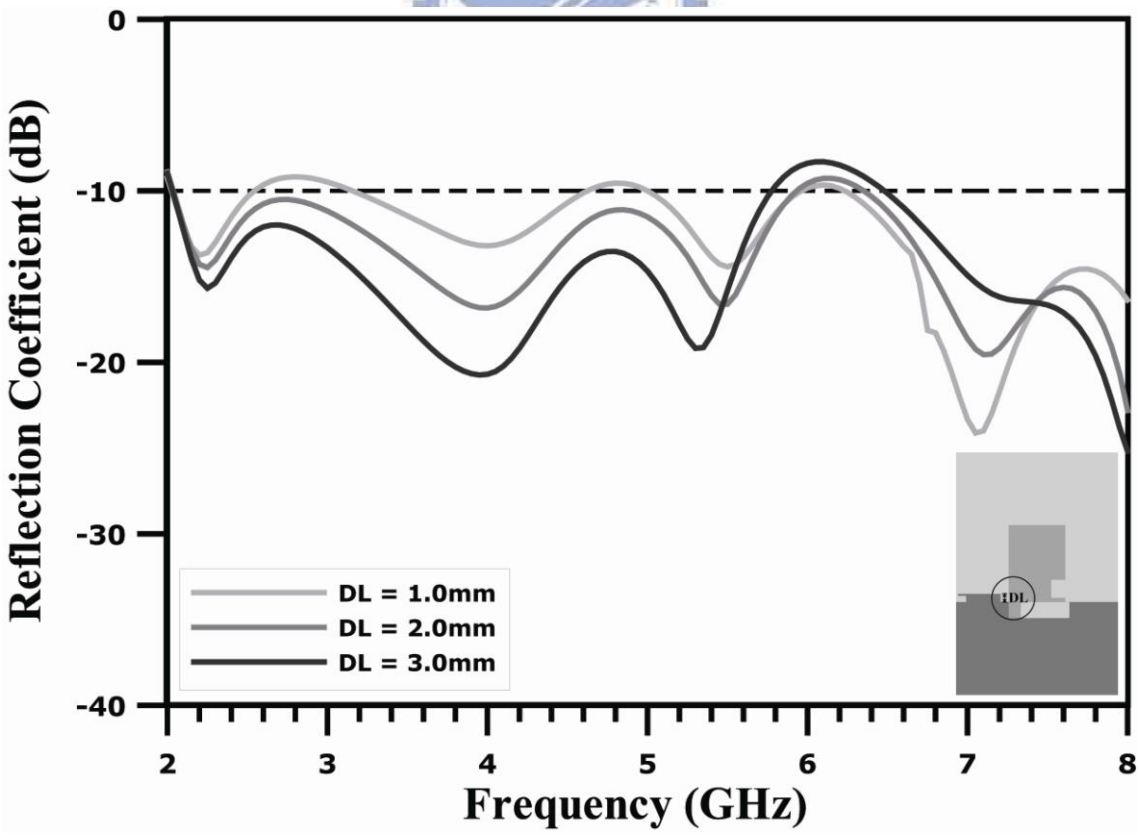

Fig. 2-22 Parametric study of *DL* for reflection coefficient

B. *Parametric Study of Phase and Axial Ratio*

The effect of varying the length of *SL1* is presented in Fig. 2-23 and it can be obtained the degradation of phase at the vicinity of 6 GHz as *SL1* decrease. While changing the view to axial ratio as shown in Fig. 2-24, a great deal of degradation at the vicinity of 6 GHz as *SL1* decrease was illustrated apparently. The good performance would be reached at higher band via selecting the length of *SL1* adequately.

The effect of varying the length of *SW1* is presented in Fig. 2-25 and it can be obtained the phase varied in differential sense at 4.5 GHz and 5.6 GHz as *SW1* was changed separately. Regarding 5.1 GHz as the division, the axial ratio of lower band will broaden as *SW1* decrease as shown in Fig. 2-26.

The effect of varying the length of *SL2* is presented in Fig. 2-27 and it can be obtained obviously the phase upgrade over broad bandwidth as *SL2* increase. It gets the agreement with the ground truncating mentioned before to meet wider bandwidth for circularly polarized operation. Turning the view to Fig. 2-28, the axial ratio bandwidth becomes wider as *SL2* set to 4mm.

The effect of varying the length of *DL* is presented in Fig. 2-29 and it can be obtained almost linear variation below 4 GHz as *DL* varies. Turning the view to Fig. 2-30, the axial ratio bandwidth moves to lower band as *DL* increase.

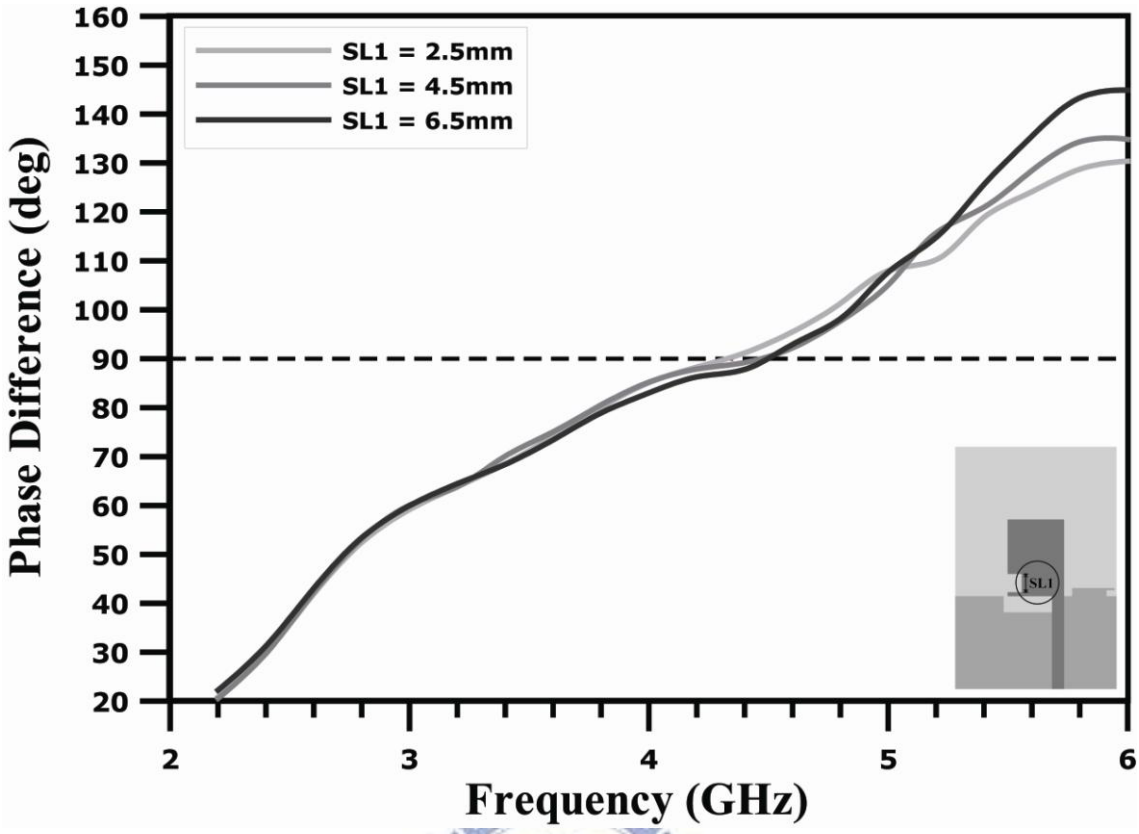

Fig. 2-23 Parametric study of *SL1* for phase difference

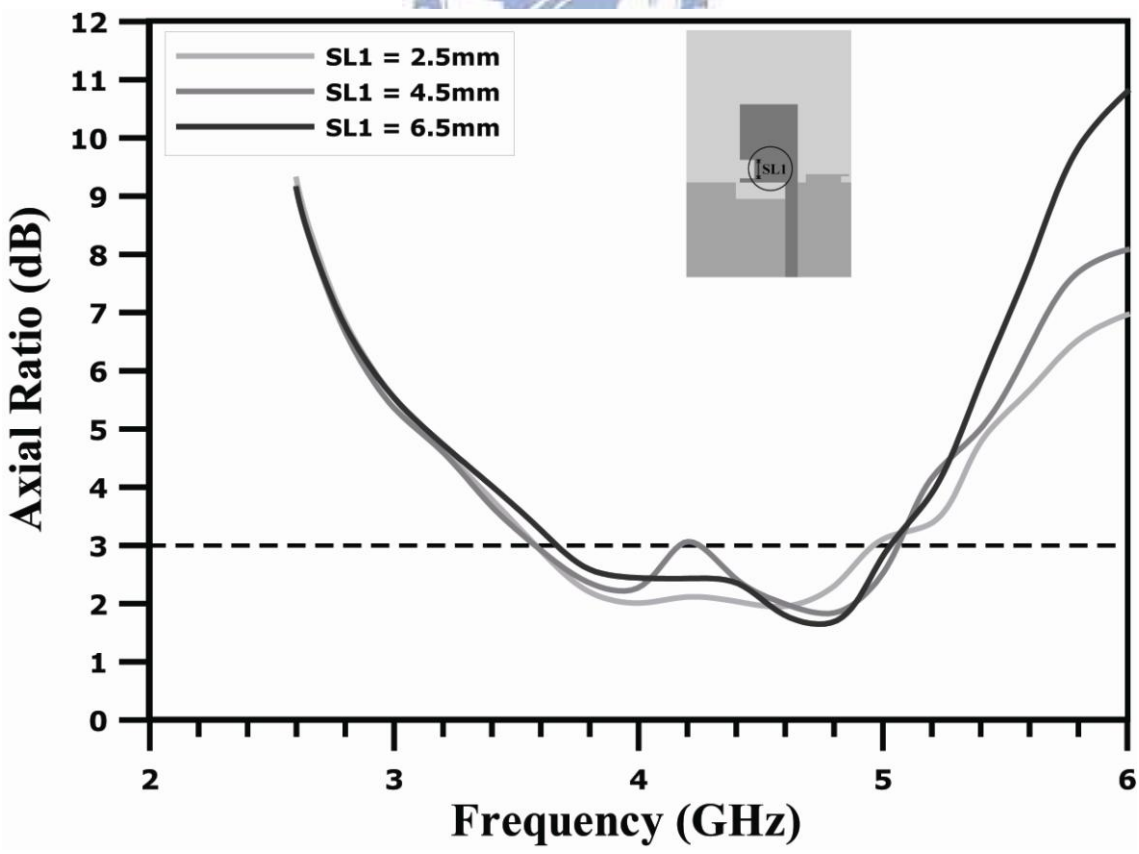

Fig. 2-24 Parametric study of *SL1* for axial ratio

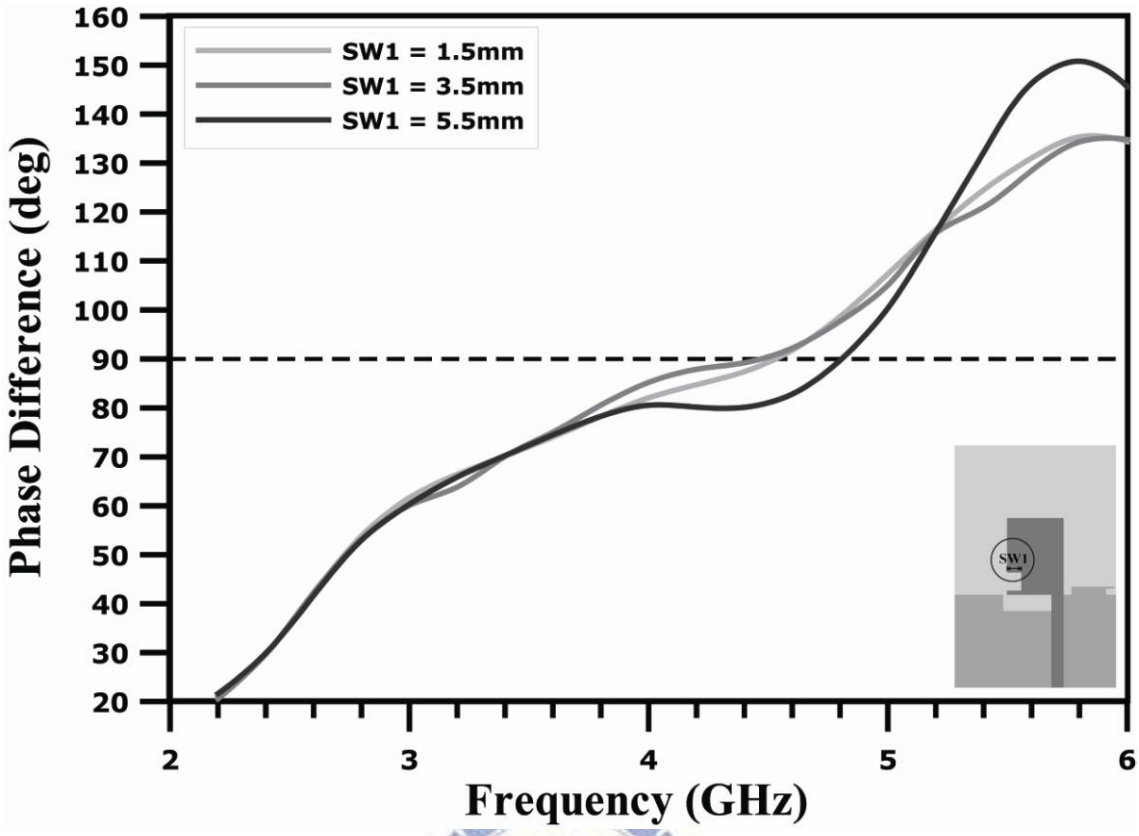

Fig. 2-25 Parametric study of *SW1* for phase difference

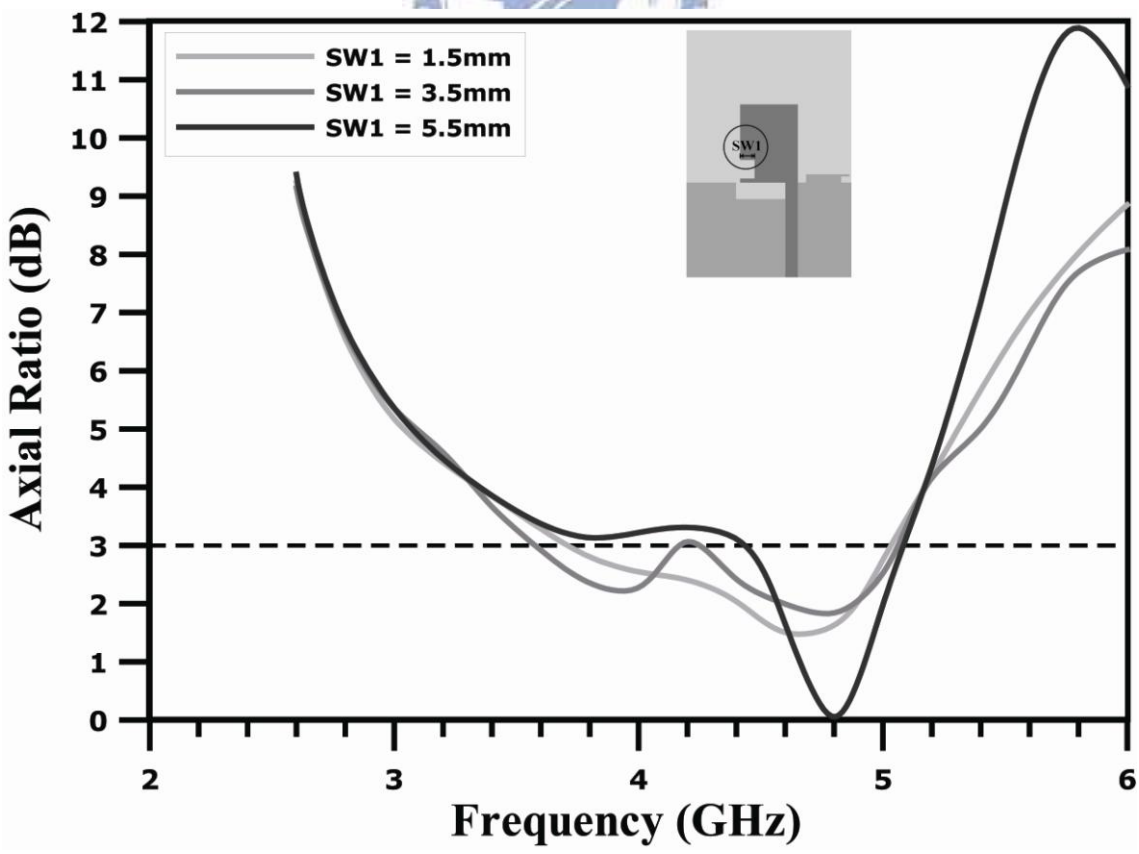

Fig. 2-26 Parametric study of *SW1* for axial ratio

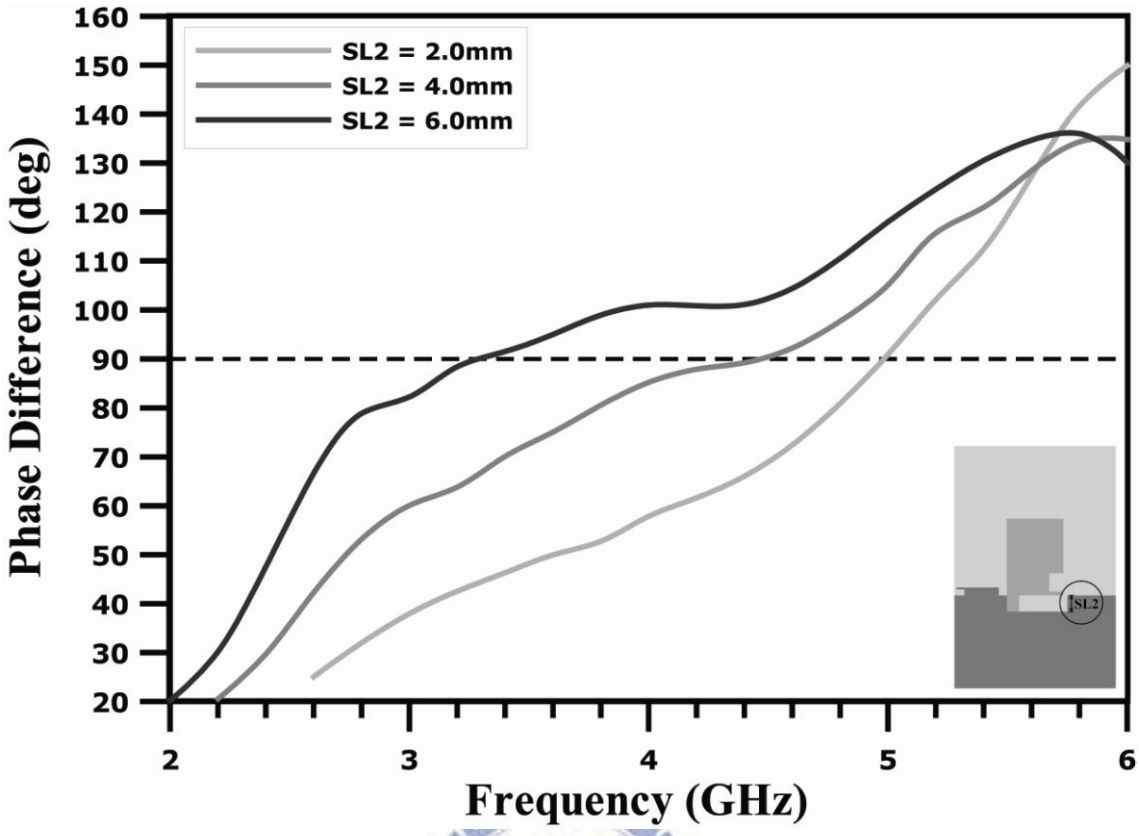

Fig. 2-27 Parametric study of *SL2* for phase difference

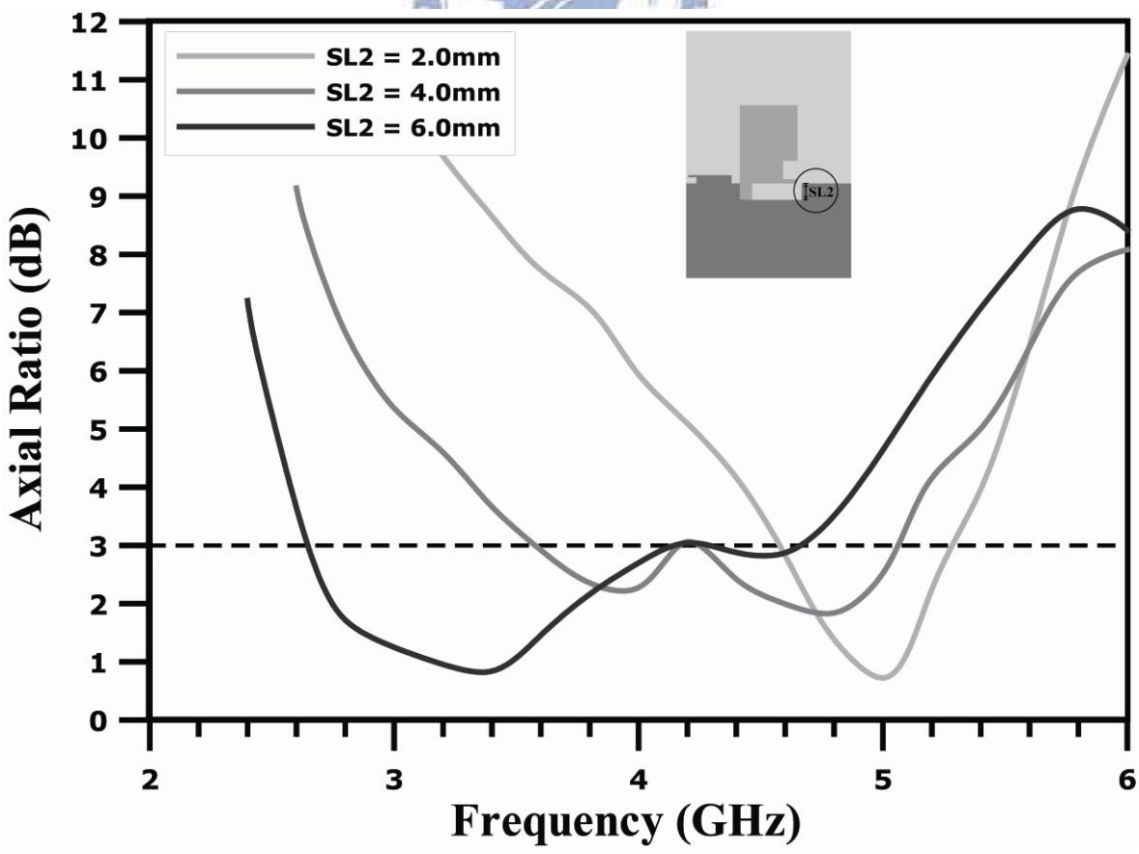

Fig. 2-28 Parametric study of *SL2* for axial ratio

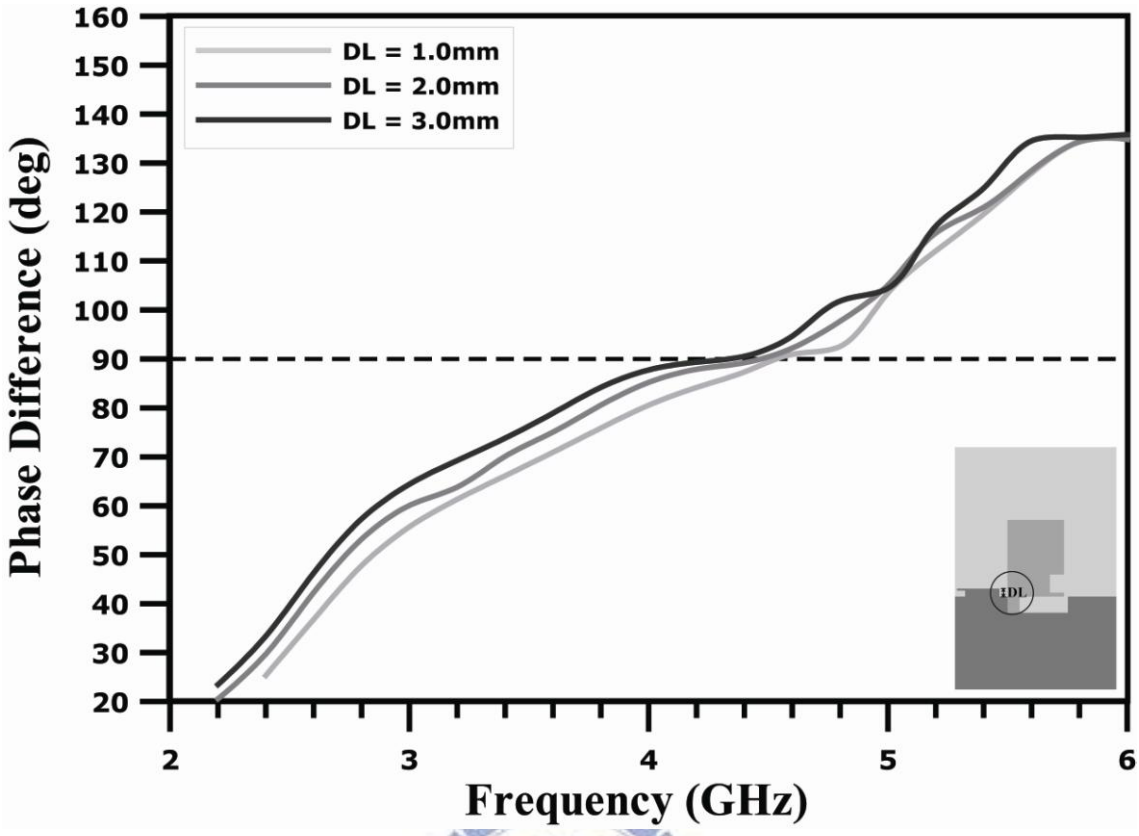

Fig. 2-29 Parametric study of *DL* for phase difference

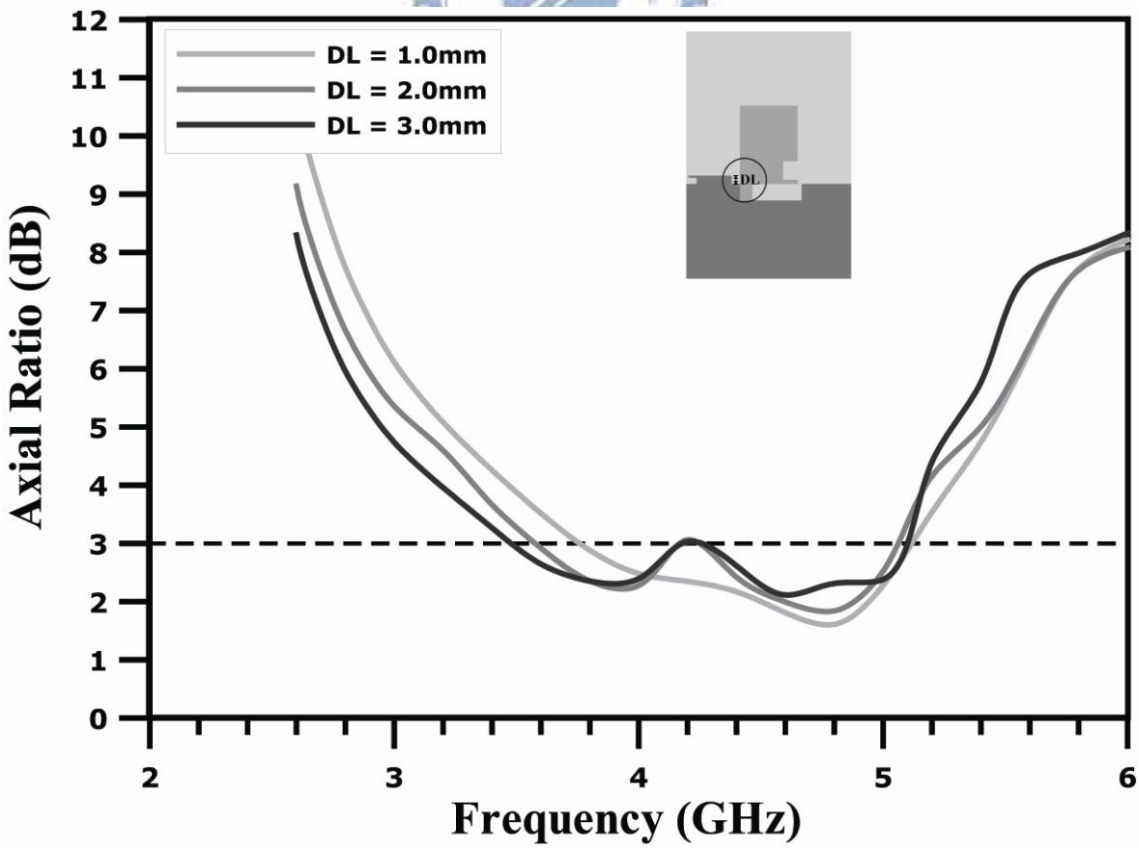

Fig. 2-30 Parametric study of *DL* for axial ratio

2.2.4 Results of Simulation and Measurement

The characteristics of these proposed monopole antennas were calculated by using Ansoft High Frequency Structure Simulator (HFSS) [28] software and measured by using HP 8722C network analyzer.

A.*Reflection Coefficient and Surface Current Distribution*

In Fig. 2-31, the reflection coefficient of simulation and measurement was illustrated good agreement. There are five modes can be obtained via simulation and they are 2.25 GHz, 4.00 GHz, 5.49 GHz, 7.13 GHz and 8.16 GHz separately. According to these five modes, the surface current distribution will be simulated and discussed in Fig. 2-32. The impedance bandwidth can be obtained from 2.2 GHz to 8.8 GHz, namely, 120% respect to 5.5 GHz.

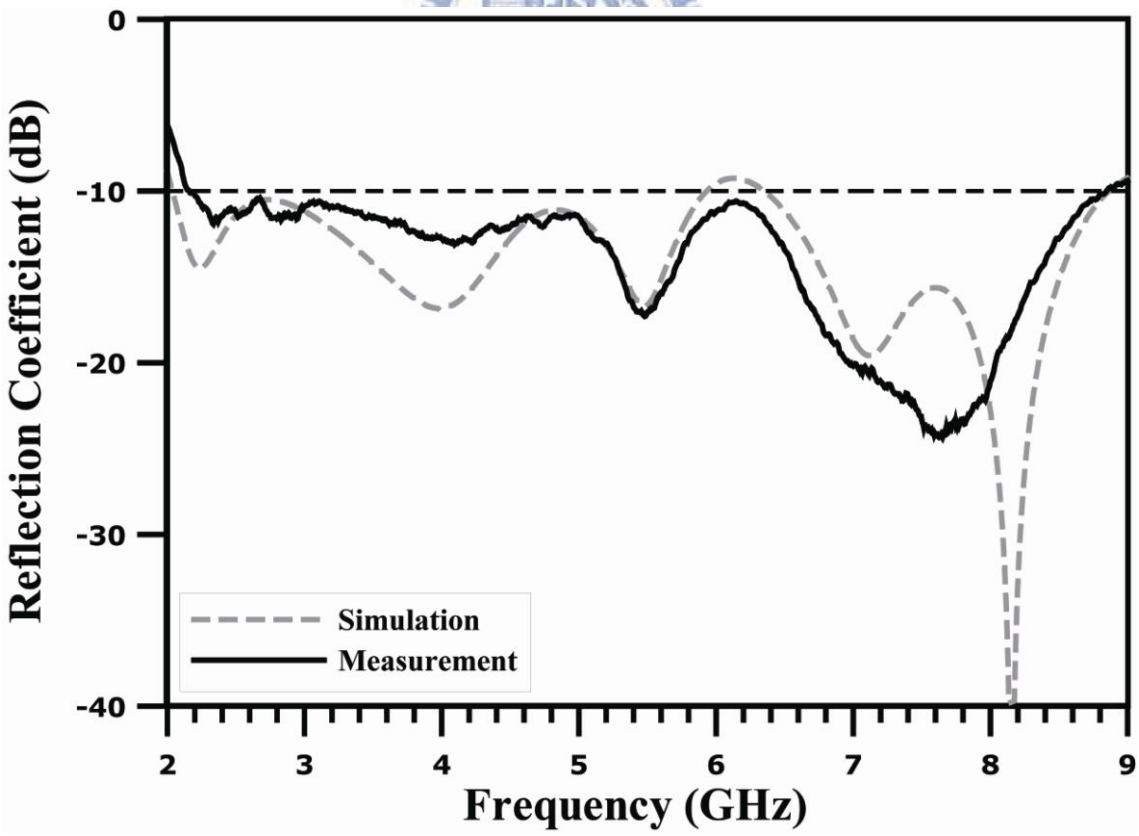

Fig. 2-31 Comparison of the reflection coefficient of proposed antenna between simulation and measurement

In Fig. 2-32, the five modes are illustrated separately and they can refer to the parametric studies mentioned before for coincidences. Meanwhile, it can be found that the current distribution at perturbation on the ground plane almost masses over the five resonant modes, and hence the perturbation can be recognized as a wideband factor. Relatively, even though the *SL2* affects the phase difference significantly, it should be chosen carefully since the current distribution arises unevenness surrounding this parameter.

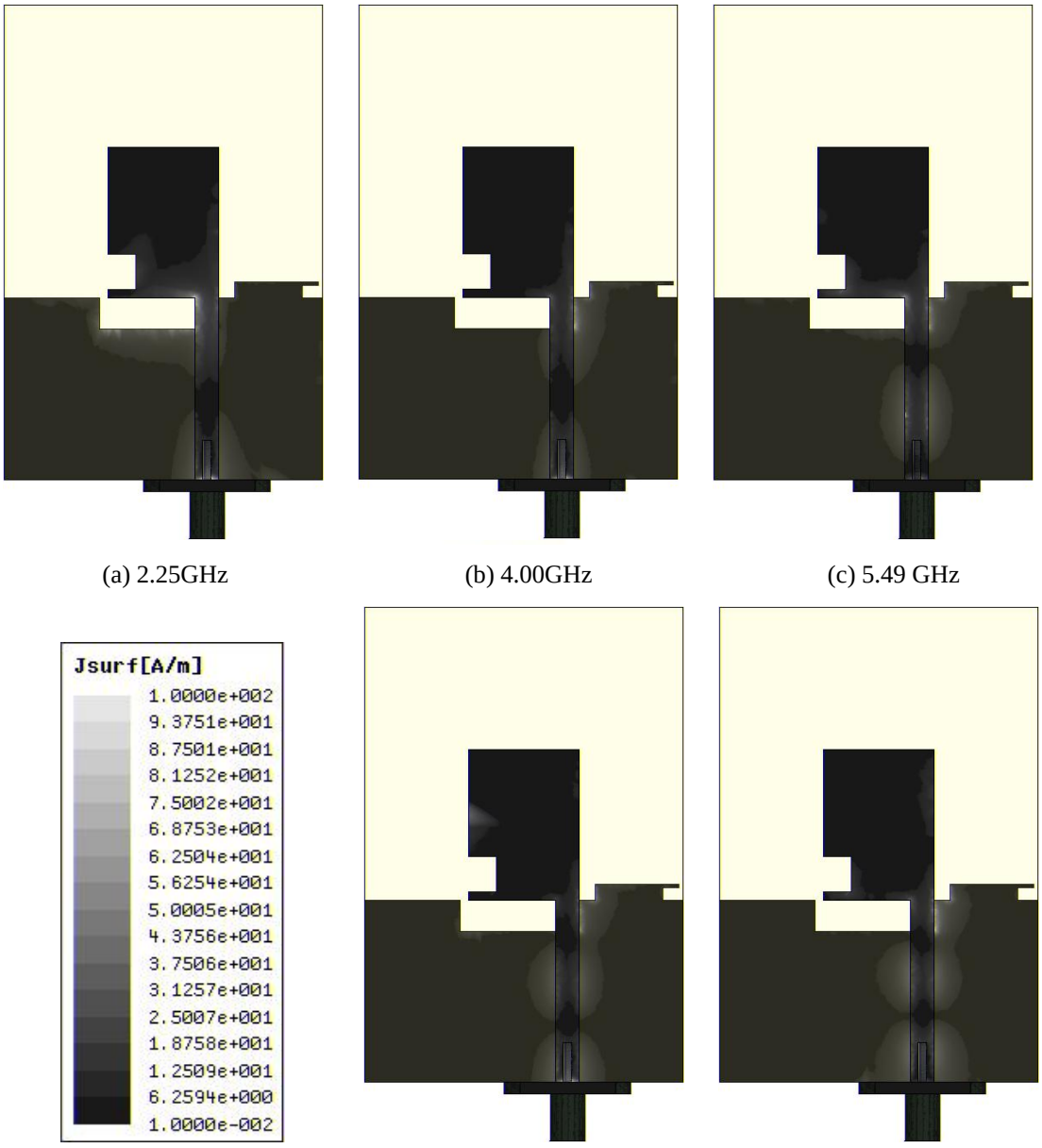

(a) 2.25GHz (b) 4.00GHz (c) 5.49 GHz

(d) 7.13 GHz (e) 8.16 GHz

Fig. 2-32 Surface current distributions corresponding to resonant modes.

B.*Axial Ratio and Far-field Behaviors*

The comparison of the phase and axial ratio for simulation and measurement would be considered in Fig. 2-33 and there exist an agreement between them. It can be obtained the axial ratio bandwidth was stated 3.2 GHz to 4.8 GHz namely 40% respect to 4 GHz and the center frequency of measurement possesses frequency shift about 0.4 GHz cf. simulation may be caused by the tolerance made during fabrication.

The peck gain can be obtained in Fig. 2-34 which expresses the agreement with simulated values besides 3GHz and 4GHz. The radiation efficiency was simulated in Fig. 2-35. Finally, the polarized pattern would be measured and lead to the results as shown in Fig. 2-46 to 2-48. They show that LHCP was excited at broadside direction within the axial ratio bandwidth of proposed antenna.

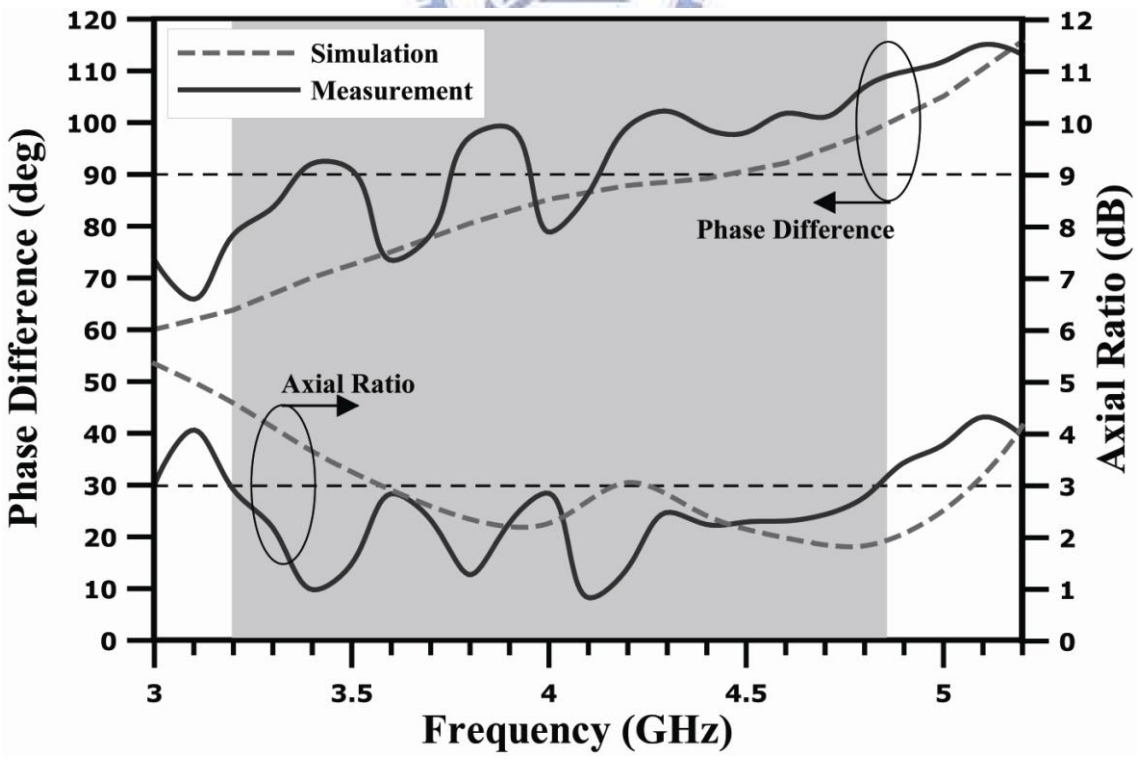

Fig. 2-33 Comparison of the phase difference and axial ratio of proposed antenna between simulation and measurement

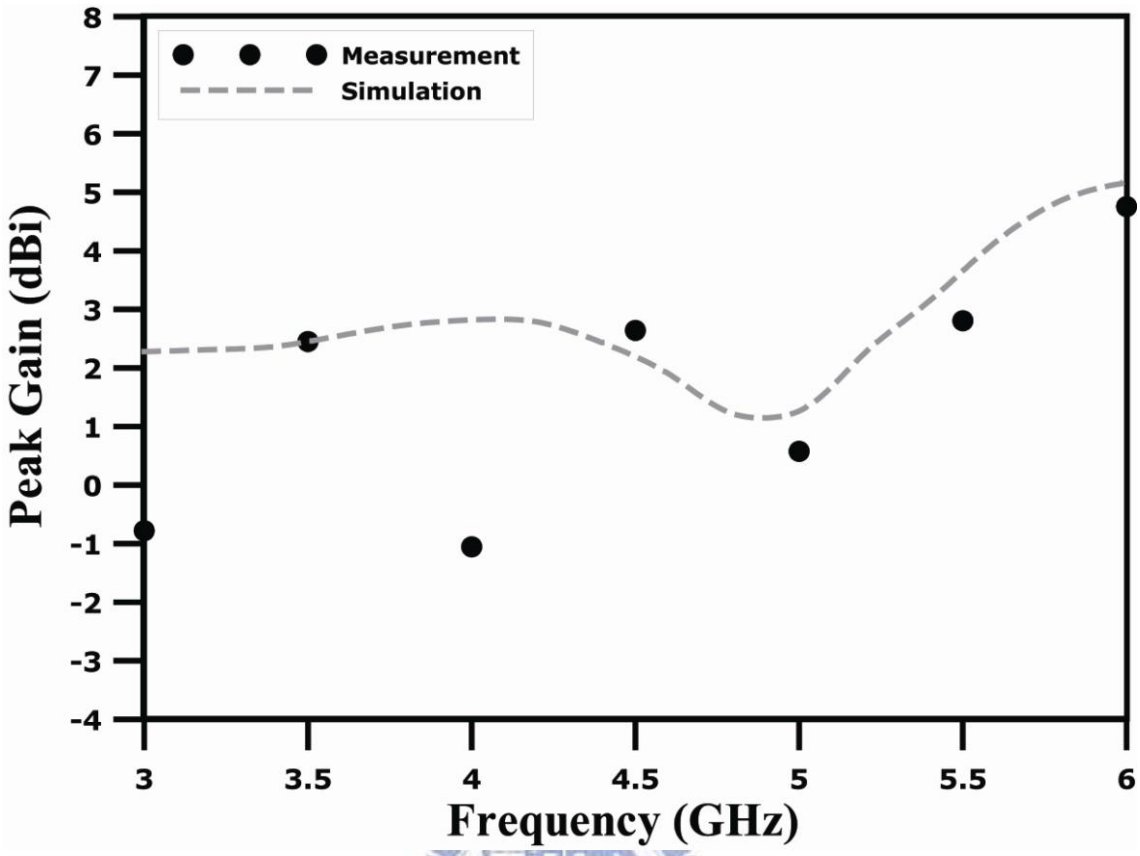

Fig. 2-34 Comparison of the peak gain of proposed antenna between simulation and measurement

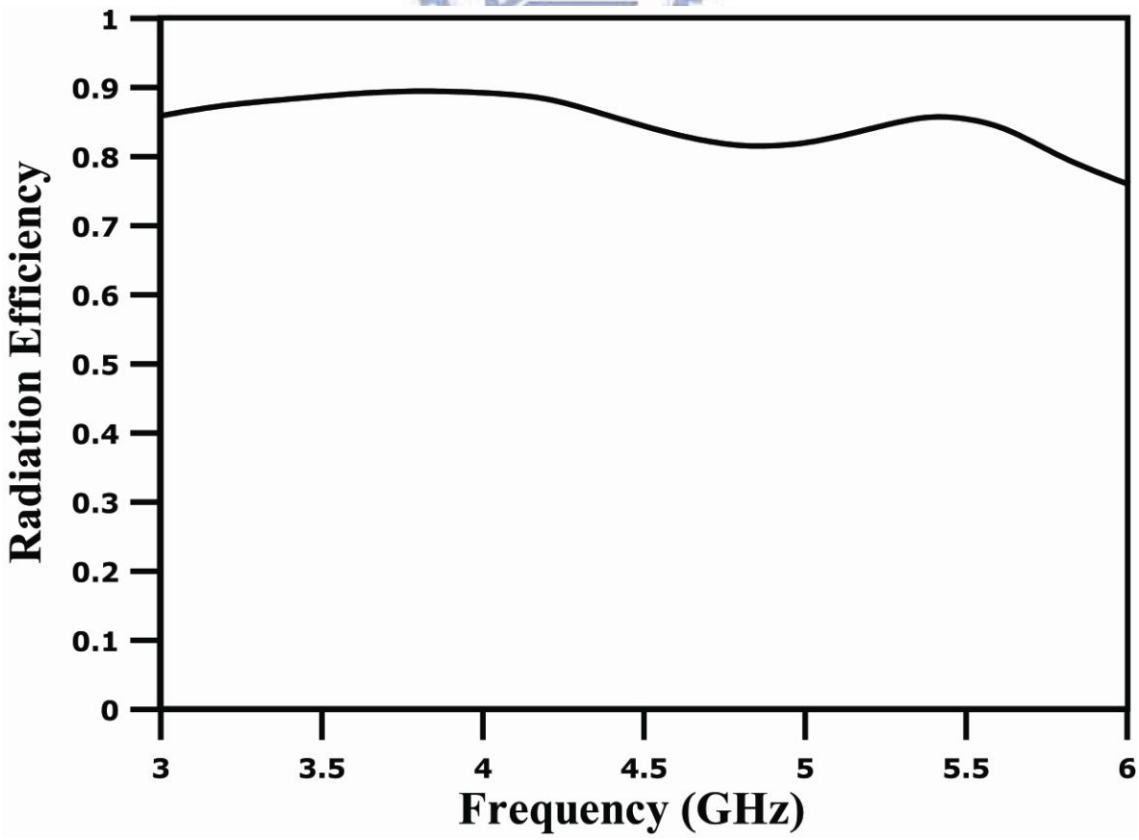

Fig. 2-35 Simulation of the radiation efficiency of proposed antenna

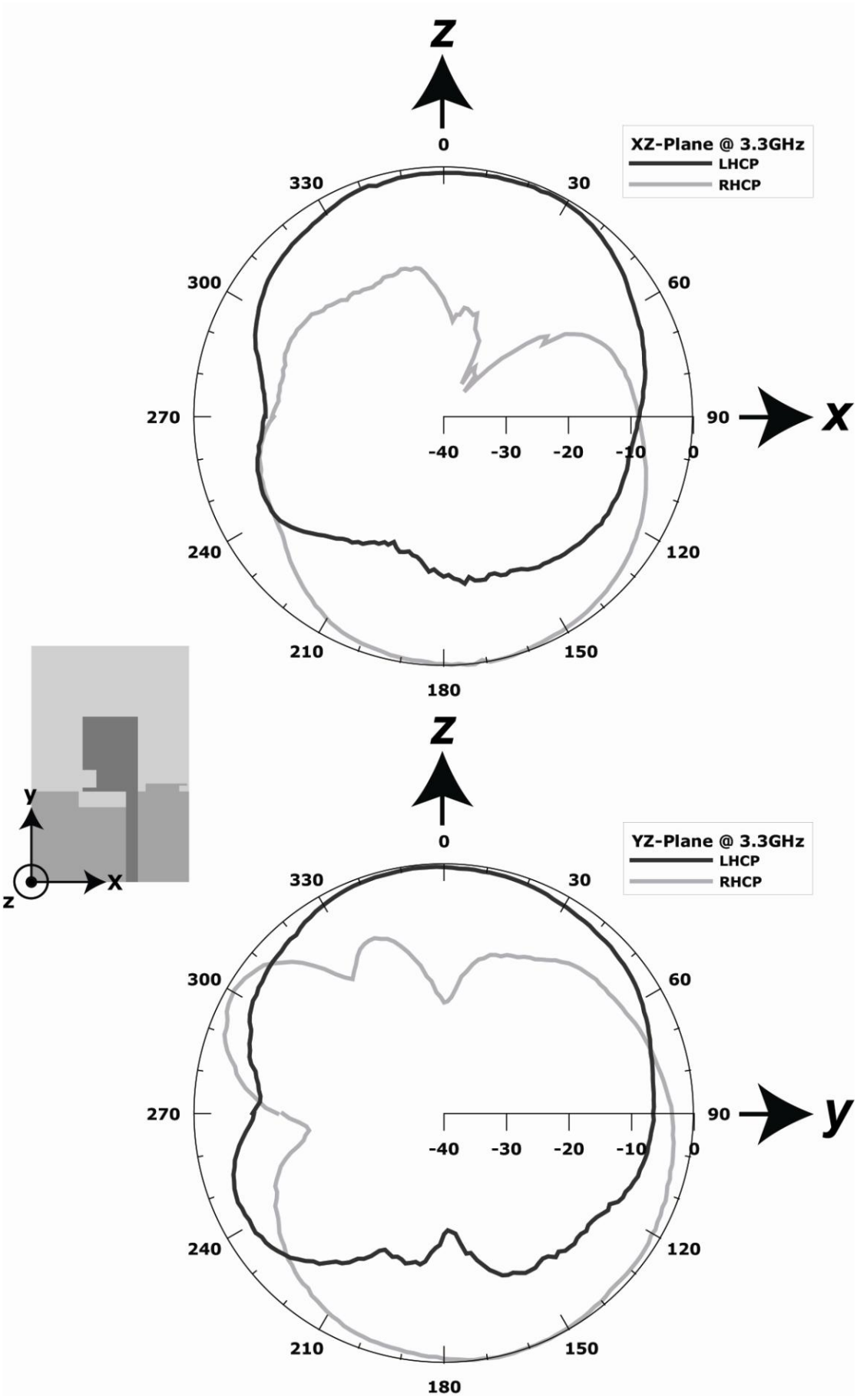

Fig. 2-36 Measurement of the polarized pattern of proposed antenna at 3.3 GHz

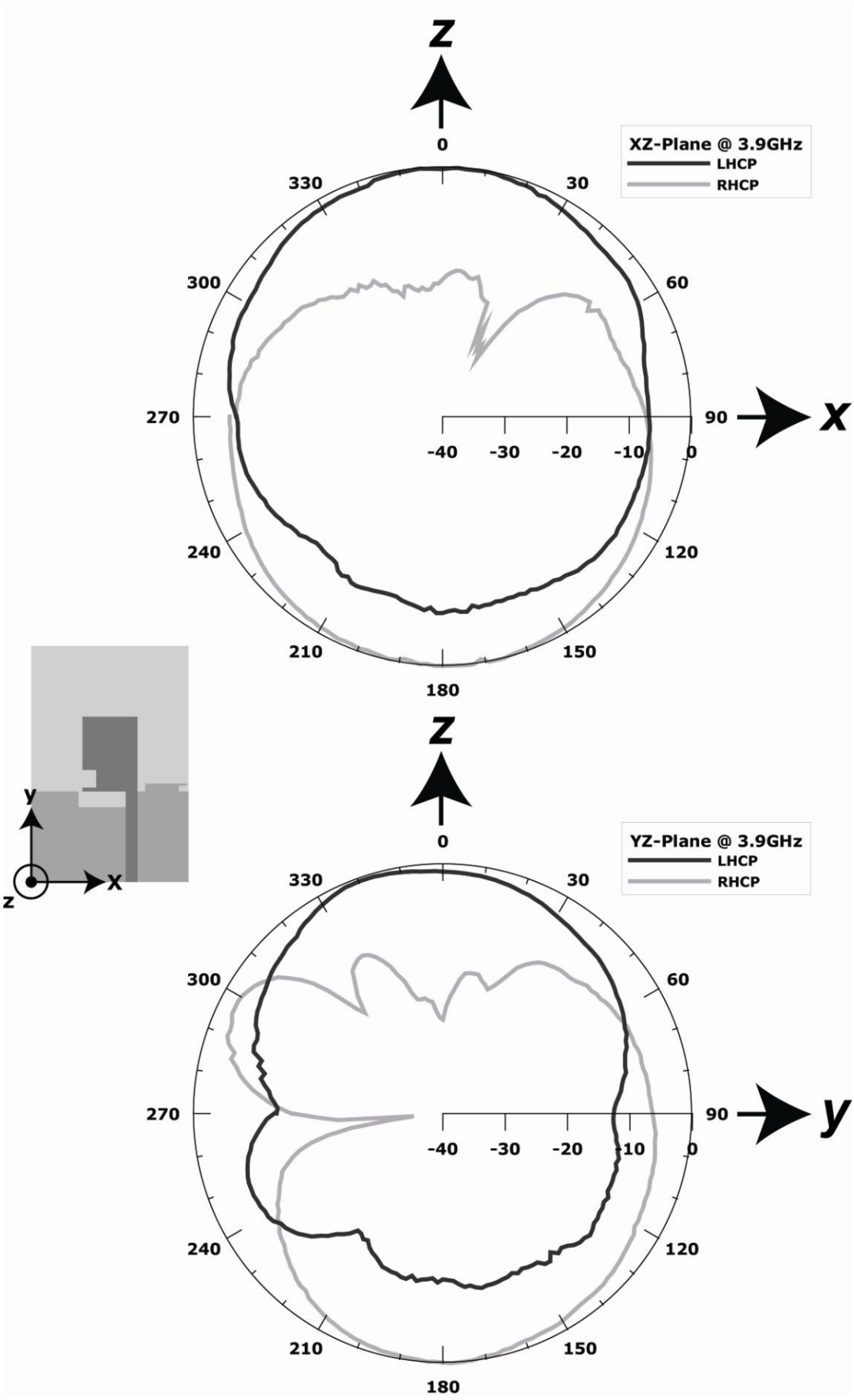

Fig. 2-37 Measurement of the polarized pattern of proposed antenna at 3.9 GHz

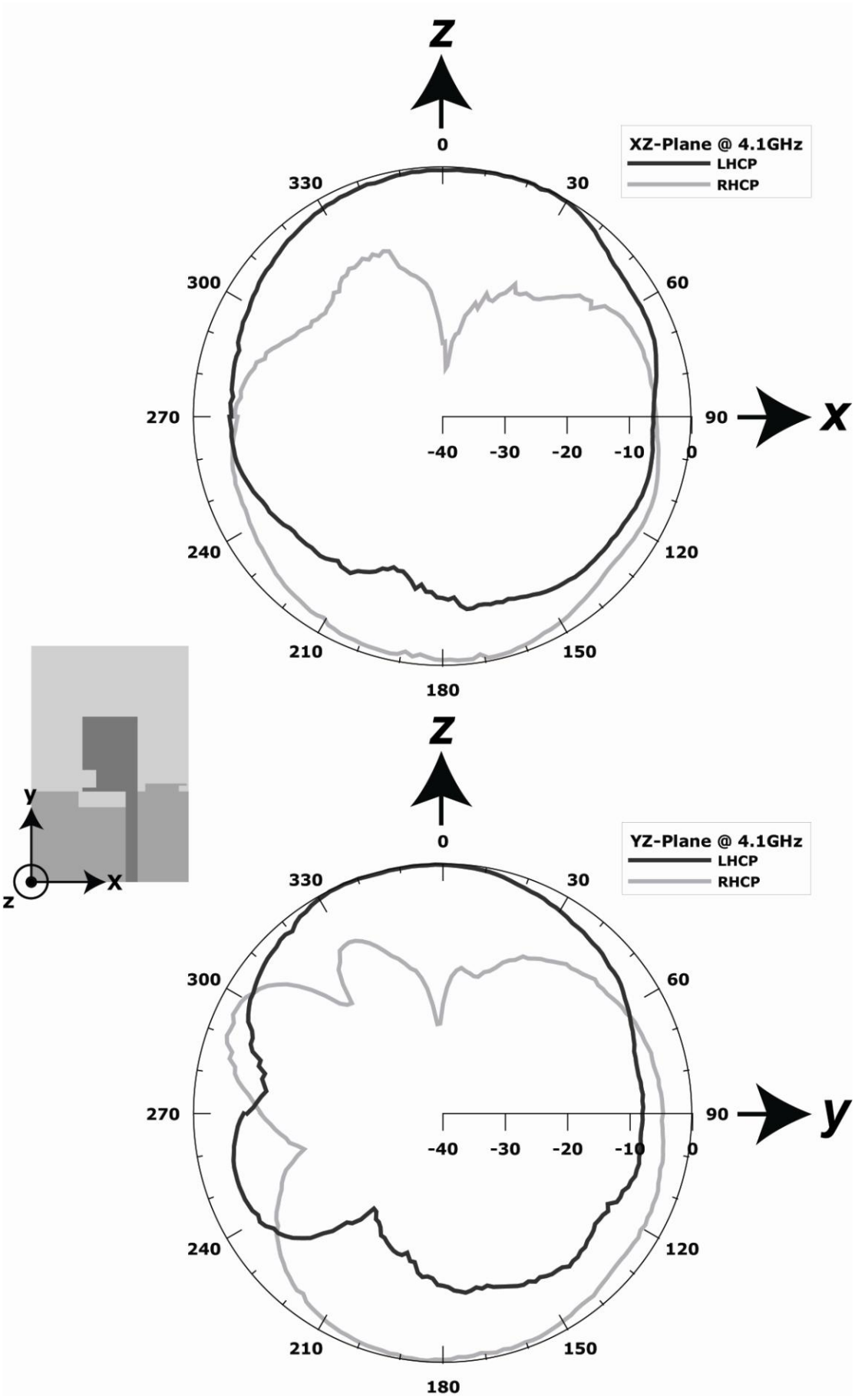

Fig. 2-38 Measurement of the polarized pattern of proposed antenna at 4.1 GHz

2.3 Conclusion

A planar monopole antenna was introduced in this chapter. It achieves the wideband characteristic through the process of truncating both ground plane and radiator of the antenna and further embedding slits both in ground plane and radiator. The proposed antenna possesses about 40% bandwidth of 3dB axial ratio at center frequency of 4GHz and excites LHCP wave at broadside direction. It would be obtained 121% bandwidth with center frequency of 5.6GHz.

CHAPTER 3

Compact Antenna Design for WLAN Purpose

3.1 Wireless LAN Technology

The application of wireless communication can trace its history to 1890s while radiotelegraph system was developed by an Italian inventor whose name is Guglielmo Marconi. The traditional image that message delivering across the distance and spaces calls for a physical connection between two ends was overturned completely. Through the duration of World War II, American soldiers integrated the technology of encryption to radiotelegraph system to avoid eavesdropping by foes. This can be as the leading edge of wireless networking so far. In view of the communication standards were followed respectively, International Standard Organization (ISO) announced the architecture of Open Systems Interconnection (OSI) [30] in 1984. There are seven layers in OSI model as shown as following:

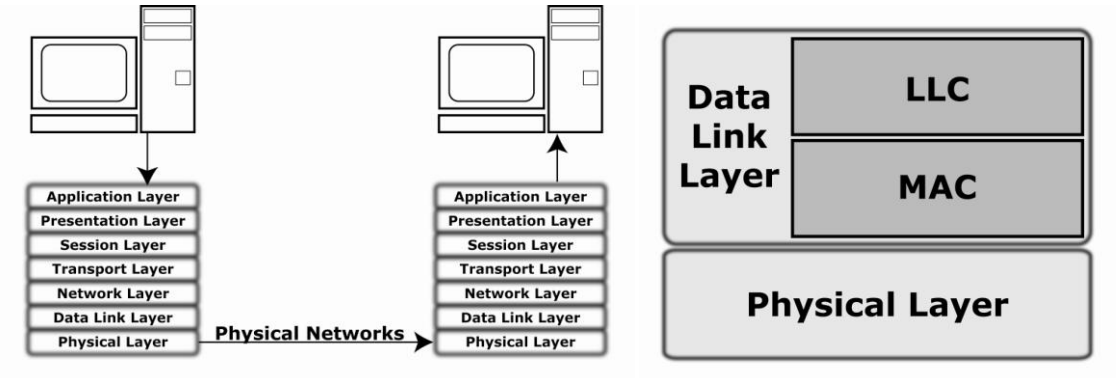

(a) (b)

Fig. 3-01 OSI model (a) Two hosts communicate via OSI model (b) Data Link Layer can be split up into Logical Link Control and Medium Access Control

The package was formed by encapsulating message in top-down manner before

transferring and then it will be delivered to another host through physical network. On the destination host, the package must be treated with bottom-up as a means of de-capsulating to extract the message. Such a mechanism attaches great importance to cooperation and responsibility in order to reduce the design complexities. Many standards were proposed according to the seven layers model afterward.

In 1997，IEEE released the origin version of the standard 802.11 [31] in which the Data Link layer and the Physical layer was defined. It specified to be transmitted the bounding data rate about 2 Mbit/sec in Industrial Scientific Medical (ISM) band at 2.4 GHz. Until 1999, IEEE released 2 versions of revision of 802.11 origin standard and hence 802.11a [32] and 802.11b [33] was published. 802.11a inherits the protocol of 802.11 but transmits the maximum data rate of 54Mbit/sec at 5G; 802.11b uses the same media access method defined in the origin version of 802.11 and delivers the data rate up to 11Mbit/sec in the same band as 802.11. There are some drawbacks in 802.11a such as Line-of-Sight (LOS) transmission and attenuation along traveling path caused by higher carrier frequency and 802.11b is popular with people relatively. In 2003, the extension of 802.11b was further generated and it so called 802.11g [34] operates at the data rate of 54Mbit/Sec and still uses the ISM band. In recent years, 802.11n builds on previous version of 802.11 standards by adding MIMO capability, and therefore improving antenna diversity and spatial multiplexing.

3.1.1 Protocols and Spectrum Allocation

IEEE 802.11 standard specifies wireless LAN architecture and its operation of Medium Access Control (MAC) and Physical (PHY) layers. As shown in Fig. 3-01(b), MAC and Logical Link Control (LLC) layers are the sub-layers of data link layer of OSI model and MAC layer interconnects with PHY and LLC layers. LLC layer is

occupied in not only multiplexing and de-multiplexing protocols amid MAC and upper layers of LLC but also providing flow and error control. It was specified independent of physical structure of network in IEEE 802 standard, and hence its upper layer needn't modify against various networks.

According to super-heterodyne model of wireless LAN, it can be divided into RF front end, IF transceiver, baseband module and MAC block surrounded by antennas and wireless devices. MAC block provides addressing mechanism to identify each address in subnetworks, besides, states some multiple access protocols such as CSMA/CA (Carrier Sense Multiple Access / Collision Avoidance). The other stages mentioned above constitute the architecture of PHY.

For the sake of improving immunity against interference and lower transmitting power within PHY, baseband technology provides some functions to spread spectrum or multiplex such as FHSS (Frequency Hopping Spread Spectrum), DSSS (Direct Sequence Spread Spectrum) and OFDM (Orthogonal Frequency Division Multiplexing). FHSS utilizes pseudo-random code to switch carrier frequency rapidly and cooperates with the capability of error correction to reduce the influence caused by interference. DSSS achieves spectrum spreading via XOR (exclusive OR) operation between signal sequence and 11-bits barker code. DBPSK (Differential Binary Phase Shift Keying) and DQPSK (Differential Quadrature Phase Shift Keying) was adopted to modulate date as system operates at 1Mbps and 2Mbps, CCK (Complementary Code Keying) was introduced to utilize as chip rate up to 5.5Mbps and 11Mbps. In order to increase spectral efficiency, OFDM allocates signal to many sub-carriers which are orthogonal sets and overlapping next door to each other. After combining each modulated channel, it will be altogether transmitted.

Finally, some standards will be listed in Table 3-01.

Standards	802.11		802.11a		802.11b		802.11g	
Frequency (GHz)	2.4000 – 2.4835		5.150 – 5.250 5.250 – 5.350 5.725 – 5.825		2.4000 – 2.4835		2.4000 – 2.4835	
Bandwidth (MHz)	83.5		300		83.5		83.5	
Modulation	BPSK, QPSK		BPSK, QPSK MQAM		BPSK, QPSK		BPSK, QPSK MQAM	
Spread Spectrum Multiplexing	FHSS, DSSS		OFDM		DSSS, CCK		OFDM, CCK	
Data Rate (Mbps)	*a.	1, 2	*c.	6, 9, 12, 18, 24, 36, 48, 54	*a.	1, 2	*a.	1, 2
					*b.	5.5, 11	*b.	5.5, 11
							*c.	6, 9, 12, 18, 24, 36, 48, 54

*a. DBPSK + DSSS for 1Mbps, DQPSK+DSSS for 2Mbps

*b. CCK for 5.5Mbps and 11Mbps

*c. OFDM modulation:

Modulations	BPSK	QPSK	16QAM	64QAM
Data Rate (Mbps)	6, 9	12, 18	24, 36	48, 54

Table 3-01 802.11 wireless LAN standards

3.2 Design of Compact WLAN Antennas

Wireless LAN Antennas widely used in handset device. Fig. 3-02 shows the configuration of our proposed compact wireless LAN antenna. It would be etched on 1.0 mm FR4 double side substrate with relatively permittivity ε_r =4.4 and loss tangent $\tan\delta$ =0.024. The overall sizes of the antenna is about ($L\times W\times H$) $45\times 14.5\times 1.0$ mm^3.

3.2.1 Schema of Antenna Structure

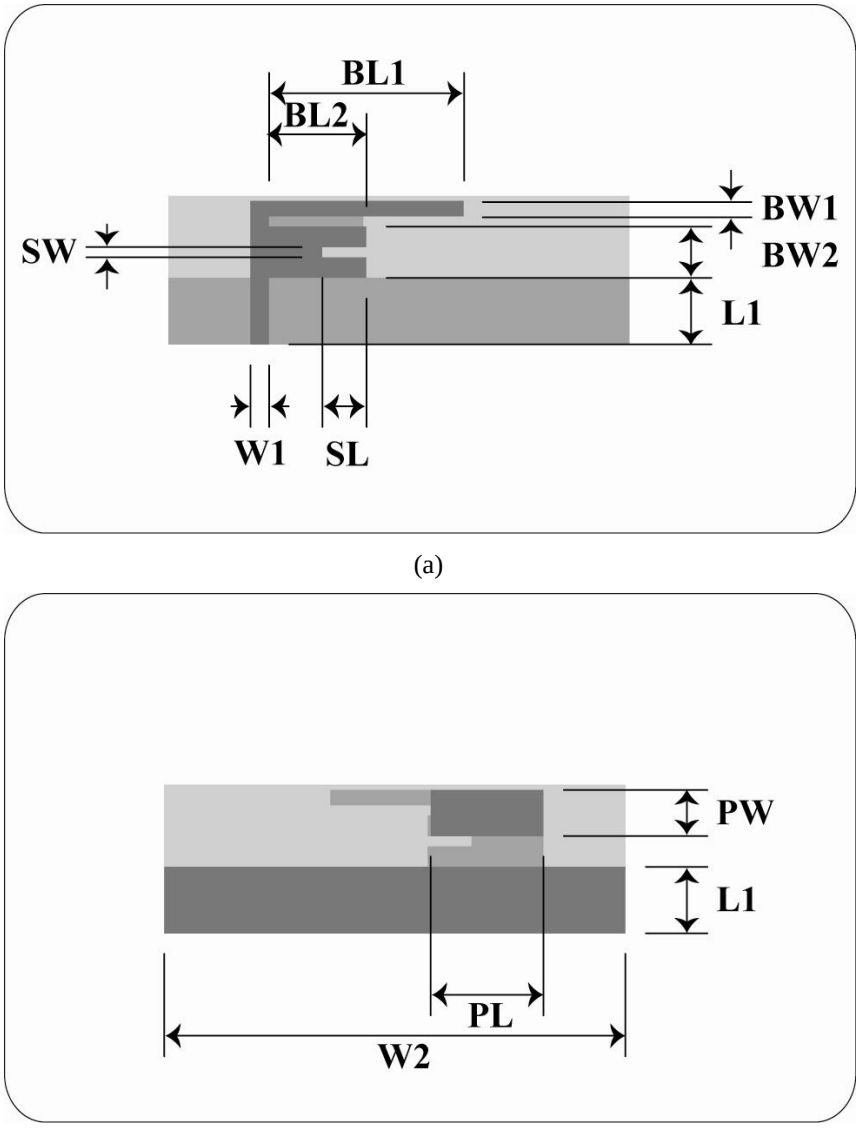

(a)

(b)

Fig. 3-02 Geometry of the proposed antenna (a) Top side view (b) Back side view

The geometry of the proposed antenna was shown as Fig. 3-02. There are three gradations of gray color to distinguish the arrangement via scenograph and they are light gray, gray and dark gray respectively. Because of the light gray always means substrate and hence it should be considered only on the others. The dark gray used to present the side near observer in this expression. Top side view of the proposed antenna was displayed in Fig. 3-02 (a) and two significant branches were connected to feeding point via a microstrip line with the size of $L1\times W1$. One of the branches with the size of $BL1\times BW1$ was designed to control lower band of the wireless LAN band. The other of the branches with the size of $BL2\times BW2$ embedded a slot with a size of $SL\times SW$ was designed to control upper band of the wireless LAN band. Turn the proposed antenna to the other side and it can be seen as Fig. 3-02 (b). A ground plane with the size of $L1\times W2$ was etched on the side of proposed antenna. In addition, a patch with the size of $PL\times PW$ was aligning to right edge of entire radiator on top side. Table 3-02 states the optimization of the architecture.

(Unit: mm)

L1	W1	BL1	BW1	BL2	BW2
6	1.8	19	1.5	9.5	5
SL	SW	PL	PW	W2	L1
4.3	1	11	4.5	45	6

Table 3-02 Parameters of Antenna Optimization

It can be seen that the proposed antenna includes two branches and one of these two branches embedding a slit to control the higher band matching. On the backside of the proposed antenna is attached a rectangular patch to couple two branch and further tuning the resonant frequency as shown in Fig. 3-04. Other parameters will be discussed as following sections.

3.2.2 Parametric Studies

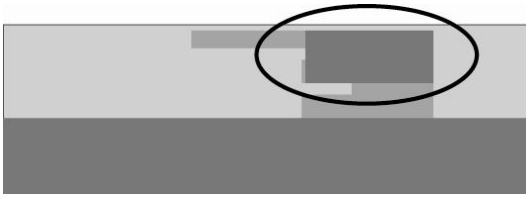

Fig. 3-03 Influence after adding the patch

Since the patch on the backside, higher band and lower band affect each other. It can be seen in Fig. 3-05, higher band and lower band were varied as the *BL1* varies. The shorter branch can be used to match upper band as shown in Fig. 3-06, and the slit embedding on the short branch can improving the matching of higher band as shown in Fig. 3-07. The backside patch influences higher band obviously. As the length of back side patch PL increasing, not only poor matching on lower band can be obtained but also moves the upper band toward lower band side as shown in Fig. 3-08. As the width of back side patch PW increasing, upper band shifts to lower band side can be obtained as shown in Fig. 3-09. These mentioned above design provides a flexible way to well match the antenna.

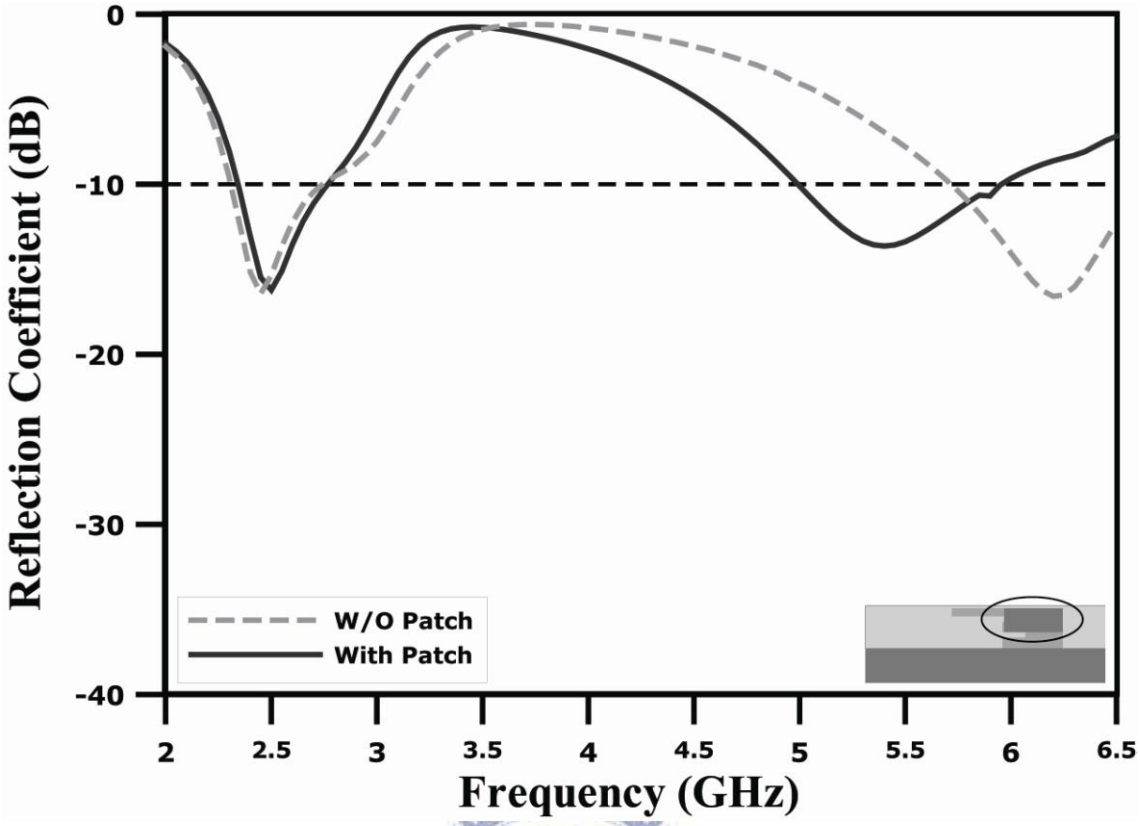

Fig. 3-04 Comparison of reflection coefficient between with and without adding the patch

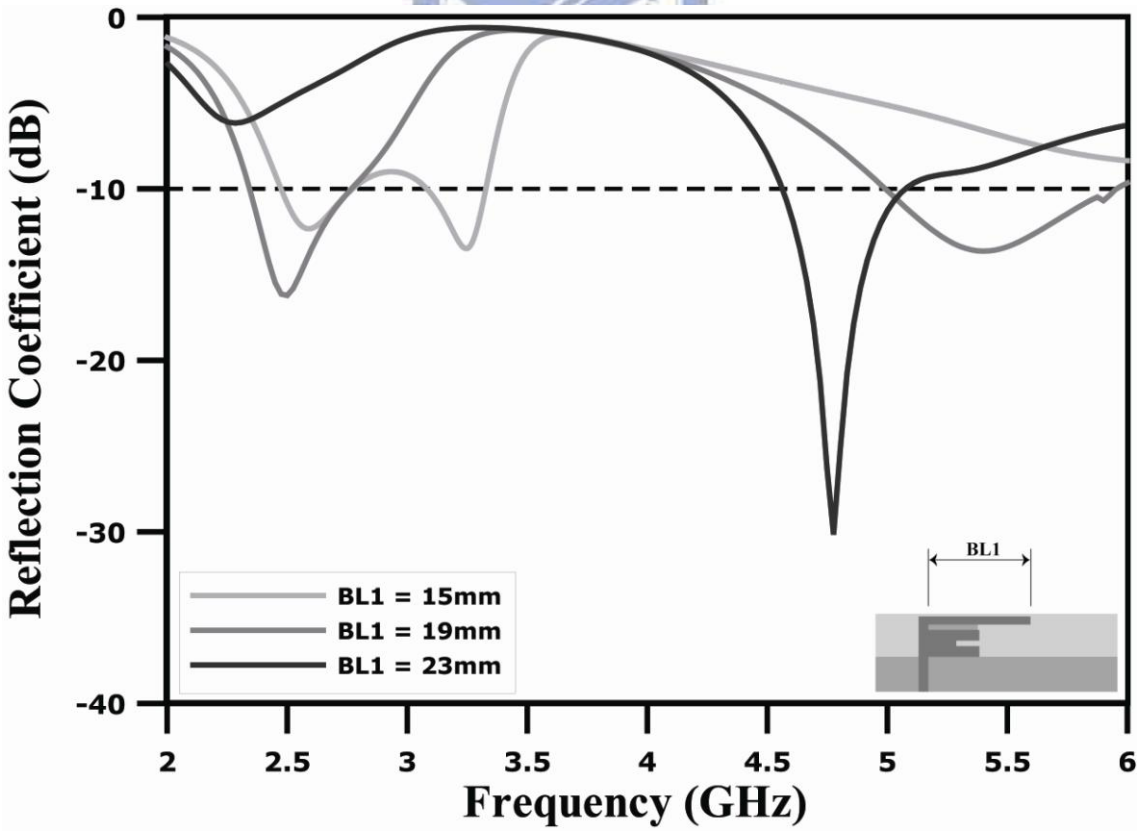

Fig. 3-05 Parametric Study of *BL1* for reflection coefficient

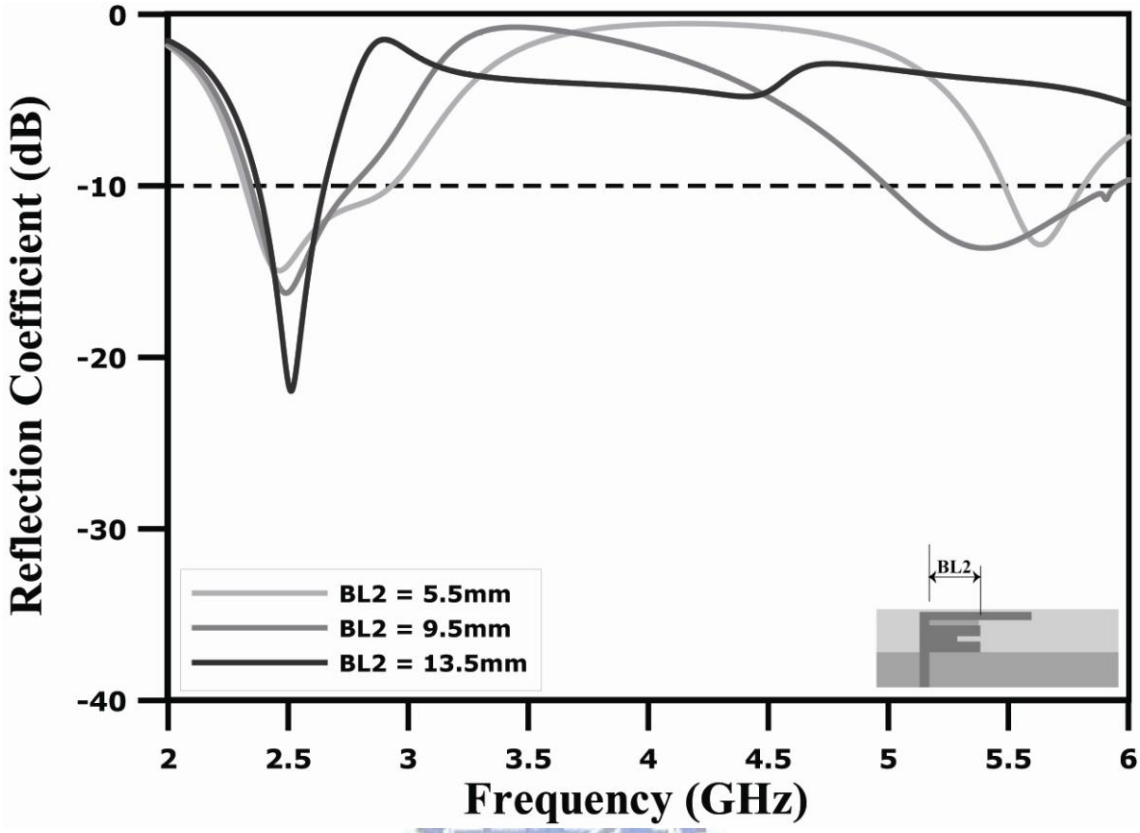

Fig. 3-06 Parametric Study of *BL2* for reflection coefficient

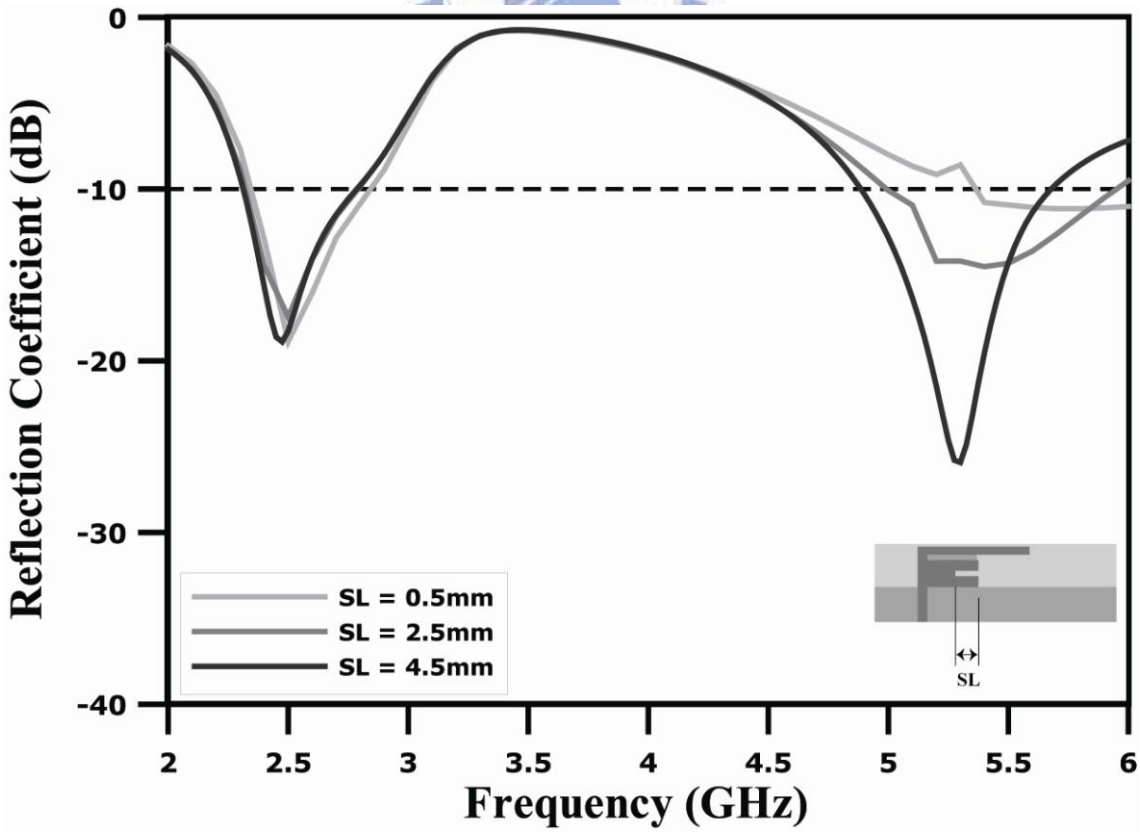

Fig. 3-07 Parametric Study of *SL* for reflection coefficient

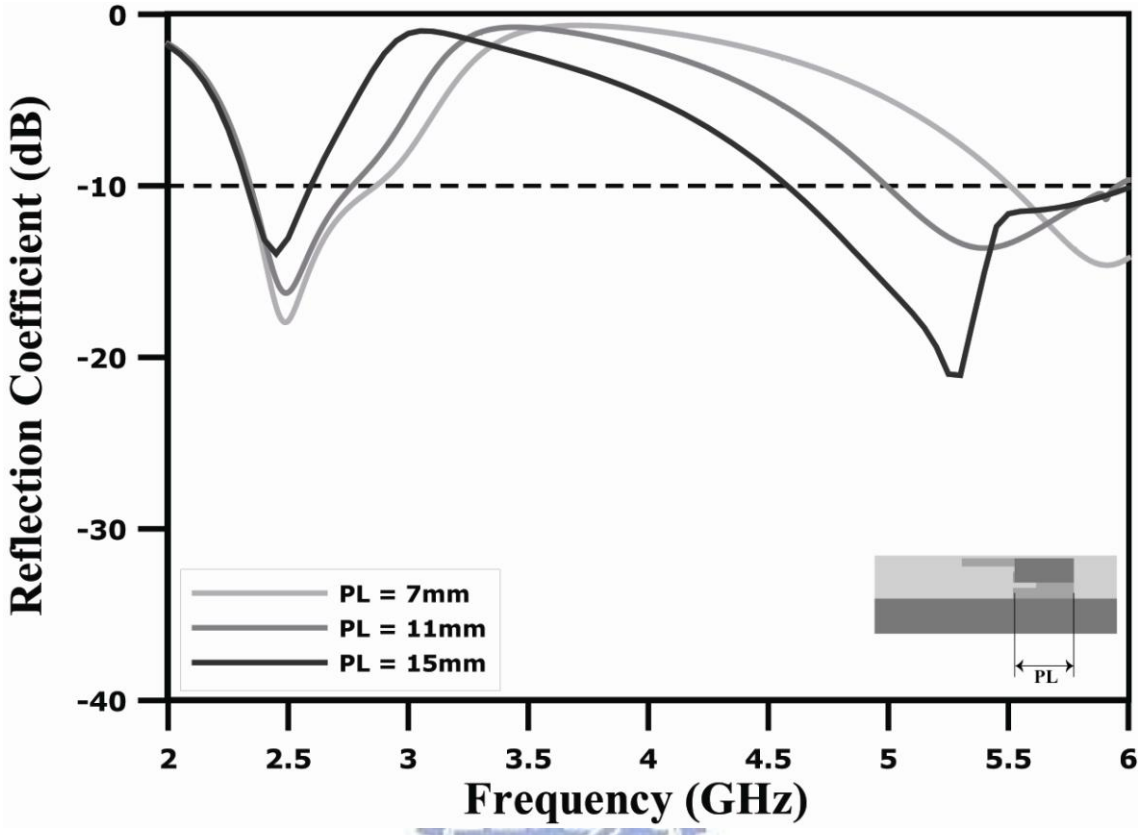

Fig. 3-08 Parametric Study of *PL* for reflection coefficient

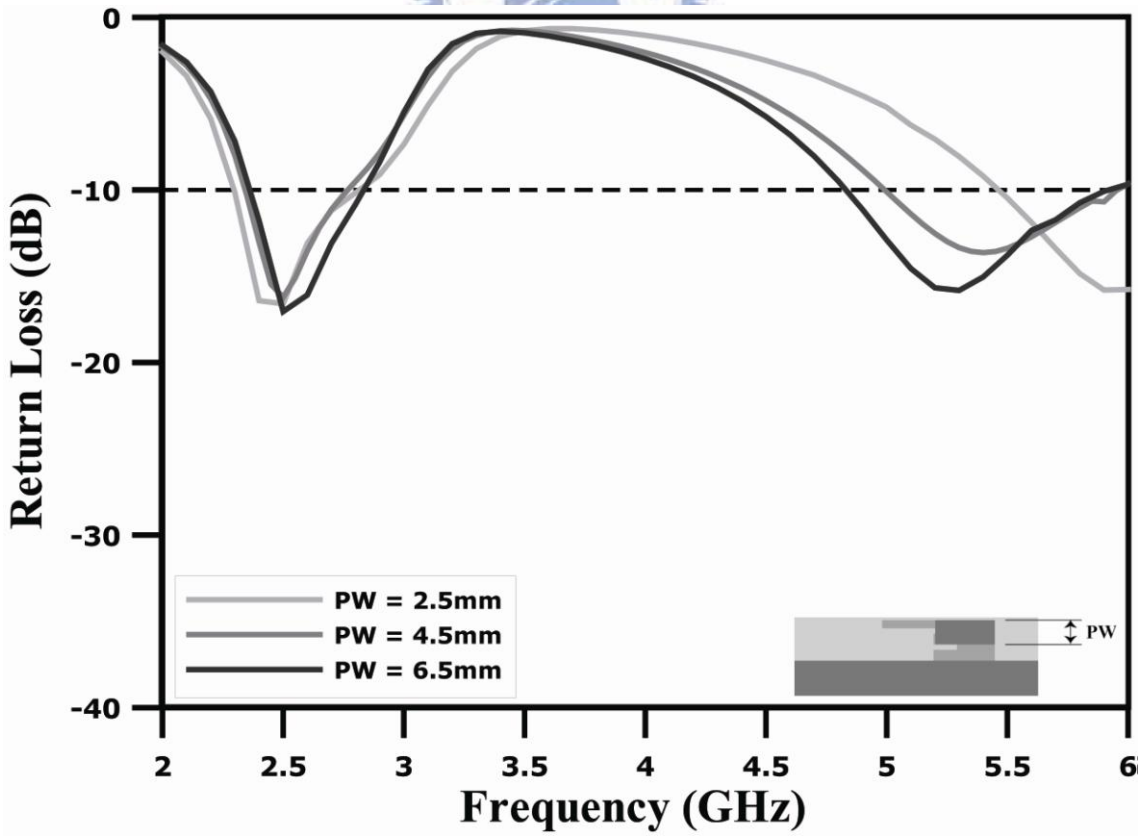

Fig. 3-09 Parametric Study of *PW* for reflection coefficient

3.2.3 Results of Simulation and Measurement

The characteristics of these proposed monopole antennas were calculated by using Ansoft High Frequency Structure Simulator (HFSS) software and measured by using HP 8722C network analyzer.

In Fig. 3-10, the reflection coefficient of simulation and measurement was illustrated good agreement but appeared some frequency shift on upper band. There are two modes can be obtained via simulation and they are 2.5 GHz and 5.4 GHz separately. According to these two modes, the surface current distribution will be simulated and discussed in Fig. 3-11. It can be obtained that surface current was distributed on the longer branch at lower band, simultaneously; it was distributed on the shorter branch at upper band.

The simulated radiation efficiency and peak gain are listed. Finally, radiation pattern was measured and listed in Fig. 3-16 to Fig. 3-19 over 802.11 family bands.

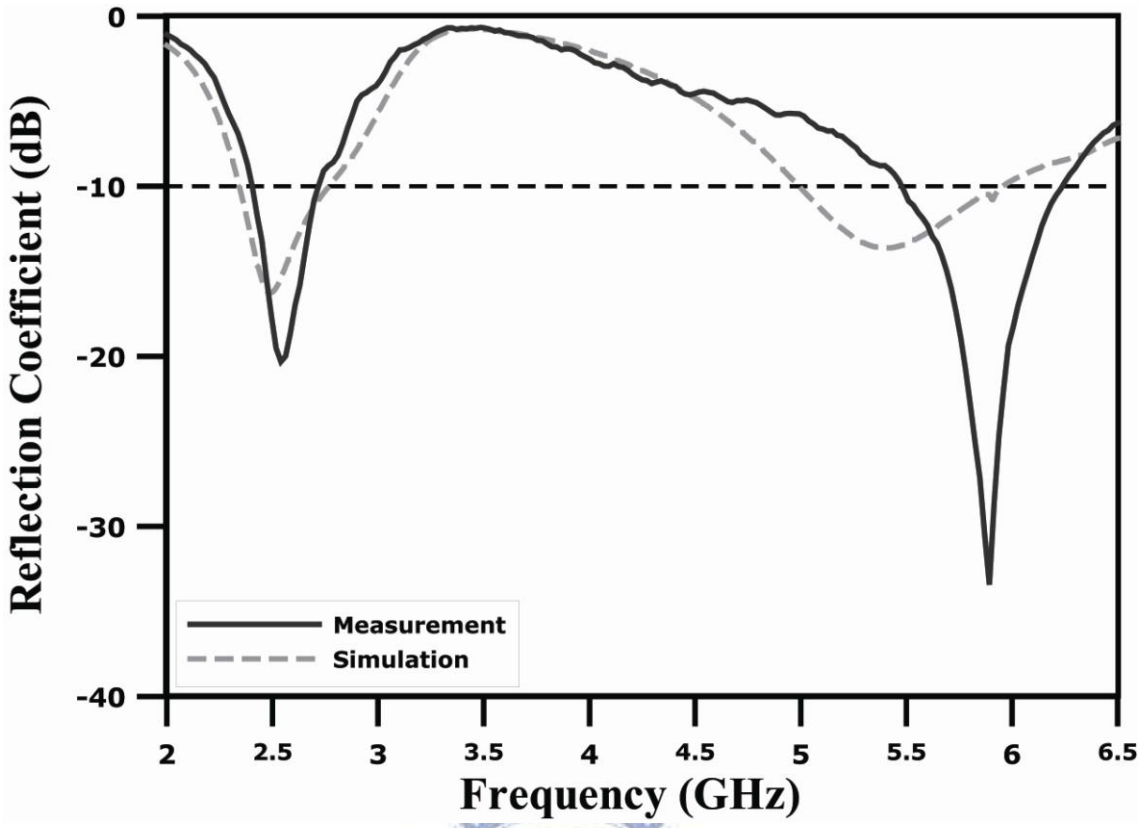

Fig. 3-10 Comparison of the reflection coefficient of proposed antenna between simulation and measurement

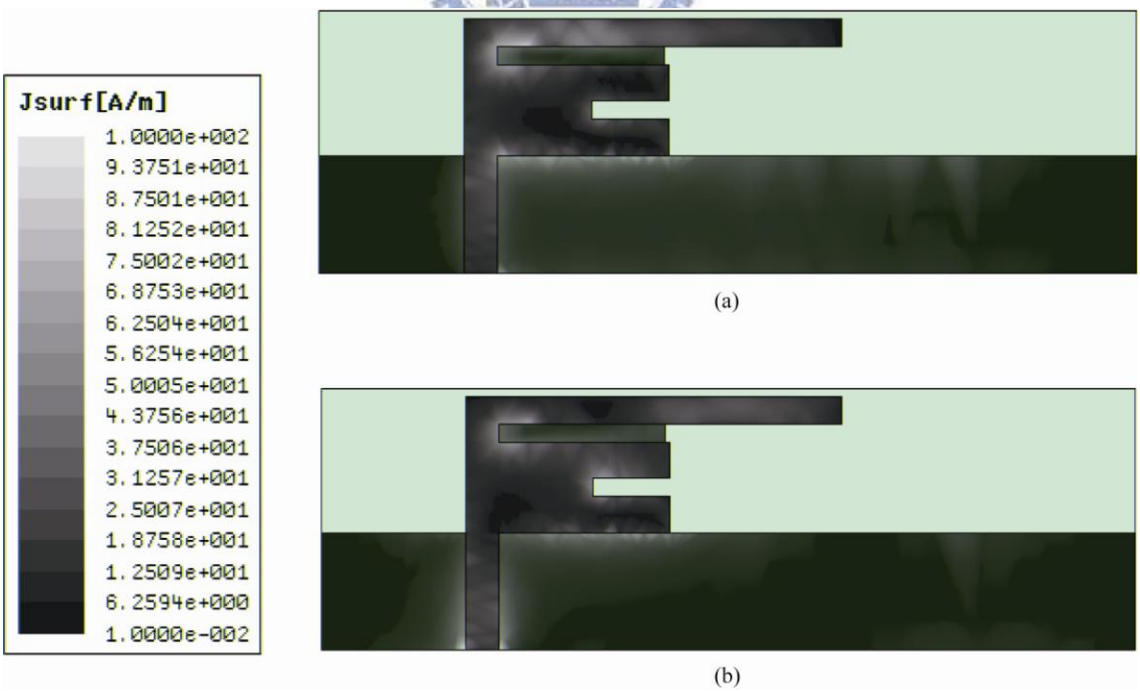

Fig. 3-11 Surface current distribution corresponding to resonant modes (a) 2.5GHz (b) 5.4 GHz

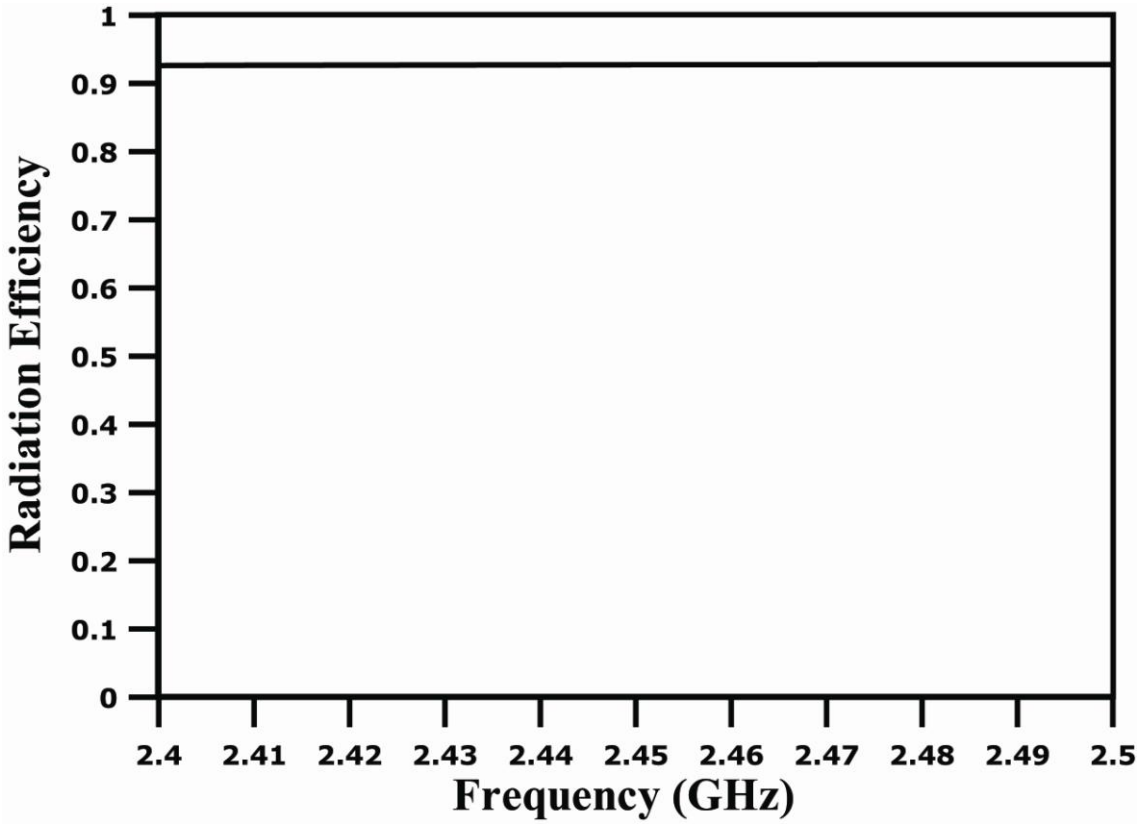

Fig. 3-12 Simulated radiation efficiency of the proposed antenna at lower band

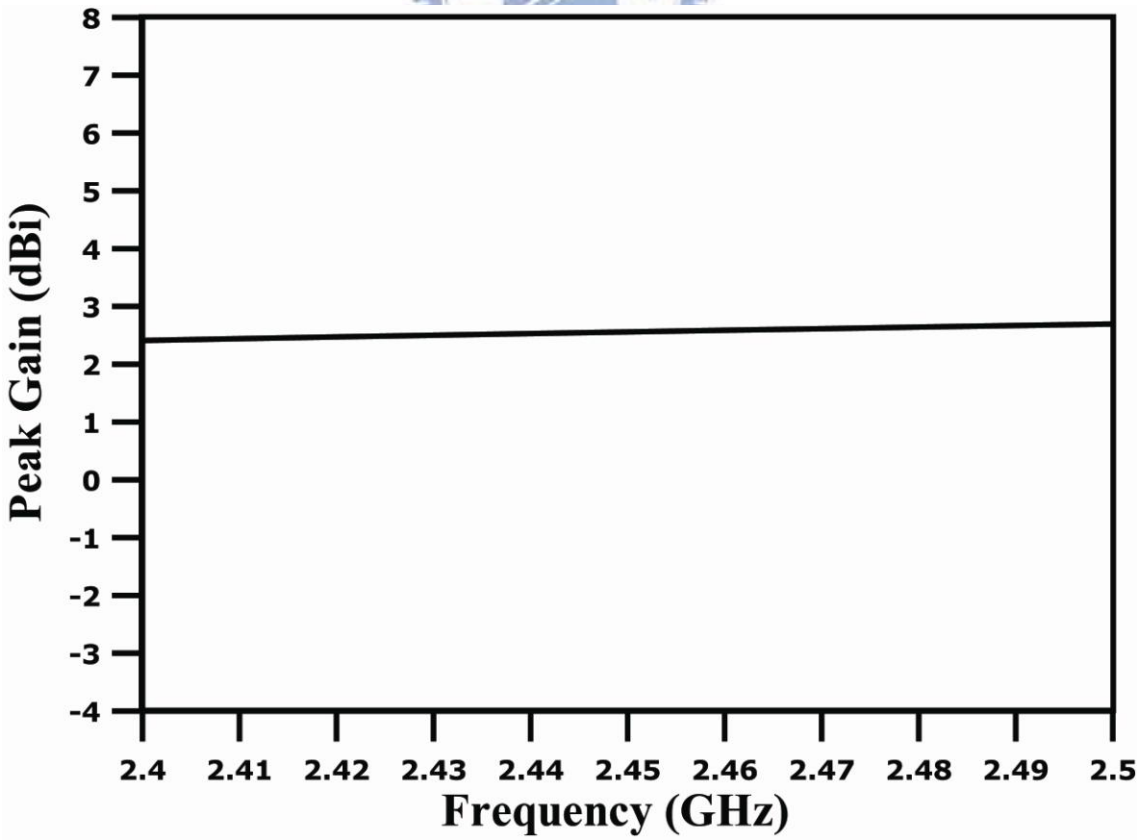

Fig. 3-13 Simulated peak gain of the proposed antenna at lower band

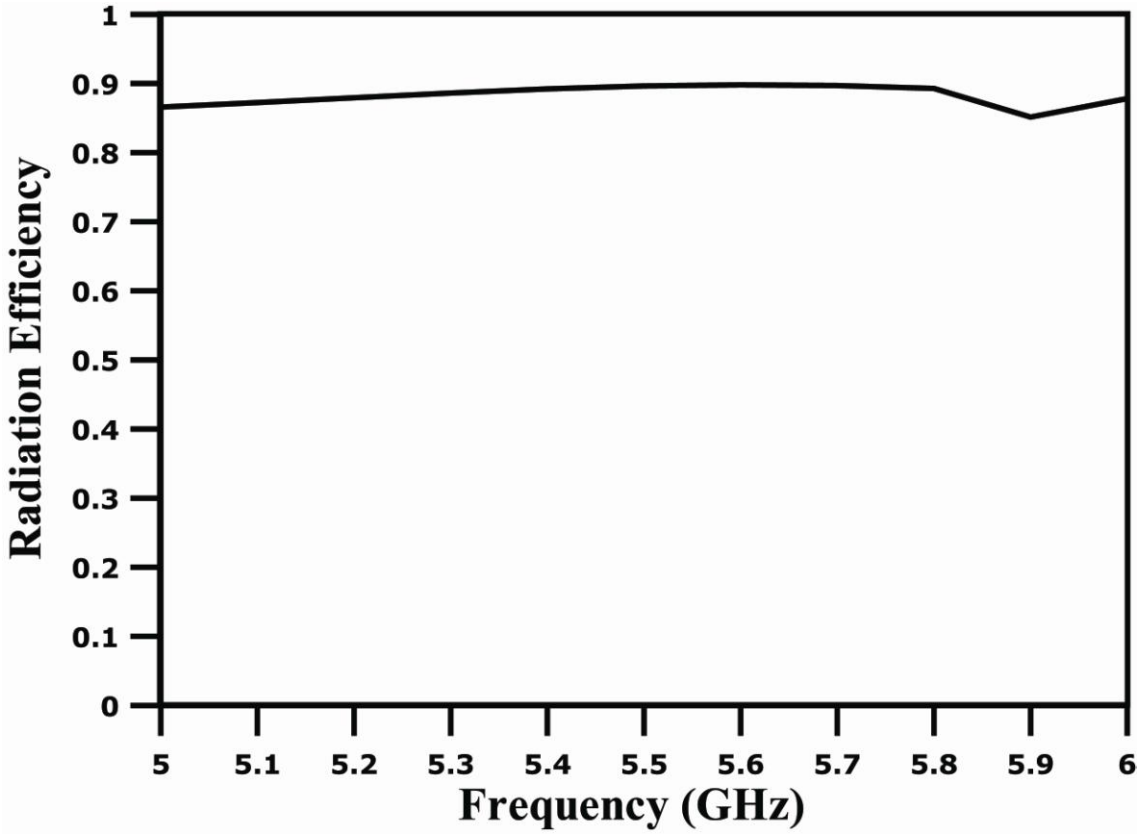

Fig. 3-14 Simulated radiation efficiency of the proposed antenna at higher band

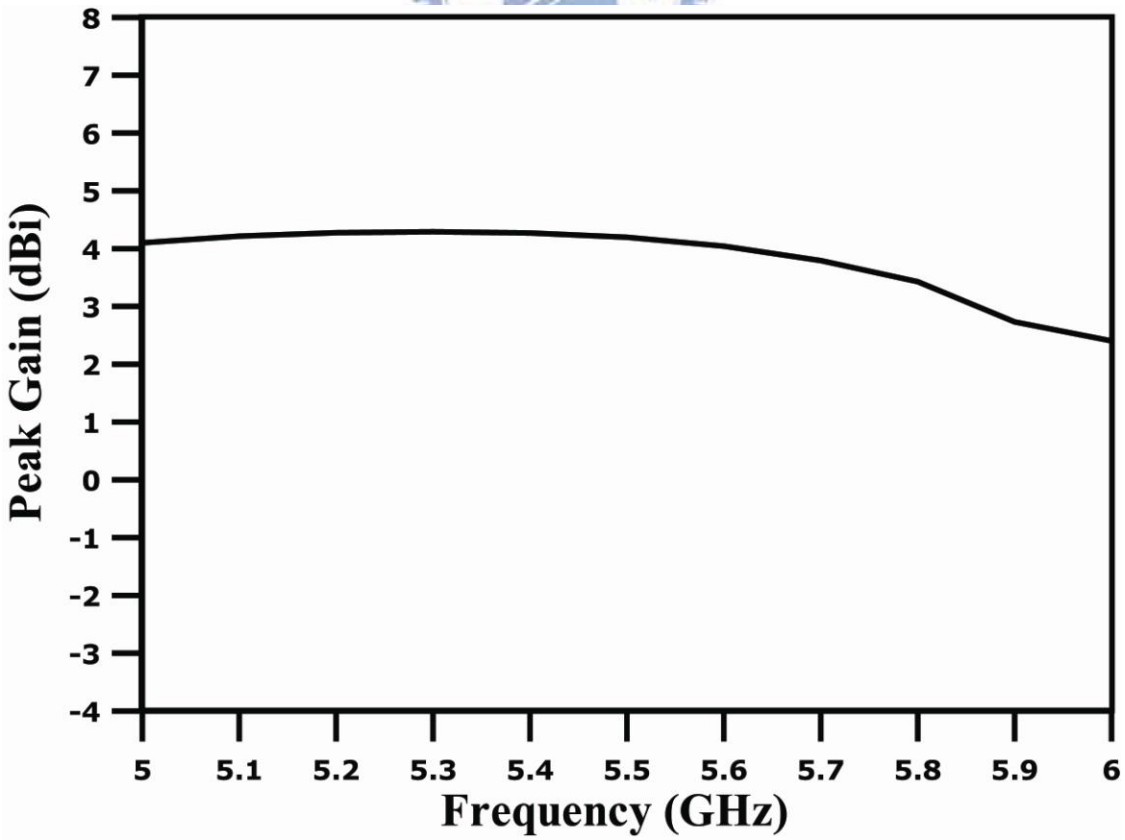

Fig. 3-15 Simulated peak gain of the proposed antenna at higher band

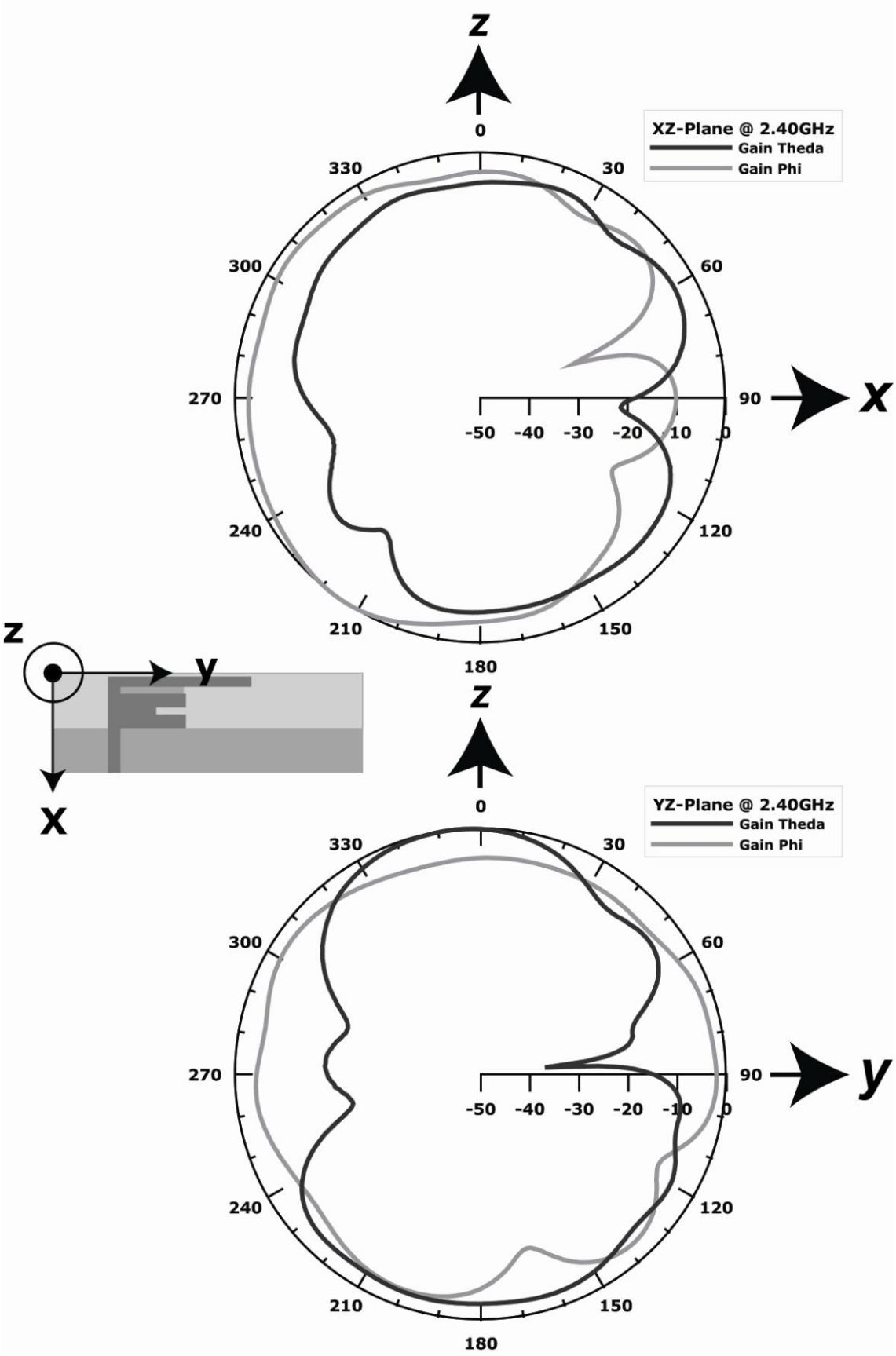

Fig. 3-16 Measurement of the radiation pattern of proposed antenna at 2.40 GHz

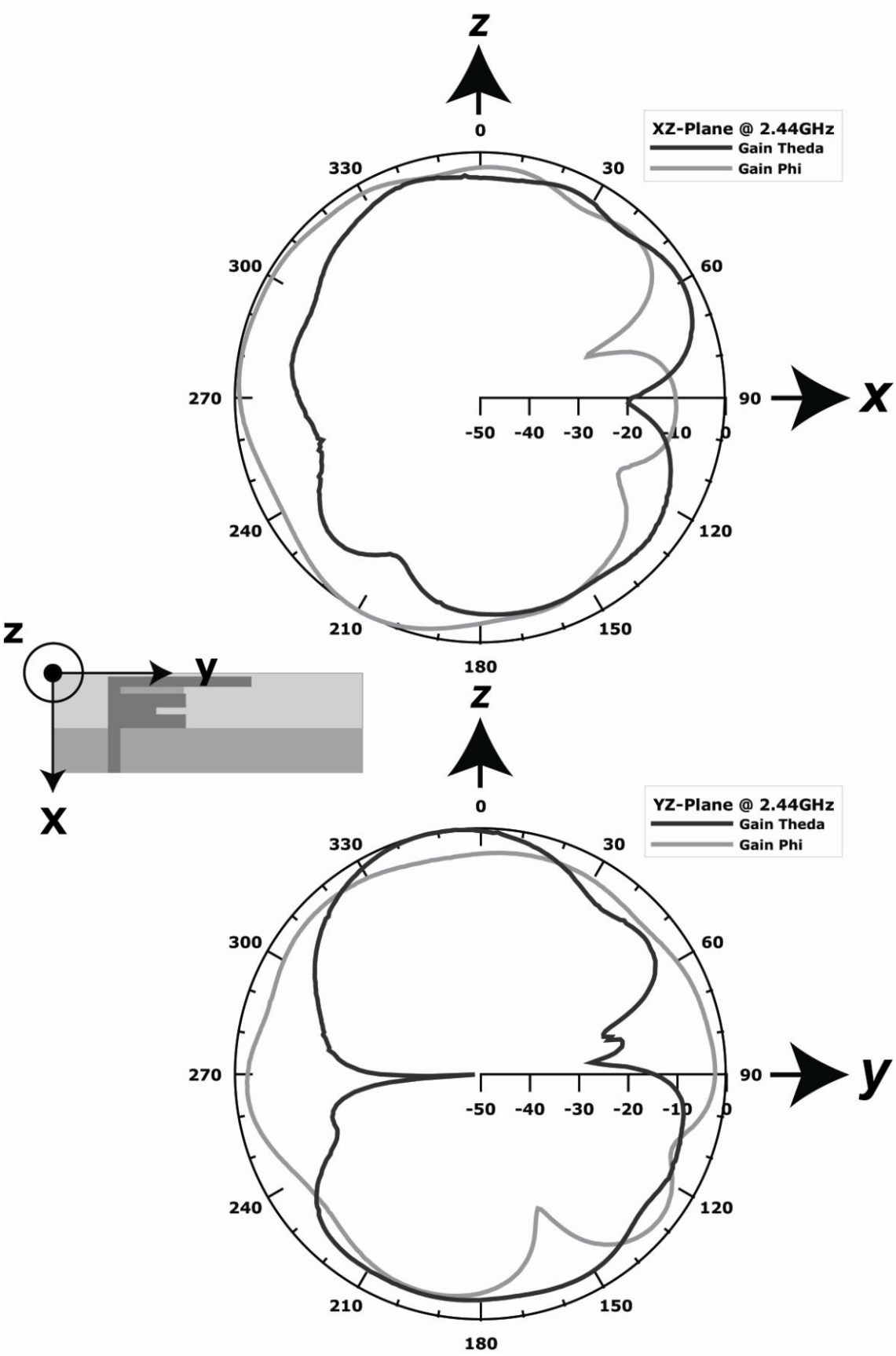

Fig. 3-17 Measurement of the radiation pattern of proposed antenna at 2.44 GHz

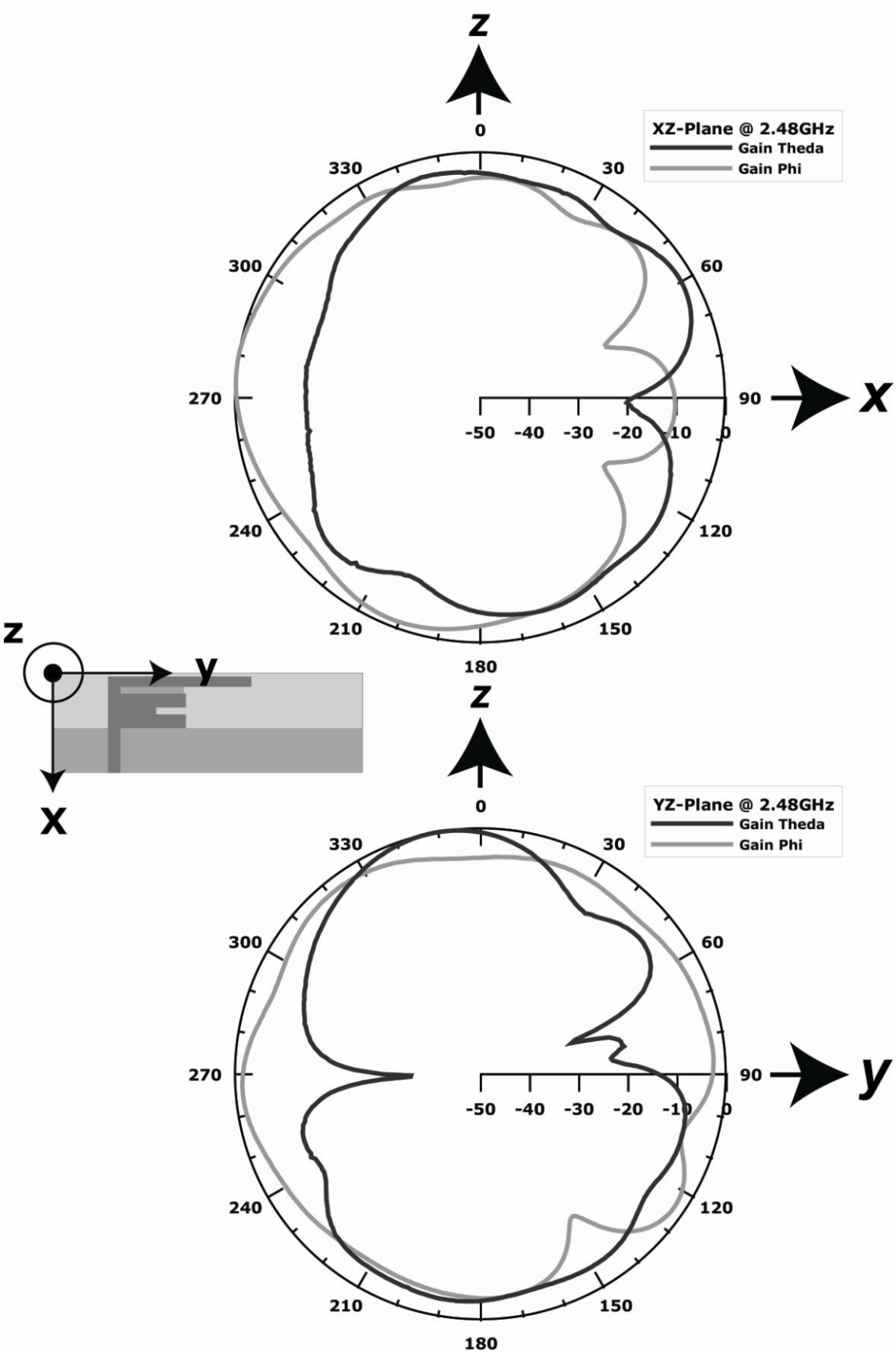

Fig. 3-18 Measurement of the radiation pattern of proposed antenna at 2.48 GHz

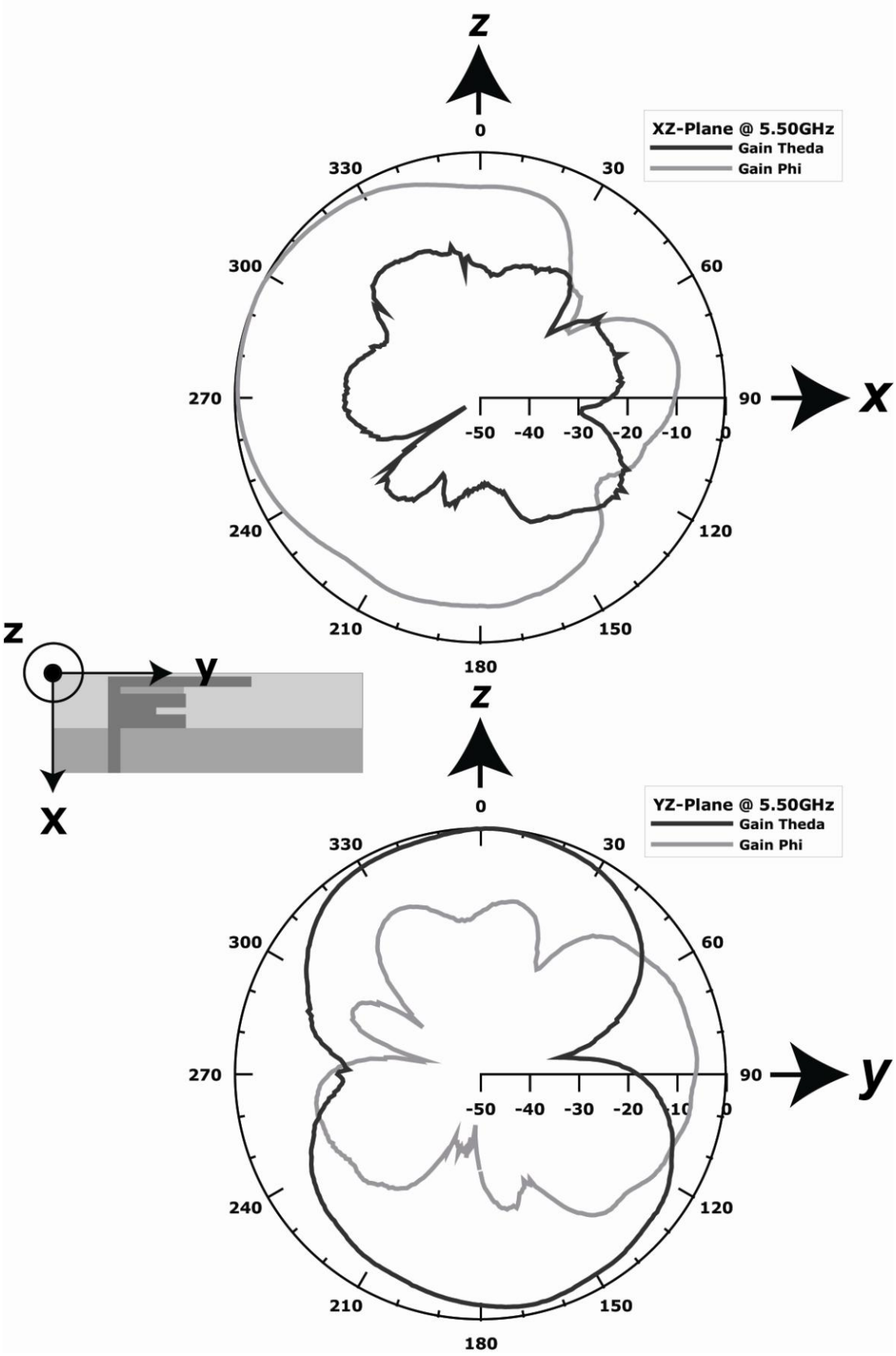

Fig. 3-17 Measurement of the radiation pattern of proposed antenna at 5.50 GHz

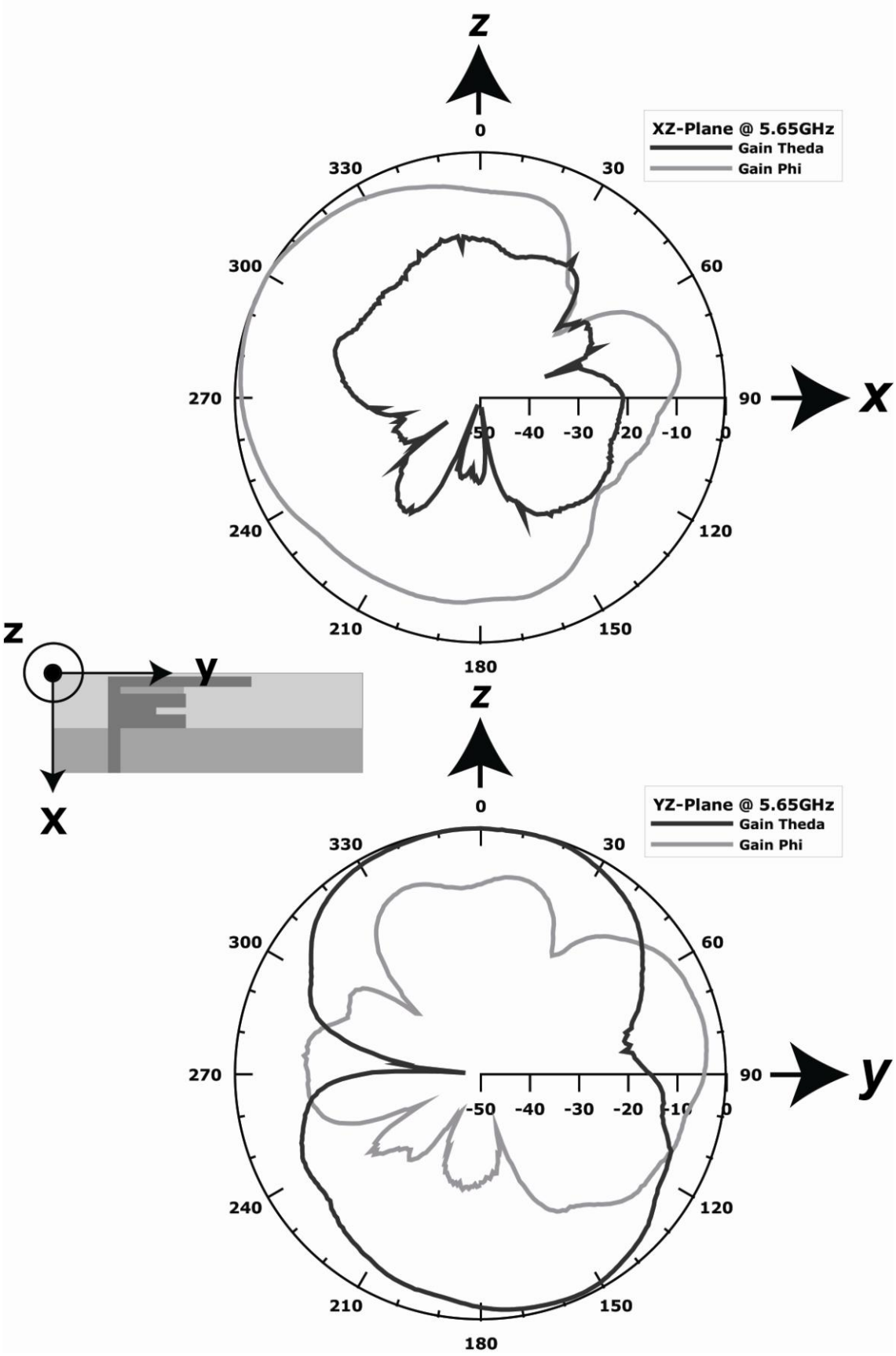

Fig. 3-18 Measurement of the radiation pattern of proposed antenna at 5.65 GHz

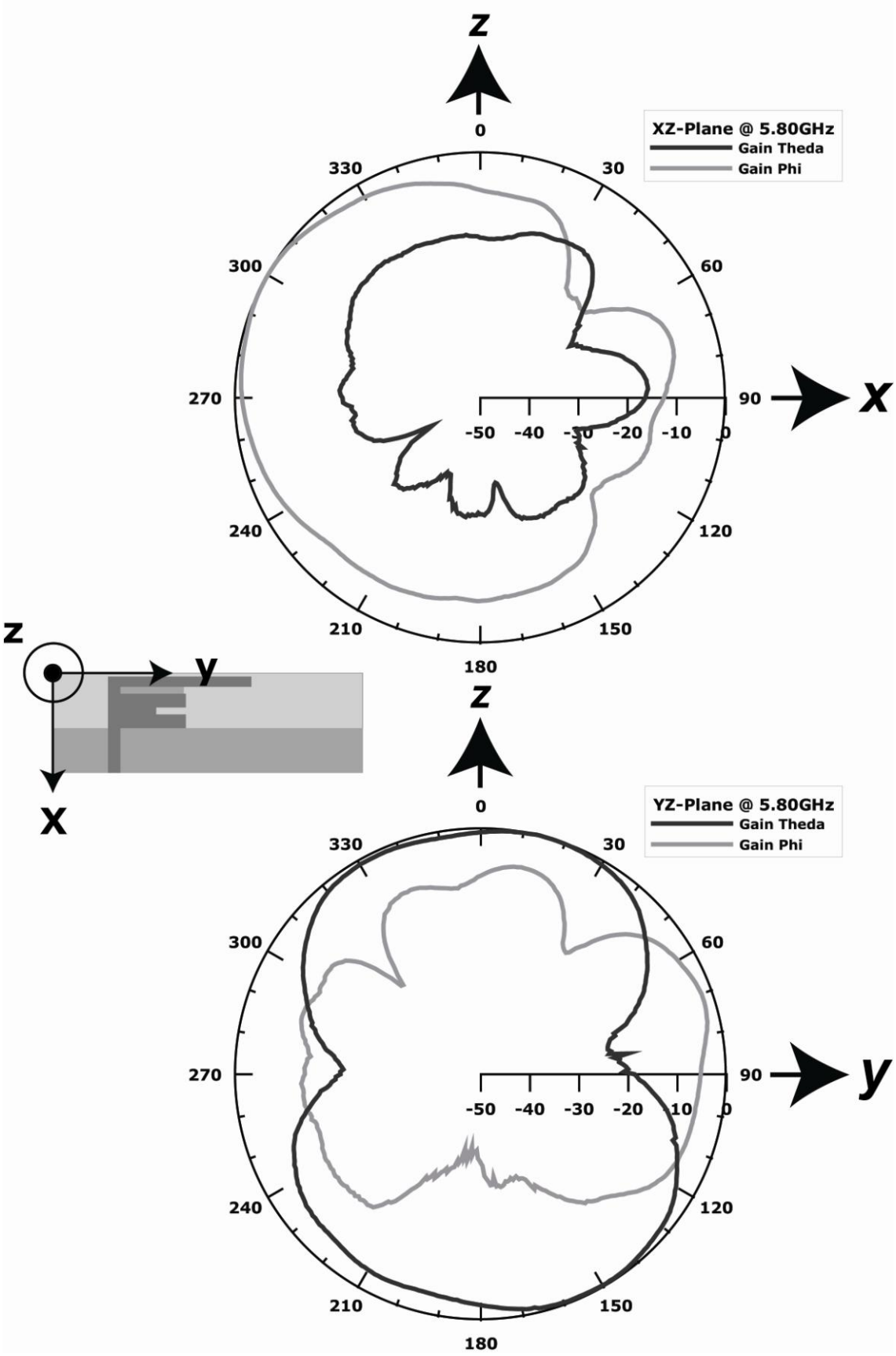

Fig. 3-19 Measurement of the radiation pattern of proposed antenna at 5.80 GHz

3.3 Conclusion

In this chapter, a wireless LAN antenna have been proposed and demonstrated. Through the feature of coupling, more flexible matching can be obtained in the structure based on conventional dual branch. The antenna can operate over ISM band, otherwise, can use in upper band of IEEE 802.11a. There is some frequency drift on 5GHz-band; it might be caused by the process of fabrication. Perfect coverage can be achieved via adequate matching if necessary.

CHAPTER 4

Future Works

4.1 Future Works

MIMO (Multiple-Input-Multiple-Output) is an effective concept to improve the channel capacity of communication system. Michael R. Andrews et al. published in Nature to illustrate the tripling of capacity via electromagnetic polarization [35]. In addition, IEEE 802.11g appended the capability of MIMO to increase channel capacity. Chi-Yuk et al. published an article [36] related to this orthogonally polarization architecture.

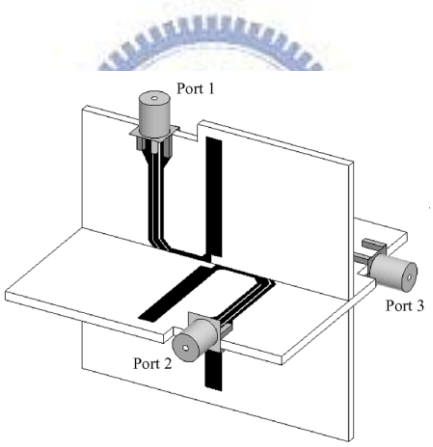

Fig. 4-01 Three-port orthogonally polarized MIMO antenna [36]

The same as the dipole element, half-slot element have also proposed in [36]. In the future, a half-patch antenna edition of the tripling capacity can be considered. Through the ground plane on the back side forms a mirror to perform image theory. According to ZOR (Zeroth Order Resonator) concept, A. Sanada et al. proposed a miniature method using left-handed transmission line [37], and hence it can be introduced to the future design. The minimizing process because of size reducing related to ground plane can achieve not only diminution of antenna size but improving image property.

REFERENCES

[1] Apple Inc., "Apple-iPhone," available in http://www.apple.com/iphone/

[2] HTC Corporation, "HTC - Touch Phone, PDA Phone, Smartphone, Mobile Computer," available in http://www.htc.com/us/

[3] W. L. Stutzman and G. A. Thiele, *Antenna Theory and Design*, 2nd ed. New York: Wiley, 1998.

[4] W. F. Richards, Y. T. Lo, and D. D. Harrison, "An improved theory for microstrip antennas and applications," *IEEE Trans. Antennas Propag*., vol. 29, pp. 38-46, Jan. 1981.

[5] Y. T. Lo, B. Engst, and R. Q. Lee, "Simple design formulas for circularly polarized microstrip antennas," in *Proc. IEE*., June 1983, pt. H, vol. 135, no. 3, pp. 213-215.

[6] S. K. Lee, A. Sambell, E. Korolkiewicz, and S. F. Ooi, "Analysis and design of a circular-polarized nearly-square-patch antenna using a cavity model," *Microw. Opt. Technol. Lett*., vol. 46, no. 4, pp. 406-410, Aug. 2005.

[7] N. Kumprasert, "Theoretical study of dual-resonant frequency and circular polarization of elliptical microstrip antennas," in *Proc. IEEE AP-S Int. Symp*., Jul. 2000, vol. 2, pp. 1015-1020.

[8] K. F. Tong and T. P. Wong, "Circularly polarized U-slot antenna," *IEEE Trans. Antennas Propag*., vol. 55, no. 8, pp. 2382-2385, Aug. 2007.

[9] H. Q. Cheng, L. B. Tian, and B. J. Hu, "Compact Circularly Polarized Square Microstrip Fractal Antenna with Symmetrical T-slits," in *Proc. IEEE WiCom Int. Conf*., Sep. 2007, pp. 613-616.

[10] K. P. Yang and K. L. Wong, "Dual-band circularly polarized square microstrip

antenna," *IEEE Trans. Antennas Propag*., vol. 49, no. 3, pp. 377-382, Mar. 2001.

[11] H. L. Zhang, H. O. Cheng, L. B. Tian, and B. J. Hu, "Novel Circularly Polarized Square Microstrip Antenna with L-Slits," in *Proc. IEEE Microw., Antenna, Propag. and EMC Technol. for Wireless Comm. Int. Symp*., Aug. 2007, pp. 665-668.

[12] K. C. Wan and Q. Xue, "A novel reconfigurable wideband circularly polarized transmitter implemented by indirect-controlled-phased-source," *Antennas Propag. Lett*., vol. 6, pp. 604-607, Nov. 2007.

[13] J. P. Thakur and J. S. Park, "An advance design approach for circular polarization of the microstrip antenna with unbalance DGS feedlines," *Antennas Propag. Lett*., vol. 5, pp. 101-103, Jan. 2006.

[14] S. Gao, Y. Qin, and A. Sambell, "Low-cost broadband circularly polarized printed antennas and array," *Antennas Propag. Mag*., vol. 6, pp. 57-64, Aug. 2007.

[15] Nasimuddin, K. P. Esselle, and A. K. Verma, "Wideband circularly polarized stacked microstrip antennas," *Antennas Propag. Lett*., vol. 6, pp. 21-24, Dec. 2007.

[16] Nasimuddin, K. P. Esselle, and A. K. Verma, "Wideband high-gain circularly polarized stacked microstrip antennas with an optimized C-type feed and a short horn," *IEEE Trans. Antennas Propag*., vol. 56, no. 2, pp. 578-581, Feb. 2008.

[17] D. J. Müller and K. Sarabandi, "Design and analysis of a 3-arm spiral antenna," *IEEE Trans. Antennas Propag*., vol. 55, no. 2, pp. 258-266, Feb. 2007.

[18] M. C. Buck and D. S. Filipovic, "Two-arm sinuous antennas," *IEEE Trans. Antennas Propag*., vol. 56, no. 5, pp. 1229-1235, May. 2008.

[19] I. C. Deng, J. B. Chen, Q. X. Ke, J. R. Chang, W. F. Chang, and Y. T. King, "A

circular CPW-fed slot antenna for broadband circularly polarized radiation," *Microw. Optical Lett.*, vol. 5, pp. 2728-2733, Nov. 2007.

[20] J. Y. Sze, K. L. Wong, and C. C. Huang, "Coplanar waveguide-fed square slot antenna for broadband circularly polarized radiation," *IEEE Trans. Antennas Propag.*, vol. 51, no. 8, pp. 2141-2144, Aug. 2003.

[21] C. H. Chen, E. K. N. Yung, and B. J. Hu, "Miniaturised CPW-fed circularly polarized corrugated slot antenna with meander line loaded," *Electron. Lett.*, vol. 43, no. 25, pp. 1404-1405, Dec. 2007.

[22] J. S. Row, "Design of aperture-coupled annular-ring microstrip antennas for circular polarization," *IEEE Trans. Antennas Propag.*, vol. 53, no. 5, pp. 1779-1785, May. 2005.

[23] J. Y. Sze, C. I. G. Hsu, M. H. Ho, Y. H. Ou, and M. T. Wu, "Design of circularly polarized annular-ring slot antennas fed by a double-bent microstripline," *IEEE Trans. Antennas Propag.*, vol. 55, no. 11, pp. 3134-3139, Nov. 2007.

[24] X. L. Bao and M. J. Ammann, "Dual-frequency circularly-polarized patch antenna with compact size and small frequency ratio," *IEEE Trans. Antennas Propag.*, vol. 55, no. 7, pp. 2104-2107, Jul. 2007.

[25] J. Huang, "A technique for an array to generate circular polarization with linearly polarized elements," *IEEE Trans. Antennas Propag.*, vol. AP-34, no. 9, pp. 1113-1124, Sep. 1986.

[26] S. L. S. Yang, R. Chair, A. A. Kishk, K. F. Lee, and K. M. Luk, "Study on sequential feeding networks for subarrays of circularly polarized elliptical dielectric resonator antenna," *IEEE Trans. Antennas Propag.*, vol. 55, no. 2, pp.

321-333, Feb. 2007.

[27] W. Kim, S. Hong, H. Park, and J. Choi, "Wide impedance bandwidth for mobile handset application," *Microw. Optical Lett*., vol. 49, no. 4, pp. 779-781, Apr. 2007.

[28] HFSS, Version 9.2, Ansoft Corporation, available in http://www.ansoft.com/products/hf/hfss/

[29] Andrea Goldsmith, *Wireless Communications*. Cambridge University Press, 2005.

[30] ITU-T Rec. X.200 (07/94) Information technology - Open Systems Interconnection - Basic reference model: The basic model

[31] IEEE Std 802.11™-2007, IEEE Standard for Information Technology--Telecommunications and information exchange between systems--LANs and MANs--Specific requirements--Part 11: WLAN MAC and PHY Specifications

[32] IEEE Std 802.11a-1999 [ISO/IEC 8802-11:1999/Amd 1:2000(E)] (Supplement to IEEE Std 802.11, 1999 Edition) Part 11: Wireless LAN Medium Access Control (MAC) and Physical Layer (PHY) specifications: High-speed Physical Layer in the 5 GHz Band.

[33] IEEE Std 802.11b-1999 (Supplement to ANSI/IEEE Std 802.11, 1999 Edition) Part 11: Wireless LAN Medium Access Control (MAC) and Physical Layer (PHY) specifications: Higher-Speed Physical Layer Extension in the 2.4 GHz Band.

[34] IEEE Std 802.11g-2003 [Amendment to IEEE Std 802.11, 1999 Edition (Reaff 2003) as amended by IEEE Stds 802.11a-1999, 802.11b-1999, 802.11b-1999/Cor 1-2001, and 802.11d-2001], Amendment 4: Further Higher Data Rate Extension in the 2.4 GHz Band.

[35] M. R. Andrews, P. P. Mitra, and R. deCarvalho, "Tripling the capacity of wireless

communications using electromagnetic polarization," *Nature Mag*., vol. 409, pp. 316-318, Jan. 2001.

[36] C. Y. Chiu, J. B. Yan, and R. D. Murch, "Compact three-port orthogonally polarized MIMO antennas," *Antennas Propag. Lett*., vol. 6, pp. 619-622, Nov. 2007.

[37] A. Sanada, M.Kimura, I. Awai, H. Kubo, C. Caloz, and T. Itoh, "A Planar zeroth order resonator antenna using left-handed transmission line," to be presented at the *European Microw. Conf*., Amsterdam, Netherlands, 2004.